Theses and Dissertations--Microbiology, Immunology, and Molecular Genetics

Microbiology, Immunology, and Molecular Genetics

2017

IMMUNE EVASION BY DIVISION OF LABOR: THE TROPHIC LIFE CYCLE STAGE OF *PNEUMOCYSTIS MURINA* SUPPRESSES INNATE IMMUNITY TO THIS OPPORTUNISTIC, FUNGAL PATHOGEN

Heather M. Evans
University of Kentucky, heather.evans3458@gmail.com
Author ORCID Identifier:
 https://orcid.org/0000-0001-7551-2367
Digital Object Identifier: https://doi.org/10.13023/ETD.2017.402

Right click to open a feedback form in a new tab to let us know how this document benefits you.

STUDENT AGREEMENT:

I represent that my thesis or dissertation and abstract are my original work. Proper attribution has been given to all outside sources. I understand that I am solely responsible for obtaining any needed copyright permissions. I have obtained needed written permission statement(s) from the owner(s) of each third-party copyrighted matter to be included in my work, allowing electronic distribution (if such use is not permitted by the fair use doctrine) which will be submitted to UKnowledge as Additional File.

I hereby grant to The University of Kentucky and its agents the irrevocable, non-exclusive, and royalty-free license to archive and make accessible my work in whole or in part in all forms of media, now or hereafter known. I agree that the document mentioned above may be made available immediately for worldwide access unless an embargo applies.

I retain all other ownership rights to the copyright of my work. I also retain the right to use in future works (such as articles or books) all or part of my work. I understand that I am free to register the copyright to my work.

REVIEW, APPROVAL AND ACCEPTANCE

The document mentioned above has been reviewed and accepted by the student's advisor, on behalf of the advisory committee, and by the Director of Graduate Studies (DGS), on behalf of the program; we verify that this is the final, approved version of the student's thesis including all changes required by the advisory committee. The undersigned agree to abide by the statements above.

<div align="right">

Heather M. Evans, Student

Dr. Beth Garvy, Major Professor

Dr. Ken Fields, Director of Graduate Studies

</div>

IMMUNE EVASION BY DIVISION OF LABOR:
THE TROPHIC LIFE CYCLE STAGE OF *PNEUMOCYSTIS
MURINA* SUPPRESSES INNATE IMMUNITY TO THIS
OPPORTUNISTIC, FUNGAL PATHOGEN

———————————————

DISSERTATION

———————————————

A dissertation submitted in partial fulfillment of the requirements
for the degree of Doctor of Philosophy in the College of Medicine
at the University of Kentucky

By
Heather Marie Evans

Lexington, Kentucky

Director: Dr. Beth Garvy,
Professor and Chair of
Microbiology, Immunology, and Molecular Genetics

Lexington, Kentucky

2017

ABSTRACT OF DISSERTATION

IMMUNE EVASION BY DIVISION OF LABOR:
THE TROPHIC LIFE CYCLE STAGE OF *PNEUMOCYSTIS MURINA* SUPPRESSES
INNATE IMMUNITY TO THIS OPPORTUNISTIC, FUNGAL PATHOGEN

Pneumocystis species are opportunistic fungal pathogens that cause severe pneumonia in immunocompromised hosts, including AIDS patients. *Pneumocystis* species have a biphasic life cycle consisting of single-nucleated trophic forms and ascus-like cysts. Both stages live within the host, and, thus, must contend with threats from the host immune system. The cyst cell wall β-glucans have been shown to stimulate immune responses in lung epithelial cells, dendritic cells and alveolar macrophages. Little is known about how the trophic life forms, which do not have a fungal cell wall, interact with immune cells. In this study, the immune response to the life cycle stages of *Pneumocystis murina* was evaluated.

Here, we report differences in the immune response of immunocompetent mice to the trophic and cystic life cycle stages of *P. murina*. Upon infection with purified trophic forms, wild-type adult mice developed a delayed innate and adaptive immune response compared to inoculation with the normal mixture of trophic forms and cysts. Cysts, but not trophic forms, stimulated T_h1-type responses in the lungs of infected mice.

Surprisingly, trophic forms are sufficient to generate protective adaptive responses, leading to clearance in immunocompetent mice. We report that $CD4^+$ T cells primed in the presence of trophic forms are sufficient to mediate clearance of trophic forms and cysts. In addition, primary infection with trophic forms is sufficient to prime B cell memory responses capable of clearing a secondary infection with *Pneumocystis* following $CD4^+$ T cell depletion. While trophic forms are sufficient for initiation of adaptive immune responses in immunocompetent mice, infection of immunocompromised $RAG2^{-/-}$ mice with trophic forms in the absence of cysts does not lead to the severe weight loss and infiltration of innate immune cells associated with the development of *Pneumocystis* pneumonia.

Dendritic cells screen the alveolar spaces for pathogens, and are in a prime position to initiate the immune response against lung pathogens, including *Pneumocystis*. Our data demonstrate that trophic forms broadly dampen the ability of dendritic cells to respond to pathogen-associated molecular patterns. Bone marrow-derived dendritic cells were stimulated with trophic forms, a mixture of trophic forms and cysts, and various

other inflammatory materials, including β-glucan. Trophic forms inhibited multiple components involved in antigen presentation by dendritic cells, including secretion of inflammatory cytokines and expression of MHC class II and costimulatory molecules on the cell surface. Furthermore, trophic forms suppressed or failed to induce the expression of multiple genes related to activation and maturation in dendritic cells. Dendritic cells silenced by trophic forms are unable to induce $CD4^+$ T cell responses. These data suggest that immune evasion by trophic forms is dependent on the suppression of innate responses, and the development of adaptive immunity represents a "point of no return" at which the trophic forms are no longer able to escape clearance.

KEYWORDS: *Pneumocystis*, fungal infection, dendritic cells, antigen presentation, immune evasion

Multimedia Elements Used: TIFF (.tiff)

Heather Evans
Student

September 20, 2017
Date

IMMUNE EVASION BY DIVISION OF LABOR:
THE TROPHIC LIFE CYCLE STAGE OF *PNEUMOCYSTIS MURINA* SUPPRESSES
INNATE IMMUNITY TO THIS OPPORTUNISTIC, FUNGAL PATHOGEN

By

Heather Marie Evans

Dr. Beth Garvy
Director of Dissertation

Dr. Ken Fields
Director of Graduate Studies

September 20, 2017
Date

This work is dedicated to my grandparents,

Raphael and Lois O'Daniel.

ACKNOWLEDGMENTS

I would like to express the deepest appreciation to my dissertation advisor, Dr. Beth A Garvy, for her persistent guidance, support, and patience. I thank the members of my dissertation committee, Drs. Don Cohen, Anthony Sinai, Sarah D'Orazio, and Nancy Webb, as well as our outside examiner, Dr. Thomas Chambers. In addition, I have greatly appreciated the mentorship provided by the various members of the MIMG department, especially Dr. Carol Pickett.

I would also like to thank current and former members of the lab: Melissa Hollifield, Luke Heil, and Drs. Cate Robbins, Samantha Oliphant, and Zhan Ye. I also thank the excellent undergraduate students that I have had the opportunity to work alongside in this project, especially Andrew Simpson, Grady Bryant III, and Nick Federico.

Finally, I am forever grateful for the love and support of my friends and family. I am especially thankful for the network of loved ones who entertained my daughter, Claire, as I completed this project.

TABLE OF CONTENTS

TABLE OF FIGURES

Chapter 1: Introduction

I. Overview

   Pneumocystis species are opportunistic fungal pathogens that cause severe pneumonia in immunocompromised hosts, including HIV/AIDS patients. Clearance of *Pneumocystis* organisms is dependent on effective $CD4^+$ T cell, B cell and macrophage responses (1-4). Failure to clear *Pneumocystis* organisms leads to severe alveolar damage due to an exaggerated inflammatory immune response (5). In spite of a reduced incidence of *Pneumocystis* pneumonia (PcP) in HIV-infected individuals due to improved highly active antiretroviral therapy (HAART), the mortality rate for patients with PcP has not improved (6). Additional studies are required to inform novel approaches to reduce morbidity and mortality due to *Pneumocystis* pneumonia.

   Outbreaks of PcP were first described in malnourished or premature infants in orphanages following the second world war (7). Evidence suggests that immunocompetent individuals of all ages are capable of mounting protective immune responses to *Pneumocystis jirovecii* that prevent progression to pneumonia. Most children encounter this opportunistic fungus at a young age, as indicated by the presence of specific antibodies in the serum of 85% of individuals by three years of age (8). Previous work from our lab has shown that the neonatal mouse immune response to *Pneumocystis murina* is delayed due in part to an anti-inflammatory lung environment (9-12). The neonatal lung environment is characterized by anti-inflammatory mediators, including transforming growth factor beta 1 (TGF-β1) and interleukin-10 (IL-10), and immature immune cells (9-12). Neonatal alveolar macrophages and T cells adoptively transferred to

1

an adult lung environment are competent to resolve *P. murina* pneumonia in mice (9, 12). In addition, neonatal alveolar macrophages are deficient in nuclear factor kappa B (NF-κB) translocation following stimulation with *Pneumocystis* organisms (9). Neonatal alveolar CD11c$^+$ cells demonstrate delayed trafficking to the draining lymph nodes (11). Together, these data indicate that both the neonatal lung environment and intrinsic immune cell deficits contribute to the delayed clearance of *P. murina* in neonatal mice.

Pneumocystis species have a biphasic life cycle (**Fig 1.1 and Fig 1.2**). Trophic forms are proposed to undergo asexual reproduction, whereas cysts are formed by sexual reproduction (13). Trophic forms are single-nucleated organisms that are typically found in clusters surrounded by a biofilm-like substance consisting of a conglomeration of DNA, β-glucan, and other sugars (14). Cysts are ascus-like structures that consist of multiple nuclei surrounded by a fungal cell wall. β-1,3 glucan and β-1,6 glucan serve as the structural components of the cyst wall (15, 16). β-glucan is not detected on the surface of trophic forms (15, 17). Both stages express surface glycoproteins and mannoproteins that may serve as pathogen-associated molecular patterns (PAMPs) that could interact with receptors on phagocytic cells (18-20). Neither life form produces the classical fungal components ergosterol, chitin or α-glucans (21, 22).

Dendritic cells are the principal antigen presenting cells in the lung. However, their role in initiating the adaptive response to *Pneumocystis* species has been understudied. Previous work has demonstrated that dendritic cells respond to β-glucans derived from the *Pneumocystis* cell wall (23). Dendritic cells activated by *Pneumocystis* cell wall-derived β-glucans increase costimulatory molecule expression and drive T cell polarization towards a T helper 1 (T$_h$1) -type response, as characterized by the production

of the proinflammatory cytokine interferon gamma (IFNγ) (23). The mechanism for dendritic cell recognition of *Pneumocystis* trophic forms, which do not express β-glucans, is unknown.

An improved understanding of innate immune interactions with the cystic and trophic life cycle stages has the potential to inform future treatment of *Pneumocystis* pneumonia. Recently, it was reported that treatment of mice with the β-1,3-D-glucan synthase inhibitor anidulafungin resulted in depletion of *P. murina* cysts (24). The mice were able to control the remaining trophic burden in the absence of an excessive inflammatory response, however, the details of how trophic forms are recognized and cleared are not known.

This dissertation examines the role of the life cycle stages of *P. murina* in shaping the immune response to this fungal pathogen. The work herein demonstrates that infection with the cyst stage provokes proinflammatory immune responses, including the early recruitment of innate and effector immune cells into the lungs. Conversely, the trophic life cycle stage inhibits critical components of the dendritic cell response to infection, including cytokine expression, proinflammatory signaling, and antigen presentation. The rapid establishment of a trophic population may be critical for this fungal pathogen to avoid preemptive clearance of the transmitted cyst stage.

II. Populations at risk

Severely immunocompromised patients are at risk for *Pneumocystis* infection that progresses to pneumonia. The history of *Pneumocystis* is closely tied to the expansion of susceptible populations in the past century. Early observations by Carlos Chagas in 1909

and by Antonio Carini in 1910 identified the cyst stage of *Pneumocystis* in association with *Trypanosoma* species ((25, 26), reviewed in (27)). The organisms were recognized as a separate species, *Pneumocystis carini*, by Pierre and Mme Delanoë in 1912 (27, 28). However, *Pneumocystis* was not associated with human disease until 1942, when M.G. van der Meer and S.L. Brug identified the organism in two infants and one young adult (27, 29). In 1951, Josef Vanek demonstrated that *Pneumocystis* was the causative agent of an epidemic of interstitial plasma cell pneumonia in preterm or malnourished infants in orphanages (27, 30). Otto Jírovec reported additional cases of PcP in neonates in 1952 (27, 31). Sporadic reports of PcP followed, including a handful of cases in the United States in the 1950s (7). The disease was most commonly associated with premature, malnourished, or otherwise immunocompromised infants 6 weeks to 4 months of age (7).

The development of chemotherapy and immunosuppressive drug treatments expanded the populations at risk for PcP. Long-term cortisone therapy has been reported in association with PcP since the 1960s (32). A report from 1968 in which an adult male who had received radiotherapy, cytotoxic agents, and steroids for chronic lymphatic leukemia was diagnosed with PcP illustrates the potential complexity of such cases (33). Early surveys of infection in bone marrow transplant patients identified *Pneumocystis* as an organism of concern (34).

Pneumocystis continued to be a sporadic cause of disease in severely immunocompromised patients through the 1970s. However, in the early 1980s, an increase in the incidence of PcP in young, homosexual men alarmed the medical community (35). The HIV/AIDS epidemic resulted in a new pool of immunocompromised patients susceptible to PcP. The development of HAART has

significantly reduced the incidence of PcP in HIV patients. A dramatic 80% reduction in the incidence of PcP among HIV/AIDS patients in the United States and Canada was observed from 2004 to 2010 (36). These improvements are attributed to improved management of HIV/AIDS with HAART, including improved CD4$^+$ T cell counts and lower viral titer (36). Despite improved management of HIV/AIDS, *P. jirovecii* remains the most common opportunistic infection associated with the disease (36). The risk remains significant among individuals who are unaware of their HIV-positive status or lack access to HAART (36).

The development of novel immunosuppressive therapies continues to expand the range of populations at risk for PcP. The rise of the use of biologics in the treatment of cancer and autoimmune disease has been associated with increased risk of PcP. Examples include anti-CD20 antibody therapy for non-Hodgkin's lymphoma (37, 38), and anti-tumor necrosis factor alpha (TNFα) antibody therapy for rheumatoid arthritis (39) or Crohn's disease (40).

P. jirovecii may serve as a co-factor in other diseases. Colonization has been correlated with chronic obstructive pulmonary disease (COPD) (41, 42). It has been proposed that *Pneumocystis* may fuel lung inflammation, including recruitment of T_h1 T cells (43), and promote the progression of COPD (44). The presence of *Pneumocystis* organisms has also been correlated with sudden infant death syndrome (SIDS) in some studies (45, 46). However, the correlation does not appear to be absolute, and it is unlikely that *P. jirovecii* is a direct cause of SIDS (47). Rather, colonization may contribute to SIDS by promoting excess mucus production in the lungs of infants (48).

Mortality due to PcP may range from as low as 10-20% in mild-to-moderate cases (49) to 65% in patients requiring artificial ventilation (50). Factors associated with death due to PcP include older age of the patient, time to diagnosis, and the need for oxygen therapy or invasive mechanical ventilation (51). The death rate in patients with AIDS diagnosis or solid organ transplant is lower than that of patients with other immune deficiencies (51). This may be partially attributed to a decreased time to diagnosis in these patients (51).

III. *Pneumocystis* biology

Pneumocystis species are members of the fungal phylum *Ascomycota*. The genus was originally described as a single species, *Pneumocystis carinii*. However, the discovery that individual host species were infected with unique species of *Pneumocystis* promoted changes in the taxonomy (52). The name *Pneumocystis carinii* is now reserved for one of the two species that infects rats. The human pathogen was renamed *Pneumocystis jirovecii*, while the species that infects mice was named *Pneumocystis murina* (52-54). Additional *Pneumocystis* species have been identified in host species as diverse as rabbits (*P. oryctolagi*), dogs, horses, bats, and chickens (55-59). While a single host species may be infected with multiple species of *Pneumocystis* (see *P. carinii* and *P. wakefieldiae* in rats), a given *Pneumocystis* species does not infect multiple host species (60, 61).

The factors that determine the strict host restrictions of *Pneumocystis* species are unknown. However, recent genome analysis of *P. jirovecii*, *P. carinii*, and *P. murina* suggest that these species evolved in close association with their respective hosts (21).

The sizes of the genomes were remarkably reduced compared to other extracellular fungi, with notable losses in ribosomal RNA genes, transcription factors, nutrient transporters, and metabolic pathways. Conversely, the number of genes encoding peptidases is expanded in *Pneumocystis* species compared to related fungi, and the genes encoding proteins related to endocytosis and the proteasome are preserved. These data suggest that *Pneumocystis* species have made significant adaptations to acquire nutrients from their respective hosts.

   Pneumocystis species have a biphasic life cycle consisting of trophic forms and cysts (**Fig 1.1**, **Fig 1.2** and reviewed in (62)). The trophic forms were formerly known as trophozoites, with the newer name reflecting their fungal, rather than protozoan identity. Trophic forms are single-nucleated organisms that may replicate asexually by binary fission. Trophic forms are also proposed to undergo conjugation to form a diploid pre-cyst (or sporocyte), which then undergoes multiple rounds of sexual reproduction to form the cyst life cycle stage. Comparative genomics suggest sexual reproduction in *Pneumocystis* involves a single mating type (primary homothallism) rather that multiple mating types (heterothallism) or mating type switching (secondary homothallism) (63).

   Trophic forms may be found in clusters surrounded by a biofilm-like substance consisting of a conglomeration of DNA, β-glucan, and other sugars (14). It has been proposed that previously-lysed cysts provided the bulk of this biofilm-like substance. Trophic forms lack a fungal cell wall, and do not express β-glucan (15). Ultrastructural studies revealed that the trophic forms tightly adhere to the luminal surface of alveolar epithelial cells via microprotusions or invaginations of the trophic plasma membrane (64). Attachment is mediated by host cell fibronectin and other extracellular matrix

components, and does not involve fusion of host-*Pneumocystis* cell membranes or invasion of the host cell (64-66).

The cyst stage of the species is more properly termed an ascus; however, this nomenclature is not yet the norm within the field. A mature cyst contains eight daughter spores, which are believed to develop into trophic forms upon lysis of the cysts. The cyst is surrounded by a fungal cell wall, with β-1,3 glucan and β-1,6 glucan serving as the major structural components (15, 16). Recent evidence indicates that cysts are the transmittable life cycle stage of *Pneumocystis* species (17).

Both the trophic forms and cysts express surface glycoproteins and mannoproteins that may serve as PAMPs that could interact with receptors on phagocytic cells (18-20). Ten antigenic glycoproteins common to both lifeforms were identified in the cell wall fractions of *P. carinii* trophic forms and cysts separated by counterflow centrifugal elutriation and sequential microfiltration (20). Gas chromatography-mass spectrometry (GC-MS) demonstrated that all ten glycoproteins contained some degree of mannose, glucose, galactose, and N-acetylglucosamine (GlcNAc), while some contained traces of fucose. As a whole, the glycoproteins on the cysts contained more mannose, while the trophic glycoproteins contained more xylose.

Neither life cycle stage produces the classical fungal components ergosterol, chitin or α-glucans (21, 22). While capable of *de novo* cholesterol synthesis, *Pneumocystis* species also use cholesterol scavenged from the host cell (67). It has recently been demonstrated that *Pneumocystis* species lack the enzymes required for the addition of outer chain N-mannans to the N- and O-linked glycan core structure (21). Tandem mass spectrometry confirmed that *Pneumocystis* cell wall proteins were glycosylated with

chains of mannose no longer than nine residues, with the majority comprised of six residues (21). Hyper-mannosylation is required for optimal C-type lectin receptor recognition of *C. albicans,* prompting Ma, et al. to propose that the lack of outer chain N-mannans may permit *Pneumocystis* organisms to escape detection by the immune system (21, 68, 69).

Transmission of *Pneumocystis* species occurs by the airborne route (70). It was initially hypothesized that suppression of the immune system would permit reactivation of a latent, subclinical infection in previously healthy adults. However, more recent evidence suggests that transient, subclinical infections in healthy hosts serve as a reservoir for *Pneumocystis* organisms that may be transmitted to susceptible immunocompromised hosts. Immunocompetent adult mice cohoused with *P. murina*-infected severe combined immunodeficiency (SCID) mice develop a subclinical infection that resolves in 5 to 6 weeks (71). Studies in mice infected with *P. murina* demonstrated that a healthy host may transmit the organisms to both healthy and immunocompromised hosts (72-74).

Clusters of PcP cases have been observed in both inpatient and outpatient facilities caring for immunocompromised patients. Several studies suggest nosocomial transmission of *P. jirovecii* in outbreaks of PcP in kidney transplant recipients (reviewed in (75)). Such outbreaks were often caused by a predominant or a single *Pneumocystis* strain, as confirmed by genotyping by comparison of the internal transcribed spacer (ITS) regions 1 and 2 or by multilocus sequence typing (MLST). The genotypes of reference samples were different that the strains associated with such outbreaks. One such cluster was identified at a nephrology outpatient clinic in which transplant patients shared a

common waiting room, suggesting that minimal patient-to-patient contact is sufficient for transmission (76).

Exposure to *P. jirovecii* appears to be extremely common, with the first encounter occurring early in life. In a study of 74 healthy Chilean infants, *P. jirovecii* DNA was detected in the nasopharyngeal aspirates of 32% of the participants, and seroconversion developed in 85% of the infants by 20 months of age (77). Genotyping of *P. jirovecii* has demonstrated that the organisms may be transmitted from healthy, colonized caretakers to infants (78). Such evidence suggests that healthy hosts may serve as an infectious reservoir in the community. An environmental reservoir has not yet been identified. The severely constricted genome of *Pneumocystis*, as well as the lack of interspecies transmission, suggest that replication of *P. jirovecii* outside of the human host is unlikely.

IV. Treatment of *Pneumocystis jirovecii* infection

The first choice treatment for PcP is trimethoprim-sulphamethoxazole (TMP-SMX) (79, 80). Unfortunately, allergic responses to the sulfa component or other adverse effects may demand the use of alternative therapies (80). Pentamidine is a second-line therapy for severe PcP, but may also have serious side effects, including nephrotoxicity. Clindamycin in combination with primaquine or trimethoprim with dapsone are used as alternative therapies in patients who are unable to tolerate TMP-SMX and/or pentamidine (79). Atovaquone may also be used to treat less severe cases of PcP (79). Corticosteroids are given in addition to antifungals to reduce the damage due to lung inflammation in moderate to severe cases of PcP (79). *Pneumocystis* species do not produce ergosterols,

therefore, drugs that interfere with ergosterol synthesis, including azole antifungals, are not effective (22).

Prophylaxis for PcP is recommended for HIV/AIDS patients with fewer than 200 CD4$^+$ T cells/µL or patients with oropharyngeal candidiasis (20, 80). TMP-SMX is the preferred prophylactic agent for PcP, and provides additional protection against toxoplasmosis and certain bacterial infections (80, 81). Dapsone or atovaquone may be used in patients who are unable to tolerate TMP-SMX, including those with sulfa allergy (20, 80). Prophylaxis may be discontinued in patients receiving HAART if their viral load is below the limit of detection and their CD4$^+$ T cell count is greater than 200 cells/µL for more than three months (80). Prophylaxis is also recommended for certain patients with cancer (including acute lymphocytic leukemia), patients with certain primary immunodeficiency, patients undergoing prolonged or strong glucocorticoid usage, and patients undergoing solid organ transplant or hematopoietic stem cell transplant (82).

Recently, it was reported that treatment of immune-reconstituted mice with the β-1,3-D-glucan synthase inhibitor anidulafungin results in depletion of *Pneumocystis murina* cysts, and the remaining trophic burden stimulate a much reduced inflammatory response (24). Anidulafungin belongs to a drug class known as the echinocandins, which have been used in combination with other antifungals, including TMP-SMX, in the treatment of PcP in human patients (83). Linke et al., propose that depletion of *Pneumocystis* cysts by echinocandins would reduce inflammation-induced lung damage in patients, especially in patients undergoing immune-reconstitution syndrome (24).

V. Host response to *Pneumocystis*

    A. Immune response in immunocompetent hosts

       The diverse range of immunocompromised states associated with the development of PcP illustrate the range of immune processes that are critical for the clearance of *Pneumocystis*. The clearance of the normal mixture of *Pneumocystis* organisms (i.e., trophic forms and cysts) from the lungs requires the participation of innate and adaptive immune cells, including macrophages, $CD4^+$ T cells, and B cells (1-4). The alveolar epithelium provides a thin barrier for gas exchange between the lung alveoli and lung capillaries. The lung immune response to infection must be carefully controlled to avoid excessive thickening of the epithelium due to inflammation, edema, and recruitment of immune cells.

       i. Dendritic cells

       Dendritic cells are the principal antigen presenting cells in the lung, and are critical for optimal B cell and T cell activation in response to pathogens (reviewed in (84)). Immature lung dendritic cells reside in the alveolar interstitium, where they project their dendritic extensions through the epithelial-tight junctions into the alveolar spaces. Encounters with antigen promote a complex maturation process that prepares the dendritic cell to serve as an antigen-presenting cell. Unlike macrophages, which remain in the periphery in response to infection, activated dendritic cells migrate to the draining lymph nodes to present antigen to lymphocytes. The involvement of dendritic cells is critical to the recruitment of T and B cells into the airway lumen, particularly as these spaces are largely free of lymphocytes prior to infection.

While the interaction between dendritic cells and *Pneumocystis* organisms has been understudied, the scarce pertinent publications suggest a complex and unusual relationship. Macagno et al. found that human monocyte-derived dendritic cells stimulated *in vitro* with a ratio of two *P. carinii* organisms per DC failed to increase surface expression of the activation marker CD83, and only minimally increased expression of MHC class II, CD40, CD80 and CD86 compared to cells stimulated with lipopolysaccharide (LPS) (85). However, the authors suggest that the DCs were sensitive to *P. carinii*, as they observed aggregation of the DCs during co-culture. These data prompted the authors to speculate that *Pneumocystis* organisms may actively suppress the maturation process of DCs, and other host-derived factors, particularly cytokines, may be critical for the activation of DCs during infection.

Kobayashi et al. demonstrated that phagocytosis of a mixed population of *P. murina* organisms by murine bone marrow-derived dendritic cells (BMDCs) was partially inhibited by the addition of mannan, implying that mannose-binding C-type lectin receptors such as mannose receptor or dectin-2 may recognize *Pneumocystis* organisms (86). Co-culture of murine BMDCs with a ratio of 10 *P. murina* organisms per BMDC failed to induce various markers of activation, including production of proinflammatory cytokines (IL-12p40, TNFα, IL-6) and surface expression of major histocompatibility (MHC) class II, CD40, CD54, CD80, and CD86 (86). *P. murina*-pulsed BMDCs were sufficient to induce *P. murina*-specific proliferation of CD4$^+$ T cells *in vitro* (86). For this experiment, Zheng *et al.* employed CD4$^+$ T cells isolated from the spleens of mice treated 3 days prior with *P. murina*-pulsed BMDCs (86). Likewise, *P. murina*-pulsed BMDCs promoted production of *P. murina*-specific immunoglobulin G (IgG) *in vivo* (86, 87).

13

Despite suboptimal activation, dendritic cells stimulated with a mixture of *P. murina* trophic forms and cysts appear to serve as effective antigen-presenting cells to CD4$^+$ T cells and B cells.

While stimulation with a mixed population of intact *Pneumocystis* organisms appears to poorly stimulate dendritic cell responses, Carmona et al. demonstrated that human dendritic cells respond strongly to β-glucans derived from the *Pneumocystis* cyst cell wall (23, 88). DCs activated by cyst cell wall-derived β-glucans display increased costimulatory molecule expression (CD40, CD80, CD86) and drive T cell polarization towards a T_h1/T_h17-type response (23, 88). In addition, the DCs express CCR7, a chemokine receptor that directs migration to the draining lymph nodes (23). Intriguingly, human dendritic cells stimulated with *Pneumocystis* β-glucans produce the proinflammatory cytokines TNFα and IL-1β (23). The mechanism for dendritic cell recognition of *Pneumocystis* trophic forms, which do not express β-glucans, is unknown.

ii. Macrophages

Alveolar macrophages are the primary phagocyte involved in the clearance of *Pneumocystis* organisms. Alveolar macrophages bind *Pneumocystis* organisms *in vitro*, and traffic the fungi to the phagolysosomes for degradation (2, 89-91). Alveolar macrophages phagocytose *Pneumocystis* organisms using pattern recognition receptors (PRRs) including mannose receptor and the β-glucan receptor dectin-1(92, 93). Opsonized organisms may be also be phagocytosed by the receptors FcγRII and FcγRIII (93).

The role of reactive oxygen species in the killing of *Pneumocystis* organisms is unclear. Rat alveolar macrophages stimulated with *P. carinii* release NO_2^- and H_2O_2 *in vitro* (94, 95). H_2O_2 appears to be partially responsible for the killing of *Pneumocystis* within the phagosome (93). However, *Pneumocystis* organisms may have mechanisms for evasion of direct killing by reactive oxygen species, as stimulation with the fungus impairs the dimerization (and thus the activation) of iNOS (96).

In addition to direct killing of *Pneumocystis* organisms, alveolar macrophages also contribute to the inflammatory environment of the lungs by releasing proinflammatory cytokines to promote adaptive responses. Recognition of *Pneumocystis* organisms by human alveolar macrophages triggers the production of proinflammatory cytokines associated with classically activated macrophages, including IL-1β, IL-6, IL-8 and TNF-α (97, 98). However, a proportion of macrophages in the lungs of mice infected with *P. murina* display characteristics of alternatively activated cells, including increased expression of mannose receptor, CD23, CCR7, and arginase (99). Polarization of macrophages towards the alternatively activated phenotype results in improved clearance of *Pneumocystis* organisms and decreased immunopathogenesis (100, 101).

Alveolar macrophages are not sufficient for clearance of *Pneumocystis* in the absence of T helper cells (102). Intriguingly, *Pneumocystis* infection promotes expression of reactive oxygen species and the proinflammatory cytokines interferon gamma (IFNγ), TNFα, and IL-12 in the lungs of T cell-deficient mice (102). This suggests that alveolar macrophages may be dependent on additional cues from CD4^{+} T cells to mediate clearance of *Pneumocystis*.

iii. Alveolar epithelial cells

Alveolar epithelial cells, or pneumocytes, compose a thin barrier between the alveolar lumen and lung capillaries. The integrity of this barrier is essential to effective gas exchange. *Pneumocystis* trophic forms bind intimately to type I alveolar epithelial cells (64). This interaction is a risky endeavor for the trophic forms, as alveolar epithelial cells are capable of producing proinflammatory cytokines. Rat alveolar epithelial cells stimulated with *Pneumocystis* cell wall β-glucans produce macrophage inflammatory protein-2 (MIP2) and TNFα (103-105). Alveolar epithelial cells do not express the β-glucan receptor dectin-1. Rather, the production of cytokines in response to *Pneumocystis* β-glucan is dependent on NF-κB-dependent signaling pathways initiated by glycosphingolipids (105). Further work demonstrated that human airway epithelial cells stimulated with *Pneumocystis* cell wall β-glucans produce IL-8 in glycosphingolipid-dependent mechanism triggered by an increase in calcium influx (106).

Stimulation of human alveolar epithelial cells with mixed *Pneumocystis* organisms also induces expression of the proinflammatory cytokine IL-6 (107). Surprisingly, pre-incubation of the cells with IL-6 promoted the production of fibronectin, and led to increased *Pneumocystis* attachment (107). These data suggest that trophic forms may manipulate the immune response with alveolar epithelial cells to promote fungal growth.

iv. T lymphocytes

The susceptibility of HIV/AIDS patients to PcP highlights the critical role of CD4^{+} T cells in the immune response to this fungus. A CD4^{+} T cell count below 200 cells/µl is associated with an increased risk for PcP in this population (20). Transfer of CD4^{+} T cells

from *P. murina* infected immunocompetent mice into SCID mice is sufficient to mediate clearance of infection (108). Effective costimulation of CD4^{+} T cells is required for control of *Pneumocystis* infection, as loss of CD40 ligand or the costimulatory receptor CD28 results in acute infection in mice (109, 110). While Th17 responses are critical for control of many fungal infections, including candidemia, a mixed T helper response is observed in response to *Pneumocystis* infection. This mixed response appears to be largely redundant, as T_h1-, T_h2-, and T_h17-type responses have all been associated with clearance of *P. murina* organisms (24, 111-115).

The role of CD8^{+} T cells in the response to *Pneumocystis* is less clear. In the immune reconstitution model, depletion of CD8^{+} T cells did not hinder clearance of *Pneumocystis* infection, but instead led to a prolonged CD4^{+} T cell response with an increased frequency of T_h1 CD4^{+} T cells compared to the untreated, infected controls (116). In contrast, transfer of CD8^{+} T cells from *P. murina* infected immunocompetent mice into immunocompromised mice led to increased lung damage rather than control of infection (116, 117). These negative inflammatory effects are associated with CD8^{+} T cell-dependent TNFα-mediated effects on lung parenchyma cells (117, 118). In contrast, IFNγ production by CD8^{+} T cells is associated with protective responses against *Pneumocystis* (119). While CD8^{+} T cells are not normally sufficient to mediate clearance of infection, overexpression of IFNγ in the lungs of mice depleted of CD4^{+} T cells led to clearance of *P. murina* organisms and increased proliferation of IFNγ-expressing CD8^{+} T cells (119).

v. B lymphocytes

B cells are required for the clearance of *Pneumocystis* organisms (3, 4). B cells are capable of playing multiple roles within the immune response, including antigen-presentation to T cells and production of antibody and proinflammatory cytokines. The immune response to *Pneumocystis* incorporates each of these functions to a varying degree of importance.

Antibody-mediated opsonization enhances phagocytosis of *Pneumocystis* organisms by alveolar macrophages, and mediates clearance of *Pneumocystis* organisms *in vivo* (3, 93, 112, 120). Clearance is delayed in the absence of antibody class switching, indicating that *P. murina*-specific IgG enhances, but is not required for, control of *Pneumocystis* infection (3). In the absence of CD4$^+$ T cells, a memory humoral response is sufficient to clear *Pneumocystis* organisms during a secondary infection (121, 122). This response requires the participation of CD8$^+$ T cells and alveolar macrophages, which phagocytose antibody-coated organisms (122). *P. murina*-specific antibody composed of isotypes produced by either T$_h$1- or T$_h$2-like responses are sufficient for mediating clearance of secondary infection (IgG1 or IgG2a/IgG2b/IgG3, respectively) (112).

B cells are required for the generation of protective effector and memory CD4$^+$ T cell responses to *Pneumocystis* (3, 123, 124). B cells expressing both MHC class II and *Pneumocystis*-specific B cell receptor are required for effective priming of CD4$^+$ T cells and clearance of *Pneumocystis* infection (123, 124). Production of TNFα by B cells in the draining lymph nodes is essential for CD4$^+$ T cell expansion and clearance of *P. murina,* and anti-TNFα therapy for rheumatoid arthritis and Crohn's disease is associated with an increased risk for PcP (39, 40, 125).

It has recently become apparent that B cells participate in the suppression of systemic inflammation due to *Pneumocystis* infection in the lungs (126). In the absence of type I interferon signaling and B cells, systemic inflammation due to *Pneumocystis* infection in the lungs leads to bone marrow failure due to increased turnover of maturing cells and decreased bone marrow progenitor function (126). The protective contribution of B cells is mediated in part by the expression of IL-10 and IL-27 (126). Increased systemic inflammation and bone marrow dysfunction has been observed in patients with chronic pulmonary diseases and HIV/AIDS (127-130). Hoyt et al propose that *Pneumocystis* infection may be a comorbidity factor for damage due to systemic inflammation in these patients, particularly as these populations are at an increased risk for PcP (126).

vi. Summary of protective responses in immunocompetent hosts

Dendritic cells, macrophages, and alveolar epithelial cells serve as early sentinels of *Pneumocystis* infection. Upon encountering antigen, dendritic cells undergo maturation and travel to the draining lymph nodes to present antigen to lymphocytes. CD4$^+$ T cells and B cells are recruited to the lungs, where they may serve as helper cells that direct the killing of *Pneumocystis* by other immune cells, including macrophages. However, the exact mechanisms of macrophage killing of *Pneumocystis* organisms are unclear.

B. Neonatal response to *Pneumocystis*

While malnourished, premature, or otherwise immunocompromised infants are at risk for PcP, evidence suggests that immunocompetent individuals of all ages are capable

of mounting protective immune responses to *Pneumocystis jirovecii*. However, the neonatal immune response to *Pneumocystis* is delayed during the first three weeks of infection (9-12).

The delayed clearance of *P. murina* in neonatal mice may be partially attributed to the tolerogenic phenotype of the neonatal lung. The neonatal lung environment is characterized by decreased expression of granulocyte-macrophage colony-stimulating factor (GM-CSF) and increased expression of anti-inflammatory mediators, including TGF-β-1 and IL-10, and immature immune cells (9-12, 131). Neonatal alveolar macrophages and T cells adoptively transferred into the immunogenic environment of adult lungs are competent to resolve *P. murina* infection without delayed kinetics (9, 12). Treatment of neonatal mice with exogenous GM-CSF and IL-4 promotes enhanced clearance of *Pneumocystis* organisms amidst increased expression of proinflammatory cytokines in the lungs (131).

The immature phenotype of neonatal immune cells also contributes to delayed immune responses to *Pneumocystis* infection compared to adults. *Ex vivo* experiments demonstrate that neonatal alveolar macrophages are deficient in NF-κB translocation following stimulation with *Pneumocystis* organisms (9). In addition, neonatal alveolar CD11c^{+} cells demonstrate delayed trafficking to the draining lymph nodes (11). Together, these data indicate that both the neonatal lung environment and intrinsic immune cell deficits contribute to the delayed clearance of *P. murina* in neonatal mice.

C. Immunopathogenesis due to *Pneumocystis*

Pneumocystis infection causes asymptomatic or subclinical infections in healthy hosts. The severely reduced genome of *Pneumocystis* species and the lack of an environmental reservoir strongly suggest that the organisms have evolved to live as obligate commensals within the healthy host (21).

It is possible that *Pneumocystis* organisms contribute to mild damage to the structure of the alveoli, as binding of *Pneumocystis carinii* organisms to type I alveolar epithelial cells leads to cell necrosis and increased permeability of the alveolar-capillary membrane (132). However, the bulk of the lung damage that occurs during PcP is associated with rampant, non-productive inflammation in immunocompromised hosts (133, 134). Severe lung damage during PcP is more closely correlated with inflammation and increased recruitment and proliferation of immune cells within the lungs, rather than the fungal burden (5, 134, 135). The recruitment of neutrophils is correlated with a poor prognosis in humans with PcP (134, 136, 137), but animal studies suggest neither neutrophils nor reactive oxygen species directly cause lung damage (138). Rather, damage appears to be strongly related to the adaptive immune response, especially CD8$^+$ T cells (134, 135). Respiratory impairment is attributed to direct damage to the alveoli, as well as impaired gas exchange due to accumulation of immune cells in the alveolar spaces. Fungal growth can contribute to impaired gas exchange in the later stages of PcP, especially in mice that lack adaptive immune cells (139).

Myeloid-derived suppressor cells (MDSCs) accumulate in the alveolar spaces of immunocompromised mice and rats with PcP (140). Recent evidence suggests that MDSCs may contribute to pathogenesis and impede fungal clearance by suppressing key

effector cells. MDSCs isolated from the lungs of immunocompromised rodents with PcP suppress CD4$^+$ T cell proliferation *ex vivo* (140). Alveolar macrophages co-cultured with MDSCs from mice with PcP exhibited reduced phagocytic capacity (141). In addition, MDSCs may directly contribute to lung injury, as adoptive transfer of MDSCs from rodents with PcP to healthy hosts resulted in increased lung albumin and lactate dehydrogenase (LDH) (140).

The restoration of the immune system in previously immunocompromised patients increases the risk for lung damage due to PcP. Bone marrow transplant patients are at increased risk for PcP following engraftment and the restoration of the inflammatory capacity of immune cells (142). Initiation of HAART in HIV/AIDs patients may provoke an overexuberant return of inflammatory responses, known as immune reconstitution inflammatory syndrome (IRIS). IRIS increases the risk for lung damage associated with PcP, and is associated with a population of rapidly expanding CD8$^+$ T cells (135). Corticosteroids are given in addition to antifungals to reduce the damage due to lung inflammation in moderate to severe cases of PcP (79).

D. Recognition of fungal pathogens by the immune system

i. Role of PRR and PAMPs in fungal immunity

Pattern recognition receptors (PRRs) expressed by cells of the innate immune system are responsible for detecting pathogen-associated molecular patterns (PAMPs) and initiating anti-microbial mechanisms including phagocytosis, production of reactive oxygen species, and the release of inflammatory cytokines. Conserved fungal cell wall PAMPs include β-glucans, α-glucans, chitin, and mannoproteins. The major classes of

pattern recognition receptors involved in recognition of fungal pathogens include the toll-like receptors (TLR), the C-type lectin receptors (CLR), and Nod-like receptors (NLR) (143). Toll-like receptors are type I transmembrane proteins with cytosolic Toll-IL-1 receptor (TIR) domains that trigger downstream signaling cascades (144). TLR1, TLR2, TLR4 and TLR6 are commonly implicated in the response to fungal pathogens, including *Candida albicans, Aspergillus fumigatus,* and *Cryptococcus neoformans* (145).

CLRs are transmembrane proteins with at least one C-type lectin-like domain capable of binding carbohydrate (144). Dectin-1 is a CLR expressed on macrophages and dendritic cells that is highly specific for β-1,3-glucans (146, 147). The cytoplasmic tail of dectin-1 contains a single tyrosine-based activation-like motif, or "hemi-ITAM" (148). Activation of dectin-1 triggers phagocytosis and Syk-and CARD9/Bcl10/MALT1-dependent signaling cascade resulting in production of reactive oxygen species (ROS), the NF-κB- or NFAT-mediated production of inflammatory cytokines, and the upregulation of costimulatory molecules on dendritic cells (149). β-glucan has been shown to stimulate NLRP3 inflammasome-mediated production of the inflammatory cytokine IL-1β (26). These responses promote the polarization of T_h1 and T_h17 cells, the effector responses of cytotoxic $CD8^+$ T cells, and antibody production (149, 150). Other C-type lectin receptors that may play a role in fungal immunity by targeting mannose, fucose, glycolipids or chitin include mannose receptor, DC-SIGN, SIGNR1, SIGNR3, dectin-2, mincle, langerin, LSECtin, Mgl1, Mgl2, and DEC-205 (**Fig 1.3** and (151)).

ii. Synergistic interactions between PRR:

Synergistic interactions between pattern recognition receptors may further influence the initiation of the innate immune response. Dectin-1 and TLR2 are recruited to phagosomes containing unopsonized zymosan, a *Saccharomyces cerevisiae* cell wall preparation consisting of β-glucans, mannans, mannoproteins and chitin (147). TLR2 activation in the absence of dectin-1 is insufficient to induce phagocytosis or the production of ROS in response to zymosan, but does result in the production of inflammatory cytokines (147). Dectin-1 enhances TLR2-mediated production of inflammatory cytokines in response to zymosan by sustaining the degradation of IκB, which increases NF-κB nuclear translocation (147, 152). TLR2 activation does not play a direct role in the tyrosine phosphorylation of dectin-1, and direct physical contact between the receptors is not believed to occur (147). Both dectin-1-mediated Syk signaling and the TLR adaptor molecule MyD88 are required for this synergistic effect, suggesting that signal integration is responsible (152). Similar collaboration has been observed between dectin-1 and TLR4, TLR5, TLR7, and TLR9 (152).

Other pattern recognition receptors may collaborate to shape the innate immune response. For example, the association of dectin-1 with the carbohydrate binding receptor galectin-3 has been shown to enhance the TNF-α response to *Candida albicans* (153). Similarly, the association of dectin-1 with DC-SIGN, a C-type lectin receptor that binds mannose, enhances the pro-inflammatory arachidonic acid cascade in dendritic cells (154).

While dectin-1 is capable of binding soluble β-glucan, activation of downstream signaling is dependent on the recognition of immobilized, particulate β-glucan (147, 148).

This recognition causes dectin-1 to cluster in synapse-like structures that exclude regulatory tyrosine phosphatases CD45 and CD148 (148). This "phagocytic synapse" forms prior to internalization of particulate β-glucan and likely facilitates downstream signaling (148). It is not known whether other PRR are specifically clustered at the site of contact with particulate β-glucan, but the previously demonstrated physical association between dectin-1 and DC-SIGN or galectin-3 suggests that the formation of the synapse may facilitate homologous and heterologous receptor crosstalk (153, 154). Collaboration between PRRs may allow innate immune cells to differentiate between situations where a complex inflammatory response is warranted (i.e., a microbe expressing multiple PAMPs), and situations where tolerance is more ideal (i.e., inhalation of fungal allergens).

iii. Innate recognition of Pneumocystis:

The *Pneumocystis* cyst wall is predominately composed of β-1,3-glucan with side chains of β-1,6- and β-1,4-linked glucose residues (155). Dendritic cells have been shown to respond to β-glucans derived from the *P. carinii* cyst wall through dectin-1 (23). Dendritic cells activated by cyst wall-derived β-glucans increase costimulatory molecule expression and drive CD4$^+$ T cell activation towards a proinflammatory T_h1/T_h17 response in a dectin-1-dependent manner (23, 88).

The mechanism for dendritic cell recognition of the trophic life cycle stage, which expresses glycoproteins but not β-glucans, is unclear. Recently, treatment of rats with the β-1,3-D-glucan synthase inhibitor echinocandin resulted in depletion of *P. carinii* cysts

(24). The rats were able to clear the remaining trophic forms in the absence of an excessive inflammatory response.

TLR2 and the β-glucan receptor dectin-1 are required for the generation of an effective response to *Pneumocystis* (69, 156). This suggests that collaboration of TLR2 and dectin-1 may play a role in the induction of the robust response to *Pneumocystis* cysts. β-glucan derived from *Pneumocystis* promotes the formation of dectin-1-containing lipid rafts at plasma membrane of dendritic cells. Lipid rafts are glycosphingolipid-enriched microdomains that promote signaling via the clustering of receptors with ITAM domains. This rearrangement of the plasma membrane is likely analogous to the "phagocytic synapse" previously observed in macrophages (148). Glycosphingolipid cluster formation in human dendritic cells stimulated with cyst cell wall-derived β-glucan promotes classical NFκB activation and expression of the T_h17-type cytokine, IL-23 (88).

Other C-type lectin receptors may play a role in immunity to *Pneumocystis* by targeting mannose, fucose, or glycolipids (20, 151). Among these, mannose receptor has been the most rigorously studied in the context of *Pneumocystis* infection. Mannose receptor, a C-type lectin receptor with carbohydrate recognition domains capable of binding mannose, fucose and GlcNAc, binds the antigenic glycoprotein A (gpA, or major surface glycoprotein, MSG) on the cell wall of *Pneumocystis* organisms, triggering phagocytosis, ROS production, NFκB translocation, and production of IL-1, IL-6, IL-8, and TNF-α (92, 97, 98, 157).

iv. CLR-mediated suppression of immune responses

Recently, it has become evident that signaling via C-type lectin receptors is highly context-specific, and, in certain situations, engagement of C-type lectin receptors may lead to suppression of proinflammatory immune responses. This phenomenon may reflect the capacity of C-type lectin receptors to shape the balance between tolerance and inflammation based on the composition, density, and architecture of the ligand. For example, arabinogalactan isolated from the dust of traditional farms is protective against allergy responses. It was recently demonstrated that arabinogalactan interacts with mannose receptor and DC-SIGN on human dendritic cells and inhibits NF-κB activation following stimulation with the TLR4 ligand LPS (158). High-molecular-weight or complex β-glucans such as curdlan promote dectin-1-mediated proinflammatory signaling, while the low-molecular-weight, soluble glucan laminarin acts as an antagonist of dectin-1.

Recent evidence suggests that fungal pathogens may manipulate interactions with C-type lectin receptors to suppress proinflammatory responses. Engagement of the C-type lectin receptor mincle by the fungal skin pathogen *Fonsecaea monophora* was shown to suppress the proinflammatory T_h1- and T_h17-type immune responses induced by dectin-1-mediated signaling (159). Opposing roles for dectin-2 and mincle have been observed in the recognition of *Fonsecaea pedrosoi* (160).

Hyper-mannose glycosylation is required for optimal C-type lectin receptor recognition of *C. albicans* (68, 69). The lack of outer chain N-mannans may permit *Pneumocystis* organisms to escape detection by the immune system (21). While mannose receptor is associated with proinflammatory responses to *Pneumocystis* (92, 98, 157),

Zhang et al. demonstrated that blockage or knockdown of mannose receptor on rat alveolar macrophages resulted in elevated TNFα production in response to unopsonized mixed *Pneumocystis* organisms (161). In the absence of a strong proinflammatory signal from the cysts (β-glucan), the interaction of weakly mannosylated proteins on the surface of trophic forms with a C-type lectin receptor such as mincle or mannose receptor may suppress proinflammatory responses.

VI. Current limitations in *Pneumocystis* research

Despite repeated effort, a long term culture system for *Pneumocystis* organisms has not yet been developed. In the absence of an *in vitro* culture system, predictions have been made about the life cycle and reproduction of *Pneumocystis* species based on methods such as genome analysis, ultrastructural imaging of fungi from host lung isolates, and complementation of probable genes in related fungi including *Saccharomyces cerevisiae*. Recent genomic studies of *P. jirovecii*, *P. murina*, and *P. carinii* suggest that *Pneumocystis* species are obligate extracellular parasites that must scavenge nutrients, including amino acids, from their hosts (21, 162-164). In addition, the stable environment of the host lung may have permitted *Pneumocystis* species to lose genes involved in pH sensing, osmotic and oxidative stress responses (21). Such information will likely be critical to the success of future attempts to devise *in vitro* culture systems for *Pneumocystis* organisms.

The inability of *P. jirovecii* to live outside of a human host has limited research on this medically important parasite and opportunistic pathogen. Rat and mouse models have driven critical advances in understanding the immune responses to *P. carinii* and *P.*

murina, respectively. The transmission of *Pneumocystis* organisms and the progression of disease, including the development of interstitial pneumonia, in immunocompromised rodents appear to be homologous to that experienced in humans. Patients with specific immunodeficiencies, including defects in immune cell populations, signaling pathways, and cytokines, have provided evidence regarding the components of the immune response that are essential for clearance of *Pneumocystis* organisms. These observations have been substantiated by a large body of research exploring the immune response to *Pneumocystis* in rodent models. In addition, rhesus macaques have been used in studies that explore *Pneumocystis* and simian immunodeficiency virus (SIV) co-infection or the development of vaccines against *Pneumocystis*.

Currently, there is no reliable method for isolation of pure *P. murina* cyst organisms, though enrichment of *P. carinii* cysts from the lungs of infected rats via counterflow centrifugal elutriation has been reported (20). Cysts are relatively rare in the lungs of infected hosts (approximately 10% of the fungal lung burden), and the lungs of an infected mouse may contain only a tenth of the *Pneumocystis* organisms found in the lungs of an infected rat. The scarcity of cysts relative to trophic forms, in the context of the lower fungal burden in the lungs of mice compared to rats, may explain our inability to isolate pure cysts from mice.

Several additional factors have likely contributed to this inability to isolate cysts, regardless of host species, including considerable overlap between the sizes of trophic forms and cysts, and the lack of unique surface markers. Our attempts to isolate organisms using density gradients or recombinant His-tagged murine dectin-1 (R&D Systems, Minneapolis, MN) were unsuccessful (unpublished data). In addition, De

Stefano *et al* demonstrate that there is a high degree of conservation in the surface glycoproteins expressed by trophic forms and cysts (20). We have found a similar degree of conservation in the lectin-staining profile of trophic forms and cysts (Zhan Ye, unpublished). Our attempts to isolate the organisms by lectin-binding resulted in a slight enrichment of cysts, but insufficient yield (Zhan Ye, unpublished).

VII. Project Overview

Prior research in the field has overwhelmingly focused on the immune response to infection with a mixture of the trophic and cystic life cycle stages. Certainly, such studies provide valuable information, as the typical immune response to *Pneumocystis* organisms is shaped in the context of infection with both trophic forms and cysts. However, such studies do not provide a nuanced understanding of the distinct roles of the trophic and cystic life cycle stages in the development of the immune response to *Pneumocystis* infection. Here, our goal was to explore the biology of the immune response to these life cycle stages. In addition to providing answers to basic research questions, these efforts may provide critical insights for vaccine development or identification of new drug targets.

There is not a reliable method for isolation of pure *P. murina* cyst organisms. For this project, we have employed three general tools for modeling the exposure of the immune system to *Pneumocystis* lifeforms: 1) isolation of purified trophic forms, 2) depletion of cysts, and 3) substitution of the cyst form with materials that are homologous to cystic PAMPs.

We are able to employ differential centrifugation to isolate a population of purified trophic forms from the standard mixed population isolated from infected RAG2$^{-/-}$ mice. We routinely recover enriched trophic forms with ratios of at least 100 trophic organisms per cyst, in contrast to the standard mixture of 10 trophic forms per cyst found in infected mice. Differential centrifugation removes less than 10% of the trophic forms from the mixed population, and therefore has a negligible effect on the proportions of trophic forms and cysts that remain in the mixture.

Trophic forms encyst *in vivo*. In this report, we use the β-1,3-D-glucan synthase inhibitor anidulafungin to analyze the *in vivo* immune response to infection with trophic forms in the absence of cysts. Treatment with anidulafungin results in rapid depletion of the cyst life cycle stage, which expresses β-1,3-glucan, but leaves the trophic burden intact (17, 24).

Finally, in lieu of purified cysts, we will treat immune cells with various materials that are homologous to PAMPs on the surface of the cysts. Included in this list of surrogates are curdlan (a β-glucan preparation from *Alcaligenes faecalis*), zymosan (a *Saccharomyces cerevisiae* cell wall preparation consisting of β-glucans, mannans, mannoproteins and chitin), and depleted zymosan (zymosan that has been treated with hot alkali to denature proteins).

Central Hypothesis: The life cycle stages of *Pneumocystis murina* have a differential interaction with immune cells. Our initial goal was to characterize the immune response generated in response to trophic forms, or a mixture of trophic forms and cysts. Multiple reports from Limper *et al*. indicated that β-1,3-D-glucan from the cyst wall was sufficient

31

to drive secretion of proinflammatory chemokines and cytokines by alveolar epithelial cells and dendritic cells (23, 103, 104, 106). Furthermore, β-1,3-D-glucan-treated dendritic cells promoted CD4$^+$ T cell proliferation and T$_h$1 polarization (23). Conversely, it was unclear which types of immune responses might be elicited by the trophic forms, which do not express β-glucan. To address this hypothesis, three aims were explored:

Aim I: To determine if optimal innate and adaptive primary immune responses to *Pneumocystis* species are dependent on stimulation with the cyst life cycle stage. We initially hypothesized that infection of immunocompetent mice with trophic forms would lead to differential immune response compared to infection with mixed *P. murina* organisms due to the absence of β-glucan. Early data indicated that inoculation with trophic forms lead to the delayed initiation of innate and adaptive responses compare to inoculation with mixed *P. murina* organisms (**Fig 3.1-6**). Despite the absence of β-glucan, trophic forms express multiple glycoproteins that have the potential to interact with pattern recognition receptors (20, 165). Therefore, if trophic forms induce a less robust immune response than the cyst, it is possible that trophic forms employ some mechanism(s) to evade or dampen innate responses to the potentially inflammatory PAMPs expressed on their surface. We address this Aim in Chapter 3.

Aim II: To evaluate the role of trophic forms in the generation of protective adaptive immunity, as measured by clearance of infection. While Linke *et al.* demonstrate that depletion of cysts results in diminished inflammatory responses in the model of immune reconstitution inflammatory syndrome, it is unclear if trophic forms are

capable of eliciting any degree of an immune response. There is no evidence to suggest that *Pneumocystis* species have adaptive features associated with long-term immune escape, such as withdrawal to sites hidden from immune pressure. Indeed, infection of rodents with their respective *Pneumocystis* species results in clearance of the infection, albeit after several weeks. These data suggest that both trophic forms and cysts are susceptible to CD4$^+$ T cell and B cell-mediated clearance. Since trophic forms may encounter immune cells and may be cleared by T cell and B cell-mediated responses, we hypothesize that trophic forms may, independently of the cyst stage, elicit immune responses. We address this Aim in Chapter 4.

Aim III: To determine if trophic forms promote inflammation-mediated pneumonia in immunocompromised mice. While adaptive immunity is required for clearance of *Pneumocystis* infection, inflammation-mediated lung damage is deleterious in many models of PcP. Linke *et al*. propose that depletion of *Pneumocystis* cysts by β-1,3-glucan synthase inhibitors would reduce inflammation-induced lung damage in patients undergoing immune-reconstitution syndrome (24). RAG2$^{-/-}$ mice are not able to develop an adaptive response to *Pneumocystis*, and thus progress to PcP within 8 weeks post-infection. We predict that treatment with the β-1,3-glucan synthase inhibitor anidulafungin would extend the life of the RAG2$^{-/-}$ host, as the trophic forms would elicit less inflammation-induced lung damage. We address this Aim in Chapter 4.

Aim IV: To determine if trophic forms hamper the response to *P. murina* by preventing dendritic cell activation. The alveolar spaces of the uninfected host are

relatively free of immune cells. Clearance of *Pneumocystis* infection requires activation of alveolar macrophages, and the recruitment of CD4$^+$ T cells and B cells into the lungs. Thus, dendritic cells, which extend their processes beyond the alveolar epithelium into the alveolar spaces, are in a prime position to raise the alarm against *Pneumocystis* infection. It is possible that the ability of trophic forms to broadly dampen immune responses is dependent on silencing this alarm. To prime protective T cell responses, dendritic cells must undergo activation and prepare to present antigen, costimulatory molecules, and inflammatory cytokines to T cells in the draining lymph nodes of the lungs. We hypothesize that *Pneumocystis* trophic forms may impair one or more steps involved in the communication between dendritic cells and T cells. We address this Aim in Chapter 5.
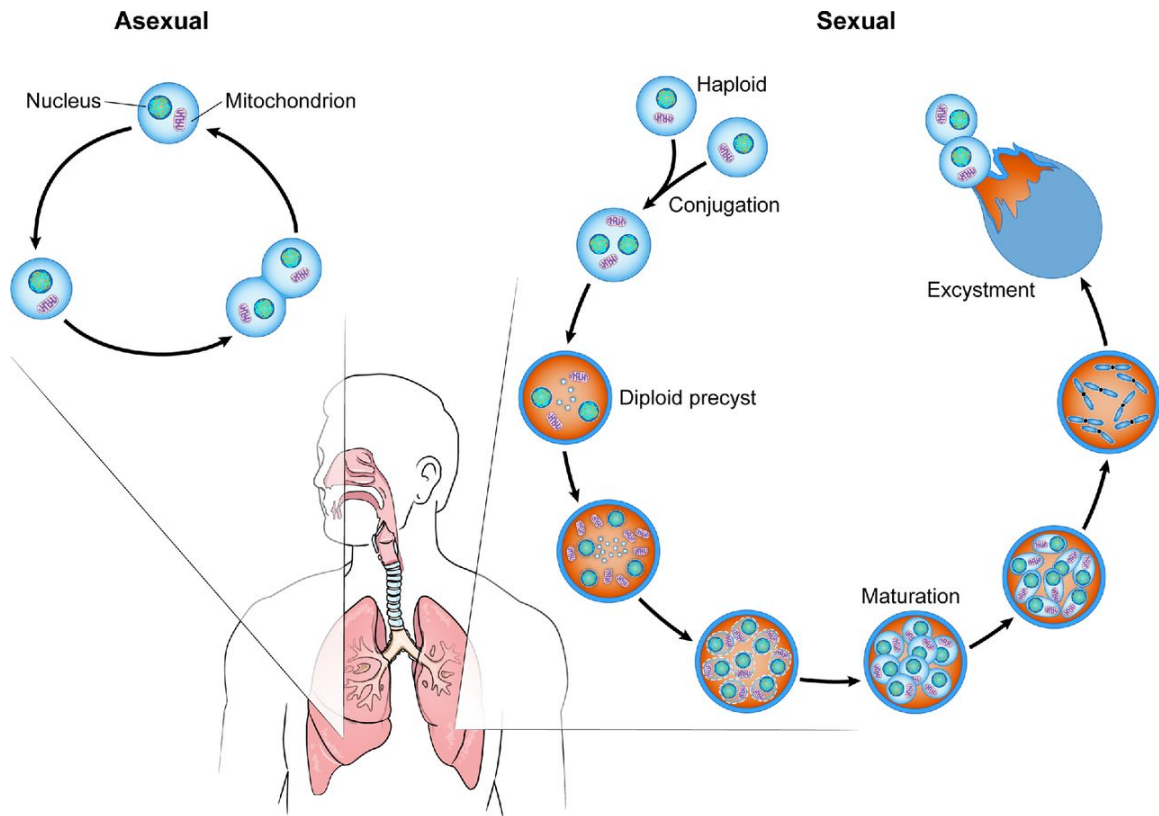
Figure 1-1 Proposed *Pneumocystis* life cycle.
Asexual reproduction of trophic forms probably occurs during acute infection. Sexual reproduction probably occurs when haploid trophic forms conjugate to form a diploid precyst. The precyst matures through the early, intermediate and late phase to form a mature cyst which ultimately releases young trophic forms.

Reproduced with permission from Skalski JH, Kottom TJ, Limper AH. 2015. Pathobiology of *Pneumocystis* pneumonia: life cycle, cell wall and cell signal transduction. FEMS Yeast Research 15: fov046. DOI: 10.1093/femsyr/fov046.
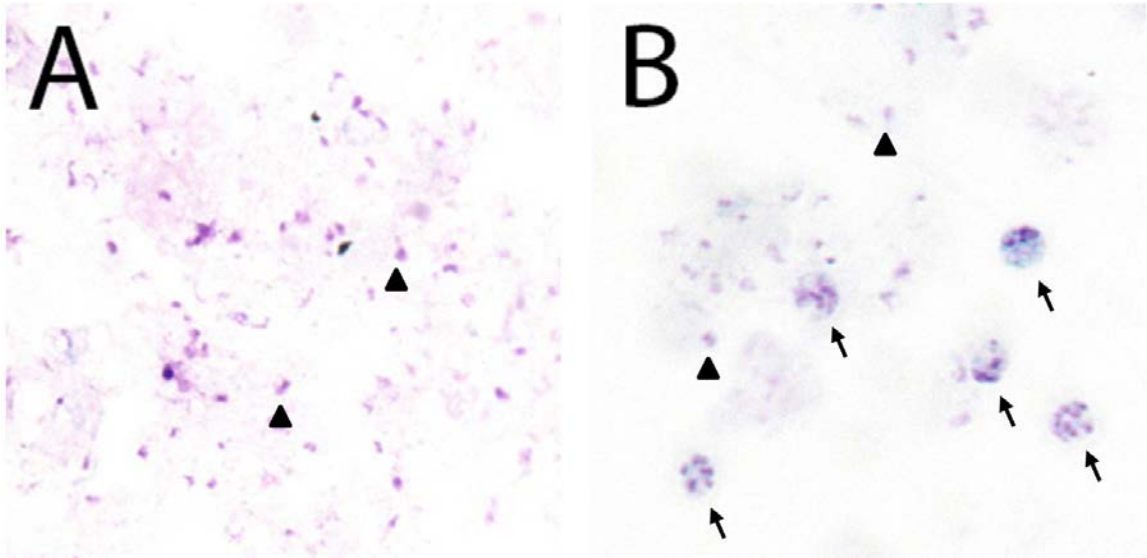
Figure 1-2 *P. murina* trophic forms and cysts.
Brightfield images (60 X magnification, oil objective, Nikon Eclipse E600 microscope) of DiffQuik-stained *P. murina* (**A**) purified trophic forms and (**B**) mixture of trophic forms (arrowhead) and cysts (arrow).
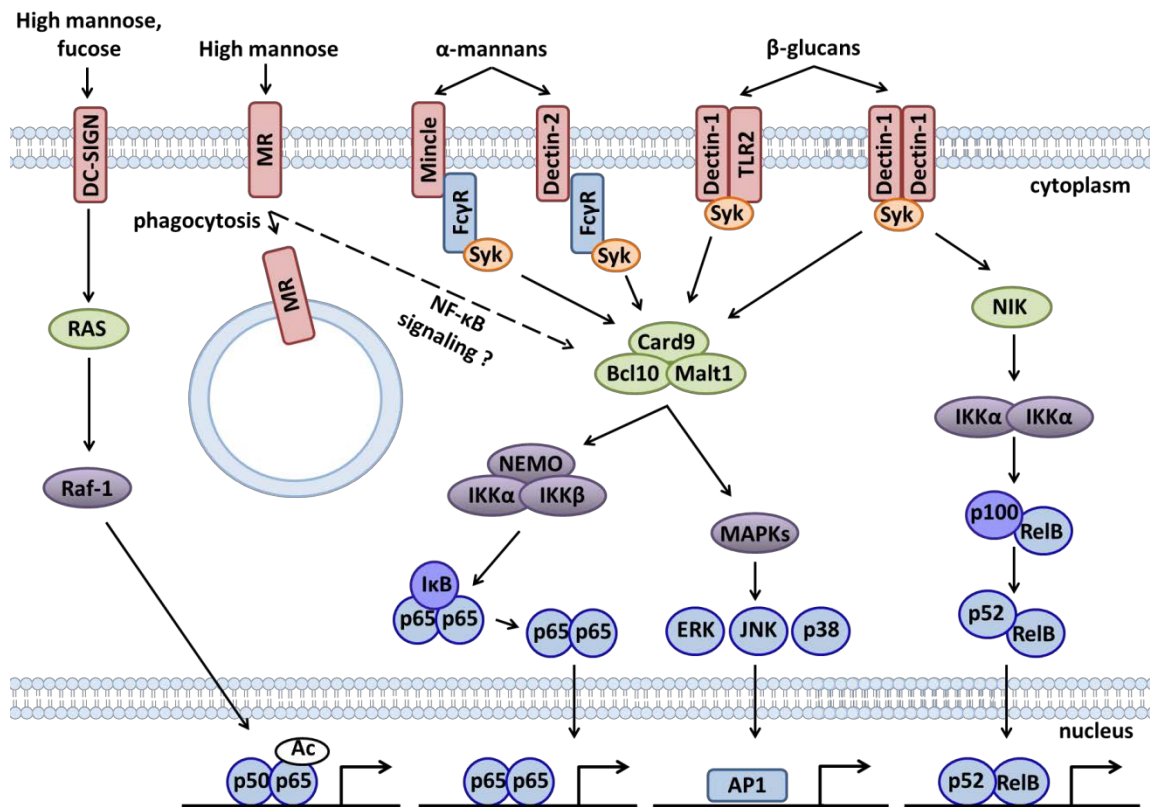
Figure 1-3 C-type lectin receptor signaling.
Engagement of DC-SIGN with fucose or highly-mannosylated structures induces acetylation of the NF-κB subunit p65 via the serine/threonine kinase Raf-1 (166). Mannose receptor (MR) is indicated in phagocytosis of *Pneumocystis* organisms (92). In human alveolar macrophages, nuclear translocation of canonical NF-κB molecules (p65, p50) and cytokine production have been shown to utilize MR (98, 167). Upon ligation with β-glucans, Syk associates with the ITAM motif within Dectin-1 to initiate downstream signaling through both the canonical and non-canonical NF-κB pathways. Dectin-2 and Mincle recognize α-mannans and require association with the FcRγ chain to initiate downstream signaling through the canonical NF-κB pathway.

Reproduced with permission from Kurkjian CJ. 2013. Environmental and intrinsic factors influence alveolar macrophage function in the neonatal immune response to *Pneumocystis*. Available from ProQuest Dissertations & Theses Global (1513271303).

Chapter 2: Materials and Methods

I. Materials

A. Reagents

Hanks Balanced Saline Solution (HBSS), Roswell Park Memorial Institute 1640 (RPMI) medium, Penicillin/Streptomycin (P/S), gentamicin reagent solution, L-glutathione, TrpLE Express cell dissociation buffer, Trypan blue, pHrodo Green Zymosan Bioparticles and Prolong Gold antifade reagent were purchased from Thermo Fisher Scientific (Waltham, MA).

DDAO-SE was purchased from Molecular Probes, Invitrogen (Grand Island, NY). Dulbecco's Phosphate Buffered Saline (PBS), albumin from bovine serum (BSA), DNase, Collagenase, glutathione, ethylenediaminetetraacetic acid (EDTA), formalin (neutral buffered, 10%), saponin, sodium azide (NaN$_3$), ionomycin, brefeldin A, dimethyl sulfoxide (DMSO), 2-Mercaptoethanol (2-ME), Tween-20, and sulfuric acid (H$_2$SO$_4$) were purchased from Sigma-Aldrich (St. Louis MO).

Heat-inactivated fetal bovine serum (HIFBS) was purchased from Atlas Biologicals (Fort Collins, CO). Methanol was purchased from BDH Chemicals (Poole Dorset, UK). MEM nonessential amino acid solution was purchased from ATCC (Manassas, VA). mGM-CSF was purchased from Peprotech (Rocky Hill, NJ). CD4 (L3T4) microbeads were purchased from (Miltenyi Biotec, San Diego, CA). DiffQuik was purchased from Siemens Healthcare Diagnostics, Inc. (Deerfield, IL). Foxp3 transcription factor staining kit and all ELISA kits were purchased from eBioscience (San Diego, CA). DNase easy kits were purchased from Qiagen (Germantown, MD). Transwell plates were purchased

from Corning Inc. (Corning NY). CFSE was purchased from Tonbo Biosciences (San Diego, CA). Direct-zol RNA miniPrep kit was purchased from Zymo Research (Irvine, CA). nCounter Mouse Immunology CodeSet was purchased from NanoString (Seattle, WA).

B. Mice

Six-week old BALB/cJ, C57BL/6, dectin-1 knockout (B6.129S6-Clec7a^{tm1Gdb}/J), and mannose receptor knockout (MR$^{-/-}$, B6.129P2-Mrc1^{tm1Mnz}/J) mice were purchased from the Jackson Laboratory (Bar Harbor, ME) and bred in our animal facilities. Male and female pups were used in the neonatal experiments. Six-week old female BALB/cJ and C57BL/6 mice were purchased from the Jackson Laboratory and infected at eight weeks of age for either the adult experiments or to generate CD4$^+$ T cells for the *in vitro* experiments. Uninfected adult female BALB/cJ, C57BL/6, dectin-1$^{-/-}$, MR$^{-/-}$, and B6.129P2 mice from the Jackson Laboratory were used to generate BMDCs for the *in vitro* experiments. Mice were maintained at the University of Kentucky Department of Laboratory Animal Resources (DLAR) under specific-pathogen-free conditions. C.129S6(B6)-Rag2^{tm1Fwa} N12 (Rag2$^{-/-}$) mice, originally from Taconic (Germantown, NY) were used to maintain a source of *P. murina* and were bred at DLAR in sterile microisolator cages with sterilized food and water. The University of Kentucky Institutional Animal Care and Use Committee approved all protocols regarding animal use. Femurs and tibias from Muc1$^{-/-}$ mice were generously provided by Dr. Sandra Gendler (Mayo Clinic, Scottsdale, AZ).

II. Methods

C. *P. murina* isolation

Lungs were excised from *P. murina*-infected Rag2$^{-/-}$ mice and pushed through stainless steel mesh in HBSS containing 0.5% glutathione at pH 7.3. Cell debris was broken up by aspirating through 20 and 26-gauge needles, then removed by centrifugation at 100 X g for 3 min. Trophic forms were isolated by removing the supernatant following centrifugation at 400 X g for 7 min. This preparation results in greater than 99% pure trophic forms (168). The pellet from the 400 X g spin contained a mixed population of cysts and trophic forms, at a typical ratio of 10:1 trophic forms to cysts. Erythrocytes in the pellet were lysed with water, and organisms suspended in an equal volume of 2X phosphate-buffered saline (PBS). Organisms were incubated with 200 U DNase at 37°C for 30 min. Clumps were broken up by aspirating through a 26-gauge needle. The remaining cell debris was removed by centrifugation at 100 X g for 3 min, followed by passage over a 70 µm filter. Aliquots of mixed *P. murina* organisms or purified trophic forms were diluted, and 100 µl aliquots were spun onto a 28.3 mm^2 area of glass slides. Slides were fixed in methanol and stained with DiffQuik (as shown in **Fig 1.2**). Organism numbers were determined microscopically using the 100X oil immersion objective of a Nikon microscope.

Purified and separated *Pneumocystis* lifeforms were pelleted by centrifugation at 1300 X g for 15 min, then resuspended in RPMI containing 10% HIFBS and 7.5% DMSO at a concentration of 10^7-10^8 *Pneumocystis* nuclei per 1ml media per cryovial. Frozen purified *Pneumocystis* was stored at -80C. As required for experiments, frozen purified *Pneumocystis* was thawed on ice and washed twice in HBSS with 1% P/S, 0.1%

gentamicin. Thawed *P. murina* was recounted (as described above) prior to inclusion in an experiment. It should be noted that the net effect of these centrifugation and wash steps would be expected to remove any matter with subcellular size. These washes, combined with the initial slow spin to remove lung debris, provide a reasonable degree of assurance that the trophic and mixed *P. murina* populations were free of any material that may confound the immunological assays employed in this dissertation. The visualization of the populations with DiffQuik stain (as seen in **Fig 1.2**) provides further assurance that the organisms were free of contamination from lung debris or bacteria.

D. Infection of mice with *P. murina*

Mice were lightly anesthetized with isoflurane to suppress the diver's reflex. Neonatal mice (24-72 hours old) were inoculated intranasally with up to 10^6 trophic or mixed *P. murina* organisms in 10 µl HBSS containing 10 units/ml penicillin, 10 µg/ml streptomycin, and 1 µg/ml gentamicin. Adult mice (6 – 8 weeks old) were inoculated intratracheally with up to 10^7 trophic or mixed *P. murina* organisms in 100 µl HBSS containing antibiotics. The adult mice were placed on an upright support rack, and the inoculations were performed using a blunted intratracheal needle designed with a curve to accommodate the trachea.

E. Adoptive transfer of CD4$^+$ T cells

Adult (8 weeks old) BALB/cJ mice were treated with saline or 1mg/kg anidulafungin (Pfizer, New York, NY) by the intraperitoneal route one day prior to infection and three times per week thereafter. Mice were anesthetized lightly with

isoflurane anesthesia to suppress the diver's reflex and inoculated intratracheally with a dose of enriched trophic forms or mixed *P. murina* equivalent to 10^6 total nuclei in 100 µl HBSS containing 10 units/ml penicillin, 10 µg/ml streptomycin, and 1 µg/ml gentamicin. The mice were placed on an upright support rack, and the inoculations were performed using a blunted intratracheal needle designed with a curve to accommodate the trachea. Infected mice were euthanized at 14 days post-infection. Tracheobronchial lymph nodes (TBLN) were collected from the infected mice followed by passage over a 70 µm filter. Erythrocytes were removed using hypotonic ammonium-chloride-potassium (ACK) lysing buffer (169). $CD4^+$ T cells were isolated with mouse $CD4^+$ T cell enrichment columns (positive selection, R&D Systems, Minneapolis, MN). $CD4^+$ T cells were washed, resuspended, and split for phenotyping or adoptive transfer. Greater than 90% of recovered cells were $CD4^+$ T cells, as determined by flow cytometry. 10^5 $CD4^+$ T cells were adoptively transferred by the intravenous retro-orbital route to $RAG2^{-/-}$ mice ("recipients").

Three days after adoptive transfer, the recipient mice were treated with either 1mg/kg anidulafungin or saline by the intraperitoneal route. This treatment continued three times per week throughout the course of the experiment. One day after the initiation of drug or saline treatment, the recipient mice were infected with a dose of enriched trophic forms or mixed *P. murina* organisms equivalent to 5 X 10^5 total nuclei. Animals were euthanized at 15 and 30 days post-infection.

F. Rechallenge with *P. murina* in CD4$^+$ T cell-depleted mice

Adult BALB/cJ mice were treated with 1mg/kg anidulafungin by the intraperitoneal route one day prior to intratracheal infection with 3 X 10^6 enriched trophic forms. Animals were treated with anidulafungin three times per week throughout the primary infection. Following clearance of the primary infection, anidulafungin treatment was stopped at day 34 post-infection to permit clearance of the drug prior to reinfection. At day 40 post-infection, 0.15 mg anti-CD4 antibody (clone GK1.5, Bio X Cell, Lebanon, NH) in 200 µl sterile saline was administered to deplete CD4$^+$ T cells. The anti-CD4 antibody treatment was administered every four days for the remainder of the study. One day after CD4$^+$ T cell depletion, mice were treated with either anidulafungin or saline followed by re-infection with a dose of enriched trophic forms or mixed *P. murina* organisms equivalent to 5 X 10^6 total nuclei. The anidulafungin or saline treatment was administered three days per week for the remainder of the study. Animals were euthanized at day 15 post-infection.

G. Isolation of cells from alveolar spaces, lungs, and lymph nodes

Mice were exsanguinated under deep isoflurane anesthesia, and lungs were lavaged with 5 washes of HBSS containing 3 mM EDTA. Bronchial alveolar lavage fluid (BALF) was centrifuged to obtain cells, and cell-free supernatant from the first wash was frozen for subsequent cytokine assays. Right lung lobes were excised, minced, and digested in RPMI containing 3% heat-inactivated fetal calf serum, 1 mg/ml collagenase A, and 50 U/ml DNase for 1 h at 37 °C. Digested lungs were pushed through 70 µm nylon mesh screens to obtain single-cell suspensions, and aliquots were taken for enumeration of *P.*

murina. Tracheobronchial lymph nodes (TBLN) were also excised and pushed through 70 µm nylon mesh screens in HBSS. Erythrocytes were removed using hypotonic ammonium-chloride-potassium (ACK) lysing buffer. Cells were washed and counted by hemocytometer.

H. Flow cytometric analysis for *in vivo* experiments

BALF, lung digest, and TBLN cells were washed with PBS containing 0.1% bovine serum albumin and 0.02% NaN3 and stained with appropriate concentrations of fluorochrome-conjugated antibodies specific for murine surface proteins (anti-CD4 clone GK1.5, anti-CD8a clone 53-6.7, anti-CD19 clone 1D3, anti-CD44 clone MEM-85, anti-CD62L clone MEL-14, anti-CD11c clone N418, anti-CD11b clone M1/70, and anti-F4/80 clone BM8).Antibodies were purchased from BD Biosciences (San Jose, CA) or eBioscience (San Diego, CA). Expression of these molecules on the surface of the cells was determined by multiparameter flow cytometry using a LSRII flow cytometer (BD Biosciences). 50,000 events were routinely acquired and analyzed using FlowJo software (TreeStar, USA).

I. Analysis of *P. murina*-specific IgG in serum

Blood was collected from rechallenged mice following euthanasia at day 15 post-rechallenge (n = 3 mice per group). Blood samples were centrifuged to pellet cells, and serum was collected and frozen at -80°C for later use. *P. murina*-specific immunoglobulin G (IgG) was measured by enzyme-linked immunosorbent assay (ELISA). A sonicate of *P. murina* trophic forms or mixed organisms (10 µg protein/ml)

was coated onto 96-well plates, and wells were blocked with 5% dry milk in HBSS containing 0.05% Tween-20. Sera were diluted and incubated on plates overnight. Serum collected from an uninfected mouse was used as a negative control. Plates were extensively washed, and bound IgG was detected using alkaline phosphatase-conjugated anti-mouse IgG (Sigma). Plates were washed and secondary antibodies detected using p-nitrophenylphosphate at 1 mg/ml in diethanolamine buffer. Optical density was read at 405 nm using a plate reader equipped with KC Junior software (Bio-Tek Instruments, Inc., Winnoski, VT). An OD of 0.1 was considered a cutoff value based on previous results from sera collected from uninfected mice. The OD of the negative control serum employed in these experiments remained below the 0.1 cutoff value.

J. Enumeration of *Pneumocystis* in the lungs of mice

Aliquots of lung homogenates were diluted in HBSS, and 100 µl aliquots were spun onto a 28.3 mm^2 area of glass slides. Slides were fixed in methanol and stained with DiffQuik. Organism numbers were determined microscopically using the 100X oil immersion objective of a Nikon microscope. The number of *P. murina* trophic forms or cysts in 50 microscopic oil immersion fields was used to calculate fungal burden. Lung burden is expressed as the number of *P. murina* organisms per right lung lobe, and the limit of detection was Log_{10} 3.12 nuclei per neonatal right lung lobe and Log_{10} 3.42 nuclei per adult right lung lobe.

K. Generation of BMDCs and CD4$^+$ T cells for *in vitro* assays.

BMDCs were generated from uninfected BALB/cJ, B6.129P2, dectin-1$^{-/-}$, and MR$^{-/-}$ adult female mice. BMDCSs were produced by flushing cells from the bone marrow of the tibias and femurs of female adult mice with PBS + 5% heat-inactivated fetal bovine serum. Erythrocytes were removed using ACK lysing buffer (169). Cells were washed and resuspended in culture media containing RPMI with 10% heat-inactivated FBS, 0.5 mM 2-mercaptoethanol, 1% MEM nonessential amino acid solution, 100 units/ml penicillin, 100 μg/ml streptomycin, and 50 μg/ml gentamycin. Cells were plated in 100 mm Petri dishes at a cell density of 4 X 10^6 in 10 ml of culture media with 20 ng/ml recombinant murine granulocyte-macrophage colony-stimulating factor. Plates were cultured at 37°C, 5.0% CO$_2$. An additional 10 ml culture media with 20 ng/ml recombinant murine GM-CSF was added to cells after 24 h of growth. Every 48 h thereafter, non-adherent cells were removed and replaced with 10 ml of fresh media containing recombinant murine GM-CSF. Cells were cultured for nine to twelve days. BMDCs were collected by vigorously washing plates with media to remove loosely adherent cells. BMDCs were washed, resuspended, and split for phenotyping or cytokine assay. Greater than 80% of recovered cells were CD11c$^+$.

CD4$^+$ T cells were generated by infecting adult BALB/cJ mice with 10^7 mixed *P. murina* organisms as described previously. TBLN were excised ten to fourteen days post-infection and pushed through 70 μm nylon mesh screens in HBSS. Erythrocytes were removed using ACK. Cells were washed and counted. CD4 (L3T4) microbeads were used for positive selection of CD4$^+$ cells. Greater than 90% of recovered cells were CD4$^+$ T cells.

L. *In vitro* cytokine production assays.

10^4 BMDCs and/or 5 X 10^4 CD4$^+$ T cells in 96-well plates were stimulated with 10 µg/ml curdlan (β-1,3-glucan from *Alcaligenes faecalis*), 20µg/ml zymosan (*Saccharomyces cerevisiae* cell wall), 20µg/ml depleted zymosan, 10µg/ml lipoteichoic acid (LTA), 100ng/ml lipopolysaccharides (LPS from *Escherichia coli* 0111:B4, purified by gel filtration to remove lipoproteins, per Sigma-Aldrich), 5 X 10^5 trophic forms and/or 5 X 10^5 mixed *P. murina* at 37°C, 5.0% CO_2 for 72 h in BMDC culture media. Supernatants were collected, centrifuged at 2700 X *g* for 1 min to remove organisms, and frozen for subsequent analysis of cytokine levels using IL-1β, IL-6, TNFα and IFN-γ ELISA. Trypan blue was used to evaluate viability of BMDCs following stimulation with 10 µg/ml curdlan, 5 X 10^5 trophic forms and/or 5 X 10^5 mixed *P. murina* at 37 °C, 5.0% CO_2 for 72 h in BMDC culture media.

M. *In vitro* phagocytosis assays

10^5 CFSE-labeled BMDCs were pre-incubated in chamber slides for one hour at 37 °C, 5.0% CO_2 in BMDC culture media. 2 X 10^5 DDAO-SE-labeled trophic forms or 2 X 10^5 DDAO-SE-labeled mixed *P. murina* were incubated with the BMDCs for 60 min. Samples were washed three times in PBS, followed by fixation in 10% neutral buffered formalin for 10 min. Slides were washed in PBS, and coverslips were mounted with Prolong Gold. Slides were cured for 48 h at room temperature. Slides were examined for internalization of *P. murina* organisms by BMDCs using a Nikon A1RSi microscope and NIS-Elements software. A minimum of 100 cells were analyzed per group.

10^5 BMDCs were incubated in round-bottom polystyrene tubes or on chamber slides for one hour at 37 °C, 5.0% CO_2 in BMDC culture media. 2 X 10^5 DDAO-SE-labelled trophic forms, 2 X 10^5 DDAO-SE-labelled mixed *P. murina*, and/or 100µg/ml pHrodo Green-labeled zymosan bioparticles were incubated with the BMDCs for 60 min. These bioparticles are labeled with a pH-sensitive dye that fluoresces within the acidic environment of the phagosome. Samples were washed three times in PBS. For confocal microscopy, chamber slides were fixed in 10% neutral buffered formalin for 10 min at room temperature. Slides were washed in PBS, and treated with 300nM DAPI for 30 min. Slides were washed in PBS, and coverslips were mounted with Prolong Gold. Slides were cured for 48 hr at room temperature. Slides were examined with a Nikon A1RSi microscope and NIS-Elements software. A minimum of 100 cells were analyzed per group. For flow cytometry, samples in round-bottom polystyrene tubes were washed twice in cold PBS. Samples were resuspended in 300ul cold HBSS. The phagocytic capacity of the cells was determined by flow cytometry using a LSRII flow cytometer. 1,000 dendritic cell events were acquired and analyzed using FlowJo software.

N. *In vitro* MHC class II and CD40 assays

10^5 BMDCs were stimulated with 20 µg/ml zymosan (*Saccharomyces cerevisiae* cell wall), 10^6 trophic forms and/or 10^6 mixed *P. murina* at 37 °C, 5.0% CO_2 for 24 h in BMDC culture media. Adherent cells were collected from the plate using TrypLE expression dissociation reagent. Cells were washed with PBS containing 0.1% bovine serum albumin and 0.02% NaN3 and stained with appropriate concentrations of fluorochrome-conjugated antibodies specific for innate immune cells (anti-CD11c clone

N418, anti-Ia^d clone AMS-32.1, and anti-CD40 clone 3/23). Antibodies were purchased from eBioscience (San Diego, CA). Expression of these molecules on the surface of the cells was determined by multiparameter flow cytometry using a LSRII flow cytometer (BD Biosciences). 1,000 CD11c$^+$ events were routinely acquired and analyzed using FlowJo software (TreeStar, USA).

O. *In vitro* CD4$^+$ T cell proliferation and polarization assays

10^5 BMDCs and/or CFSE-labelled 5 X 10^5 CD4$^+$ T cells were stimulated with 20 µg/ml zymosan (*Saccharomyces cerevisiae* cell wall), 5 X 10^5 trophic forms and/or 5 X 10^5 mixed *P. murina* at 37°C and in 5.0% CO$_2$ for 6 days in BMDC culture media. Media was collected from the plates and spun at 400 X *g* for 7 min to separate cells from the supernatant. Supernatant was stored at -80°C for use in IFNγ, IL-13, and IL-17A cytokine ELISAs (eBioscience, San Diego CA). Adherent cells were collected from the plate using TrypLE Express dissociation reagent. Dissociated cells were combined with cell pellet from the plate media and washed in fresh culture media.

Cells were washed in sterile PBS and stained with Fixable Viability Dye eFluor780 (eBioscience, San Diego, CA). Cells were washed with PBS containing 0.1% bovine serum albumin and 0.02% NaN3 (PBA) and stained with PerCP-efluor710-conjugated anti-CD4 clone GK1.5. Cells were washed with PBA and resuspended in 300µl HBSS. CD4$^+$ T cell proliferation was evaluated by multiparameter flow cytometry using a LSRII flow cytometer. 1,000 lymphocyte events were routinely acquired and analyzed using FlowJo software.

P. NanoString gene expression assay

3 X 10^4 BMDCs in 96-well Stripwell plates were stimulated with 10 µg/ml curdlan (β-1,3-glucan from *Alcaligenes faecalis*), 1.5 X 10^6 trophic forms, or 1.5 X 10^6 mixed *P. murina* at 37 °C, 5.0% CO_2 for 2, 4, and 8 h in BMDC culture media. Additional controls, including BMDCs treated with curdlan and trophic forms, were allowed to incubate for 72 h. The control supernatants were screened for IL-1β, IL-6, and TNFα cytokine production by ELISA, as described above.

At the conclusion of the 2, 4, and 8 h timepoints, the appropriate Stripwell segments were removed from the plate structure. Strips were washed once with PBS. Cells were lysed in TriReagent and RNA was extracted with the Direct-zol RNA MiniPrep kit (Zymo Research, Irvine CA). The Direct-zol RNA MiniPrep kit permitted optimal hybridization of samples to the NanoString probes, presumably due to reduced contamination of chaotropic salts compared other RNA extraction protocols.

RNA concentration was confirmed by using a NanoDrop machine, and purity was evaluated by using an Agilent 2100 Bioanalyzer. More than 50% of the RNA fragments from each sample were larger than 300 bp, satisfying the quality requirements for NanoString. The RNA integrity number (RIN) for all samples was above 8.0. 200 ng of each sample was sent to the Microarray Core at the University of Kentucky for NanoString processing. The NanoString nCounter Mouse Immunology kit was used to quantify the expression of 561 genes related to the murine immune response. Briefly, samples were hybridized to a panel of capture probes and reporter probes labeled with fluorescent barcodes. Hybridized samples were immobilized and aligned on the nCounter

cartridge. Reporter probes were read using the nCounter Analysis System, and counts were tabulated for each target transcript.

Analysis and normalization of the raw NanoString data were conducted using nSolver Analysis Software 2.0. Raw counts were normalized to the internal positive controls and to the following housekeeping genes: Alas1, Eef1g, G6pdx, Gapdh, Gusb, Hprt, Oaz1, Polr1b, Polr2a, Ppia, Rpl19, Sdha, Tbp, Tubb5. Heat maps and principal component analysis were prepared with the nSolver Analysis Software 2.0.

Q. Transwell contact assay

1×10^5 BMDCs, 10 µg/ml curdlan, and/or 5×10^6 trophic forms were plated in the upper or lower compartments of Transwell plates with a polyester membrane with 0.4µm pores. Cells were incubated at 37°C in 5.0% CO_2 for 72 h in BMDC culture media. Cytokine levels were analyzed as described above. To confirm that trophic forms did not cross the membrane, samples were centrifuged directly onto slides, DiffQuik stained, and 50 fields were screened.

Additional Transwell replicates were screened for *P. murina* DNA by quantitative PCR. Briefly, DNA was isolated from both the top and bottom compartments of the Transwell dishes using the Qiagen QIAamp Mini Kit. Presence of *P. murina* DNA was detected using primers designed to amplify a portion of the 18S rRNA gene of *P. murina*. Sequences of the primers are: forward 5'-GGGCTTCTTAGAGGGACTGTTGG-3', reverse 5'-CGTGCGGCCCAGAACATCTA-3' (IDT, Coralville, IA). The control plasmid for quantification of *P. murina* DNA contains the region of the 18S rRNA gene amplified by these primers (GenScript USA Inc., Piscataway, NJ). DNA was also isolated

from 10^4, 10^5 and 10^6 *P. murina* trophic forms. The quantitative PCR amplification was performed with DNA samples in triplicate for 39 cycles of 95°C for 5 seconds and 57°C for 30 seconds using a C1000 Thermal Cycler with a CFX96 real-time PCR detection system (Bio-Rad, Hercules, CA). The amount of trophic DNA calculated to have crossed from the Transwell insert to the bottom chamber would be equivalent to 2×10^3 organisms. *Pneumocystis* trophic forms reside in a biofilm-like substance consisting of a conglomeration of DNA, β-glucan, and other sugars (14). It is possible that the trophic DNA detected across the Transwell represents shed DNA rather than intact organisms. Therefore, fewer than 2×10^3 trophic forms may have crossed the Transwell barrier.

The number of organisms required to suppress cytokine expression in the Transwell system was determined by incubating 1×10^5 BMDCs, 10 µg/ml curdlan, and increasing numbers of trophic forms (ranging from 10^3 to 10^6 organisms) in the lower compartments of Transwell plates. Plates were incubated 37 °C, 5.0% CO_2 for 72 h in BMDC culture media. Cytokine levels were analyzed as described above.

R. Heat-killed trophic forms

Trophic forms were heat-killed by incubation at 56 °C for 1 hr. Non-viability of the organisms was confirmed by inoculation of immunocompromised Rag2$^{-/-}$ mice. 10^4 BMDCs were stimulated with 10 µg/ml curdlan, 5×10^5 trophic forms and/or 5×10^5 heat-killed trophic forms at 37 °C, 5.0% CO_2 for 72 h in BMDC culture media. Cytokine levels were analyzed as described above.

S. Statistical analysis.

Analysis and normalization of the NanoString data were conducted using nSolver Analysis Software 2.0. Differences among the groups were identified by two-way ANOVA followed by pairwise comparisons using the Least Significant Difference Method. Five biological replicates were used per group. A change was deemed significant if the p-value was < 0.01.

All other data were analyzed utilizing the SigmaStat statistical software package (SPSS Inc., Chicago, IL). Student's t-test, one way or two way analysis of variance (ANOVA) was used to determine differences between groups, with Student-Newman-Keuls or Holm-Sidak multiple comparisons *post hoc* tests. Kruskal-Wallis one-way ANOVA on ranks was used to analyze differences between groups when the data were nonparametric. Data were determined to be significantly different when the p-value was < 0.05.

Chapter 3: Robust innate and adaptive immune responses to Pneumocystis murina are dependent on stimulation with the cyst life cycle stage, while the trophic forms suppress proinflammatory responses.

The following chapter is modified from: Evans HM, Bryant GL, III, and Garvy BA. 2016. The life cycle stages of *Pneumocystis murina* have opposing effects on the immune response to this opportunistic fungal pathogen. Infect Immun. 84:3195–3205.

I. Introduction

Prior research in the field has overwhelmingly focused on the immune response to infection with a mixture of the trophic and cystic life cycle stages. Certainly, such studies provide valuable information, as the typical immune response to *Pneumocystis* organisms is shaped in the context of infection with both trophic forms and cysts. However, a nuanced understanding of the role of the trophic and cystic life cycle stages in the development of the immune response to *Pneumocystis* infection may provide critical insights for vaccine development or identification of new drug targets. Recently, it was reported that treatment of mice with the β-1,3-D-glucan synthase inhibitor anidulafungin resulted in depletion of *P. murina* cysts (24). The mice were able to control the remaining trophic burden in the absence of an excessive inflammatory response, however, the details of how trophic forms are recognized and cleared are not known.

Clearance of infection involving a mixture of *Pneumocystis* organisms is dependent on effective CD4^{+} T cell, B cell, and macrophage responses (1-4). In addition, failure to clear a mixture of *Pneumocystis* organisms leads to severe alveolar damage due to the

exaggerated inflammatory immune response (5). Both the neonatal lung environment and intrinsic immune cell deficits contribute to the delayed clearance of a mixture of *P. murina* organisms in neonatal mice (9-12).

Dendritic cells are the principal antigen presenting cells in the lung. However, their role in initiating the adaptive response to *Pneumocystis* has been understudied. Previous work has demonstrated that dendritic cells respond to β-glucans derived from the *Pneumocystis* cell wall (23). Dendritic cells activated by *Pneumocystis* cell wall-derived β-glucans increase costimulatory molecule expression and drive T cell polarization towards a T_h1-type response (23). The mechanism for dendritic cell recognition of *Pneumocystis* trophic forms, which do not express β-glucans, is unknown.

Here, we demonstrate that both the adult and neonatal immune response to infection with *P. murina* trophic forms alone was less robust than the response to infection with a physiologically normal mixture of cysts and trophic forms. Infection with trophic forms alone resulted in reduced recruitment of activated $CD4^+$ and $CD8^+$ T cells into the lungs of both neonatal and adult mice compared to infection with a normal mixture of trophic forms and cysts. Infection with a mixture of *P. murina* organisms drove recruitment of nonresident innate immune cells into the lung parenchyma and alveolar spaces. *In vitro*, trophic forms suppressed production of the proinflammatory cytokines IL-1β, IL-6, and TNFα by bone marrow-derived dendritic cells (BMDCs) stimulated with β-glucan, zymosan, LTA, or LPS. In addition, trophic form-stimulated BMDCs failed to stimulate production of the T_h1-type cytokine IFN-γ by $CD4^+$ T cells. We report for the first time that the trophic forms of *P. murina* suppress proinflammatory responses induced by multiple PAMPs.

II. Results

P. murina trophic forms encyst by day 14 post-infection in neonatal mice.

Recent evidence indicates that cysts are the transmittable life cycle stage of *Pneumocystis* species (17). However, there is a paucity of data regarding how the immune system handles the trophic forms of the organisms. We previously published that alveolar macrophages from either adult or neonatal mice failed to translocate NFκB in response to trophic forms (9). Therefore, we first wanted to know how the immune response differed when cysts were absent early in the infection and how quickly after infection trophic forms transitioned to cysts. To evaluate the differential immune response to the life cycle stages, we infected wild-type neonatal mice with either pure trophic forms or a physiologically normal mixture of *P. murina* trophic forms and cysts (**Fig 1.2**). Neonatal mice infected with a normal mixture of *P. murina* organisms fail to mount adaptive immune responses until 21 days of age (9). This presents an opportunity to observe the growth of the life cycle stages of *P. murina* in the absence of protective responses.

Trophic forms were detected at day 5 post-infection in the lungs of BALB/cJ neonates infected with 1×10^6 trophic forms or 1×10^6 mixed *P. murina* organisms (**Fig 3.1A**). The mixed *P. murina* inoculum consisted of 9.01×10^5 trophic forms and 9.90×10^4 cysts. Neonates infected with trophic forms had a higher trophic burden in the lungs at days 7 and 14 post-infection compared to mice infected with mixed *P. murina* (**Fig 3.1A**). However, the trophic lung burdens were similar between the groups by day 21 post-infection (**Fig 3.1A-B**). The cyst burden was below the limit of detection of Log_{10}

3.12 organisms per lung during the first week post-infection in BALB/cJ neonates infected with either trophic forms or mixed *P. murina* (**Fig 3.1C**). Cysts were detected at day 14 post-infection in both groups. Neonates infected with trophic forms had a higher cyst burden in the lungs at day 14 post-infection compared to mice infected with mixed *P. murina*, but there was no statistically significant difference in the cyst burden between the groups by day 21 post-infection (**Fig 3.1C**). Neonates infected with trophic forms and mixed *P. murina* displayed no differences in the clearance of either trophic forms or cysts (**Fig 3.1B and D**).

Cysts drive the early recruitment of activated T cells into alveolar spaces of neonatal mice.

Based on previously published reports, we predicted that the absence of cysts in the inoculum of neonatal mice infected with trophic forms would yield a less robust response than infection with a normal mixture of trophic forms and cysts (24). Clearance of *Pneumocystis* organisms requires the generation of effective adaptive immune responses. We have previously shown that adaptive responses are not observed in immunocompetent neonatal mice until week 3 post-infection (9). To determine if the absence of cysts in the inoculum affects the neonatal adaptive immune response, T and B cells in the lungs of neonates infected with trophic forms were compared with those of neonates infected with a normal mixture of *P. murina* organisms. The numbers of activated CD44^{high} CD62L^{low} CD4$^+$ and CD8$^+$ T cells in the alveolar spaces (represented by cells collected in the BALF) was significantly increased by week 3 post-infection in pups infected with organisms that included cysts in the inoculum compared to pups

infected with trophic forms (**Fig 3.2A and C**). No differences were observed in the numbers of T cells in the lung parenchyma (lung digest) (**Fig 3.2B and D**). These data indicate that the intensity of the early T cell response to *P. murina* in the alveolar spaces is dependent on the presence of cysts in the inoculum. The numbers of $CD19^+$ B cells in the lungs did not differ in pups infected with mixed *P. murina* organisms compared to pups infected with trophic forms (**Fig 3.2E**). The numbers of activated T cells and $CD19^+$ B cells in the alveolar spaces and lung parenchyma were equivalent between the groups at day 28 and 40 post-infection.

To determine if the absence of cysts in the inoculum affects the neonatal innate immune response, the expansion or recruitment of alveolar or non-resident innate immune cells in neonatal mice infected with trophic forms was compared with that of neonates infected with a normal mixture of *P. murina* organisms. The recruitment of $CD11c^-$ $CD11b^+$ non-resident innate immune cells to the alveolar spaces (BALF) by week 3 post-infection was higher in the mice infected with mixed *P. murina* organisms compared to trophic forms alone, but these differences were not statistically significant (**Fig 3.2G**). The numbers of $CD11c^+$ $CD11b^+$ innate immune cells increased by three weeks post-infection in the alveolar spaces of neonates infected with either trophic forms or mixed *P. murina* (**Fig 3.2H**). There were no differences in these responses at days 28 and 40 post-infection (**Fig 3.2G and H**).

P. murina **trophic forms will encyst by day 7 post-infection in adult mice.**

Quantification of the fungal lung burden in neonatal mice demonstrates that the cysts were below the limit of detection during the first week post-infection with either

trophic forms or mixed *P. murina* organisms. To determine if similar kinetics would be observed in adults, we infected immunocompetent BALB/cJ adult mice with trophic forms or mixed *P. murina* organisms. Trophic forms were detected at day 5 post-infection in the lungs of adults infected with trophic forms or mixed *P. murina* (**Fig 3.3A, C**). Cysts were first detected at day 7 post-infection in the lungs of adults infected with trophic forms or mixed *P. murina* (**Fig 3.3B, D**). The trophic and cystic lung burdens were similar between the groups at all timepoints, and peaked at day 14 post-infection (**Fig 3.3A-D**). The difference in the cyst burden at day 7 post-infection (**Fig 3.3B**) was not consistent in a repeat of the experiment (**Fig 3.3D**). The trophic and cystic lung burdens were below, or approaching, the limit of detection of Log_{10} 3.42 organisms per lung by day 21 post-infection, indicating that there were no differences in the clearance of *P. murina* organisms by either group (**Fig 3.3A-D**).

Cysts drive the early recruitment of T and B cells into the lungs of adult mice.

To determine if cysts were required for the early recruitment of T and B cells into the lungs of immunocompetent adult mice, we infected BALB/cJ adult mice with either trophic forms or a normal mixture of *P. murina* organisms (**Fig 3.4**). The robust early recruitment of activated $CD44^{high}$ $CD62L^{low}$ $CD4^+$ and $CD8^+$ T cells into the alveolar spaces (BALF) was dependent on the presence of cysts in the inoculum (**Fig 3.4A-B**). An increase in the numbers of activated $CD4^+$ and $CD8^+$ T cells was also observed at day 5 post-infection in the lung parenchyma of mice infected with a mixture of trophic forms and cysts compared to mice infected with trophic forms alone (**Fig 3.4A-B**). Cysts in the inoculum also promoted the early recruitment of $CD19^+$ B cells into the alveolar spaces

and an early increase in the number of CD19$^+$ B cells in the TBLN (**Fig 3.4C**). T and B cell numbers in mice infected with trophic forms were similar or greater than those in mice infected with mixed *P. murina* as the mice approached clearance at week 3 post-infection.

Cysts promote the early infiltration of non-resident innate immune cells in adult mice.

The recruitment of CD11c$^-$ CD11b$^+$ non-resident innate immune cells to the alveolar spaces (BALF) and lung parenchyma (lung digest) of adult BALB/cJ mice by day 14 post-infection was higher in mice infected with cysts in the inoculum compared to trophic forms alone (**Fig 3.5A**). The numbers of CD11c$^+$ CD11b$^+$ innate immune cells increased during the first week post-infection in the alveolar spaces and parenchyma of adults infected with mixed *P. murina* (**Fig 3.5B**). The numbers of lung resident CD11c$^+$ CD11b$^-$ innate immune cells increased in the lung parenchyma of adults infected with mixed *P. murina* at day 5 post-infection, but no statistically significant differences were observed in the alveolar spaces of the two groups (**Fig 3.5C**). Surface expression of the major histocompatibility complex class II molecule I-A^d was higher on both CD11c$^+$ CD11b$^-$ and CD11c$^+$ CD11b$^+$ innate immune cells in the alveolar spaces of mice infected with mixed *P. murina* compared to mice infected with trophic forms alone (**Fig 3.5D-E**). These data indicate that the presence of cysts in the initial inoculum shapes the phenotype of the early innate immune response in adult mice.

Cysts drive the early production of IFN-γ in the alveolar spaces of adult mice.

T_h1-, T_h2-, and T_h17-type responses have all been associated with clearance of *P. murina* organisms (112, 114, 115). To determine if cysts promoted the early development of T_h1-type responses in the lungs, we evaluated cytokine production following infection of BALB/cJ adult mice with either trophic forms or a normal mixture of *P. murina* organisms. The early production of IFN-γ in the BALF was higher in mice infected with cysts in the inoculum compared to trophic forms alone (**Fig 3.6A**). IFN-γ production in the lungs of mice infected with trophic forms remained low at all timepoints compared to mice infected with a mixture of *P. murina* organisms, despite the presence of cysts by day 7 post-infection (**Fig 3.6A**). In addition, the proportion of CD4$^+$ T cells producing intracellular IFN-γ at day 7 post-infection was higher in the lungs of mice infected with mixed *P. murina* organisms compared to mice infected with trophic forms (**Fig 3.6B**). These data suggest that cysts are required in the inoculum for optimal T_h1-type responses.

Trophic forms suppress β-glucan-induced proinflammatory cytokine production by dendritic cells.

β-glucan from the cell wall of *Pneumocystis* cysts has been previously shown to stimulate production of IL-1β, IL-6, and TNFα in dendritic cells and induce IFN-γ production in cocultured T cells (23). To evaluate whether trophic forms are able to stimulate proinflammatory cytokines, we measured IL-1β, IL-6, and TNFα production by bone marrow-derived dendritic cells (BMDCs) following stimulation with trophic forms, a normal mixture of *P. murina* organisms, and/or curdlan (**Fig 3.7**). Curdlan is a high-molecular-weight β-1,3-glucan isolated from *Alcaligenes faecalis*, and is similar to the β-

1,3-glucan that composes the *P. murina* cyst wall (15). IL-1β and IL-6 production was stimulated by 5 X 10^5 mixed *P. murina* organisms and 10 µg/ml curdlan, but not 5 X 10^5 trophic forms (**Fig 3.7A-B**). These data demonstrate that cysts are required for production of IL-1β and IL-6 by BMDCs. Stimulation of BMDCs with curdlan induced IL-1β, IL-6, and TNFα production (**Fig 3.7A-C**). Conversely, our data indicate that trophic forms suppress curdlan-induced IL-1β, IL-6, and TNFα production by BMDCs in a dose-dependent manner (**Fig 3.7A-C**). Interestingly, 10^6 trophic forms suppressed the IL-6 production induced by 5 X 10^5 mixed *P. murina* organisms (**Fig 3.7B**), but were insufficient to induce suppression of IL-1β production (**Fig 3.7A**). In contrast to IL-1β and IL-6 production, TNFα production was stimulated by curdlan, but not trophic forms or mixed *P. murina* organisms (**Fig 3.7C**). Moreover, incubation of BMDCs with a high number of trophic forms or mixed *P. murina* organisms suppressed curdlan-induced production of TNFα (**Fig 3.7C**). This reduction in cytokine production was not due to a toxic effect on the BMDCs (**Fig 3.8**).

The *P. murina* cell wall has been shown to contain more complex branching patterns, including β-1,6-glucan, than those contained in curdlan. The *P. murina* cell wall also includes mannosylated proteins. To evaluate the ability of trophic forms to suppress responses to a fungal cell wall, we measured cytokine production following stimulation with trophic forms, zymosan, and/or depleted zymosan (**Fig 3.9**). Zymosan is a protein-carbohydrate preparation from the cell wall of *Saccharomyces cerevisiae*. Depleted zymosan is treated with hot alkali to prevent engagement of the toll-like receptors. Trophic forms suppressed zymosan and depleted zymosan-induced production of IL-1β, IL-6, and TNFα (**Fig 3.9A-F**).

Trophic forms suppress TLR2 and TLR4-induced proinflammatory cytokine production by dendritic cells.

In addition to C-type lectin receptors such as dectin-1, *Pneumocystis* species have been shown to stimulate cytokine production by antigen presenting cells via Toll-like receptors (TLRs) 2 and 4 (156, 170). We measured IL-1β, IL-6, and TNFα production by BMDCs following stimulation with TLR2-agonist LTA, TLR4-agonist LPS and/or trophic forms (**Fig 3.10**). Stimulation of BMDCs with LTA or LPS induced IL-1β, IL-6, and TNFα production (**Fig 3.10A-F**). The addition of $5x10^5$ trophic forms suppressed this cytokine response to LTA and LPS.

The suppression of the response to curdlan is not mediated by mannose receptor.

Carbohydrate PAMPs on the surface of fungi and other microorganisms may be recognized by C-type lectin receptors. Mannose receptor and dectin-1 have been implicated in the immune response to *Pneumocystis* species (69, 92, 98, 151, 157, 161). To evaluate the role of mannose receptor and dectin-1 in the response to trophic forms and β-glucan, we stimulated BMDCs deficient in those C-type lectin receptors with trophic forms, mixed *P. murina* organisms, and/or curdlan (**Fig 3.11**). Surprisingly, neither mannose receptor nor dectin-1 was required for IL-6 or TNFα production in response to mixed *P. murina*. IL-1β production in response to mixed P. murina was modestly dependent on dectin-1. As expected, mannose receptor was not responsible for the response to curdlan. Depletion of dectin-1 did not fully abolish the IL-6 and TNFα response to curdlan. It is possible that other receptors such as complement receptor 3 (CD11b/CD18) or lactosylceramide may recognize curdlan (105, 106, 171-173).

Alternatively, the curdlan used in this project may have contained additional PAMPs beyond β-1,3-glucan.

Regardless, our data demonstrate that neither mannose receptor nor dectin-1 was exclusively required for the trophic form-mediated suppression of IL-1β, IL-6, and TNFα production. In the absence of mannose receptor or dectin-1 there was a modest increase in IL-6 production in BMDCs treated with curdlan and trophic forms compared to wild-type BMDCs. Together, these data demonstrate that dectin-1 does not contribute significantly to the IL-1β, IL-6, or TNFα response to mixed *P. murina*, but is involved in signaling β-glucan responses, though not exclusively. Furthermore, mannose receptor has only a minor role in the inhibitory effects of trophic forms on β-glucan stimulation of IL-6 production. These data suggest that other pattern recognition receptors are involved in signaling both proinflammatory and suppressive functions of *P. murina* life forms.

Finally, it should be noted that mixed *P. murina* organisms stimulated modest TNFα production by BMDCs from the C57BL/6 mouse strain background. TNFα production was not detected in response to mixed *P. murina* organisms when cells of a BALB/cJ background were used. Generally, cells from C57BL/6 mice exhibit a stronger T_h1-type bias than cells from BALB/cJ mice. The immune response of C57BL/6 adult mice following inoculation with trophic forms or mixed *P. murina* organisms was similar to that observed in BALB/cJ mice (data not shown). Regardless, our data suggest that trophic form-mediated suppression of inflammatory responses is not limited to the BALB/cJ background.

Dendritic cells co-cultured with trophic forms fail to induce IFNγ production by CD4$^+$ T cells.

To evaluate whether dendritic cells are able to induce T_h1-type responses when loaded with trophic forms, we stimulated BMDCs co-cultured with CD4$^+$ T cells with either mixed *P. murina* or trophic forms. BMDCs loaded with mixed *P. murina*, but not trophic forms, stimulated IFN-γ production in CD4$^+$ T cells (**Fig 3.12**). The addition of curdlan did not improve IFN-γ production in response to trophic forms (data not shown). These data demonstrate that cysts are required for effective T_h1-type responses *in vitro* and are consistent with our findings *in vivo* that cysts drive the early T cell response to *P. murina*.

III. Discussion

Our data confirm that cysts drive proinflammatory responses to infection with *P. murina*. Cysts promote the early recruitment of activated CD4$^+$ and CD8$^+$ T cells into the lungs of neonatal and adult mice. Cysts also promote the early recruitment of nonresident innate immune cells and CD19$^+$ cells into the alveolar spaces of adult mice. Cysts in the inoculum stimulate the production of IFN-γ. Importantly, we found for the first time that trophic forms suppress β-glucan-, LTA-, and LPS-induced proinflammatory cytokine production by dendritic cells. Furthermore, dendritic cells cultured with trophic forms failed to stimulate production of IFN-γ by CD4$^+$ T cells. Our data is consistent with the cyst life cycle stage driving proinflammatory responses that direct the early recruitment of innate and adaptive immune cells. However, the trophic life cycle forms dampen the β-glucan and TLR-induced inflammation. This is a novel finding and suggests that the two life forms of *Pneumocystis* balance the immune response to the organisms.

We have previously reported that there is a delay in the immune response to *P. murina* in neonatal mice compared to adults (9-12). Despite the delay, the immune response is sufficient to mediate clearance of *P. murina* organisms. This delayed response represents a balance between clearance of a pathogen and avoidance of inflammatory damage during postpartum development. Here, we report that cysts in the inoculum drive adaptive immune responses to *P. murina* in neonatal mice by day 21 post-infection. The fungal burden in neonates infected with trophic forms or mixed *P. murina* was similar by day 21 post-infection. These data suggest that the composition of the inoculum shapes the development of the immune response to *P. murina* organisms.

Redundant T_h1-, T_h2-, and T_h17-type responses are associated with clearance of *Pneumocystis* organisms (1, 3, 4, 112, 114, 115). Here we report that cysts are required in the inoculum to stimulate the production of intracellular IFN-γ by $CD4^+$ T cells in adult mice at day 7 post-infection. $CD8^+$ T cells are not required for clearance of *Pneumocystis* organisms, but contribute to the production of proinflammatory cytokines, including IFN-γ, that mediate effector responses (119). The concentration of extracellular IFN-γ in the alveolar spaces of adult mice infected with trophic forms did not change over the course of infection, despite an eventual increase in the cyst burden and the numbers of activated $CD4^+$ and $CD8^+$ T cells. This may suggest that trophic forms suppress T_h1-type responses, which would be consistent with our *in vitro* data.

Mice infected with trophic forms developed detectable cysts by day 7 in adult mice and day 14 post-infection in neonates. We were unable to discern in our models whether trophic forms are capable of inducing protective immune responses, or if the response to trophic forms is merely delayed. The reduced ability of trophic forms to stimulate IFN-γ expression does not preclude generation of protective responses, as there is redundancy in the types of T helper responses that can mediate clearance of *Pneumocystis* organisms (112, 114, 115). It has been previously reported (24), and our preliminary data using an echinocandin to prevent formation of cysts suggests, that infection with trophic forms is sufficient to generate protective $CD4^+$ T cell and antibody responses (**Chapter 4**).

Clearance of *Pneumocystis* organisms is also dependent on alveolar macrophage responses (2). Our data demonstrate that cysts drive increases in the numbers of $CD11c^+$ $CD11b^+$ lung resident innate immune cells. This population includes activated alveolar macrophages (9). We found that cysts promote MHC class II expression on the surface of

immune cells in the alveolar spaces. Decreased antigen presentation in the absence of cysts may have contributed to the less robust T cell response observed in mice infected with trophic forms. Additionally, cysts drive early infiltration of CD11c$^-$ CD11b$^+$ innate immune cells into the lungs. This population consists of monocytes, small macrophages, and neutrophils. Neutrophils are not required for clearance, but their accumulation in the lungs correlates with disease severity in human *Pneumocystis pneumonia* patients (5, 136). The CD11c$^-$ CD11b$^+$ population may also include myeloid-derived suppressor cells (MDSCs). MDSCs are recruited into the lungs of immunocompromised rodents during PcP (140). MDSCs isolated from the lungs of mice with PcP suppress key effector cells, including CD4$^+$ T cells and alveolar macrophages, and may directly contribute to lung injury (140, 141). The role of MDSCs in the lungs of immunocompetent hosts during *Pneumocystis* infection is unclear.

Infection with trophic forms in the absence of cysts leads to the establishment of an immunosuppressive environment in the lungs that persists for up to one week following the formation of the cystic stage. If cysts are in the inoculum, the trophic form is unable to suppress inflammatory responses in the lungs as definitively. We would predict that infection with pure cysts, in the absence of trophic forms, would lead to accelerated inflammatory responses compared to infection with a mixture of organisms. Unfortunately, there is not a reliable method to isolate *P. murina* cysts in appreciable quantities.

Other groups report difficulties in stimulating IL-1β, IL-6, and TNFα cytokine production by antigen presenting cells using unopsonized mixed *P. murina* organisms (161). We found that a multiplicity of infection of 50 mixed *P. murina* organisms to 1

BMDC was sufficient to induce IL-1β and IL-6 production. We attribute the necessity of this relatively high multiplicity of infection to the presence of trophic forms in the mixture, as our data demonstrate that trophic forms suppressed production of the β-glucan-induced proinflammatory cytokines IL-1β, IL-6, and TNFα by BMDCs. A multiplicity of infection of 50 *P. murina* organisms per dendritic cell is composed of approximately 5 cysts capable of stimulating positive cytokine responses plus 45 trophic forms that will act to suppress these responses. Gene expression data demonstrate that BMDCs stimulated with trophic forms express less express IL-1β, IL-6 and TNF*α* mRNA than cells stimulated with curdlan or mixed *P. murina* organisms (**Chapter V**). This suggests that the trophic forms suppress cytokine production rather than cytokine secretion.

Interestingly, mixed *P. murina* organisms failed to induce TNFα in BMDCs in our model. TNFα production is associated with protection against *P. murina*, and its production has been reported in BMDCs following stimulation with β-glucan extracted from the cell wall of the cyst life cycle stage (23). We propose that trophic forms, which comprise approximately 90% of the organisms in mixed *P. murina* infection, are sufficient to suppress production of TNFα by BMDCs that would otherwise be induced by β-glucan on the surface of the cysts. Consistent with this contention, we found that trophic forms inhibited cytokine production by curdlan-stimulated BMDCs.

C-type lectin receptors are transmembrane proteins that bind carbohydrates (144). Activation triggers phagocytosis, as well as signaling cascades that culminate in the activation of antigen presenting cells and the production of inflammatory cytokines. Dendritic cells have been shown to respond to *P. carinii* cyst wall β-glucans via dectin-1

(23). Dectin-1 is required for the generation of an effective response to *Pneumocystis* infection (69). Previous work has shown that mannose receptor binds glycoprotein A on the cell surface of *Pneumocystis* organisms, triggering phagocytosis, reactive oxygen species production, and NF-κB-mediated production of IL-8 (92, 98, 157). Here, we demonstrate that neither dectin-1 nor mannose receptor were exclusively required for the production of IL-1β, IL-6, and TNFα by BMDCs in response to *P. murina*. Our data suggest redundancy in the receptors that recognize cysts and trophic forms.

Conversely, some C-type lectin receptors may suppress proinflammatory responses. Engagement of the C-type lectin receptor mincle by the fungal skin pathogen *Fonsecaea monophora* was shown to suppress proinflammatory responses induced by dectin-1-mediated signaling (159). Zhang et al. demonstrated that blockage or knockdown of mannose receptor on rat alveolar macrophages resulted in elevated TNFα production in response to unopsonized mixed *Pneumocystis* organisms (161). Here, we demonstrate that the deletion of mannose receptor on dendritic cells resulted in a modest decrease in the ability of trophic forms to suppress the production of IL-6 in response to β-glucan, indicating that suppression is mediated through mechanisms other than mannose receptor. We are currently examining whether mincle could mediate the suppressive activity of trophic forms as was found for *F. monophora*.

Our data indicate that trophic forms suppress cytokine responses to the TLR2 agonist LTA and the TLR4 agonist LPS. In one paper, mice with mutant TLR4 were shown to have reduced IL-10, IL-12p40, and MIP-2 in the BALF of *Pneumocystis* infected mice and enhanced levels of TNF and IL-6 with no difference in clearance of the organisms (170). In addition, dectin-1 acts synergistically with TLR2 and TLR4 to

70

promote cytokine production following stimulation with curdlan (174). Simultaneous inhibition of dectin-1-, TLR2-, and TLR4-mediated signals may permit the trophic forms to broadly dampen the proinflammatory response and protect the colonization of *Pneumocystis* organisms in the immunocompetent host. Suppression of zymosan and depleted zymosan-stimulated cytokine production provides evidence that trophic forms can broadly dampen the response to carbohydrate and protein agonists.

The inflammatory potential of the cysts in the face of a 10-fold excess of suppressive trophic forms should not be understated. The ability of trophic forms to suppress cytokine production is dose-dependent, and our data suggest that slight changes in the ratio of trophic forms to cysts may shift the balance between suppression and stimulation. Increasing the trophic form to cyst ratio from 10:1 to 12:1 (by the addition of 10^5 trophic forms) is sufficient for the trophic forms to begin to reduce the IL-6 response to the mixed population. Our *in vivo* data indicate that the cyst burden remains low during the first week post-infection, but that cysts in the inoculum drive the initial inflammation. The rapid establishment of an immunosuppressive trophic population may be critical to avoid preemptive detection and clearance in immunocompetent hosts. Conversely, immunocompromised mice with severe pneumonia experience a final burst of trophic growth, in which the ratio of trophic forms to cysts reaches as high as 30:1 (unpublished observation). This population shift may prolong the life of the immunocompromised host by dampening inflammation, and may extend the window of opportunity for the transmission of cysts to additional hosts.

The inoculation with trophic forms employed within this paper does not mimic the natural route of infection, as cysts are the transmittable life cycle stage of *Pneumocystis*

species (17). Consistent with our goal, our approach allows conclusions to be formed about the differential immune responses generated to the life cycle stages of *Pneumocystis* species. Recently, it was reported that treatment of immune-reconstituted mice with the β-1,3-D-glucan synthase inhibitor anidulafungin results in depletion of cysts, with the remaining trophic burden stimulating a much reduced inflammatory response (24). Anidulafungin belongs to a drug class known as the echinocandins, which have been used in combination with other antifungals in the treatment of *Pneumocystis* pneumonia in human patients (83). Linke *et al*., propose that depletion of cysts would reduce inflammation-induced lung damage in patients (24). Our data corroborates this suggestion, and highlight the need for a greater understanding of the response to the trophic stage. We propose that depletion of the immunostimulatory cysts in the presence of the immunosuppressive trophic forms may hamper the ability of immunocompromised patients or infants to control the infection. However, the net outcome may be positive, as lung damage during *Pneumocystis* pneumonia is predominately due to the inflammatory immune response.

In summary, our data indicate that cysts are the primary form of *Pneumocystis* responsible for provoking adult and neonatal immune responses to infection with *P. murina*. These responses include infiltration of nonresident innate immune cells and the recruitment of $CD19^+$ B cells and activated $CD4^+$ and $CD8^+$ T cells. Cysts are required to stimulate the production of IFN-γ by $CD4^+$ T cells *in vitro*, and in the alveolar spaces of immunocompetent adult mice. We found that trophic forms suppress β-glucan-induced proinflammatory cytokine production by dendritic cells. We propose that the suppression of immune responses by the trophic forms promotes the colonization of *Pneumocystis* in

immunocompetent hosts and may be beneficial to immunocompromised hosts by dampening the inflammatory responses that contribute to lung pathology during PcP. This differential immune response to *Pneumocystis* trophic forms and cysts is most certainly a leading contributor to the success of the organisms as human pathogens.
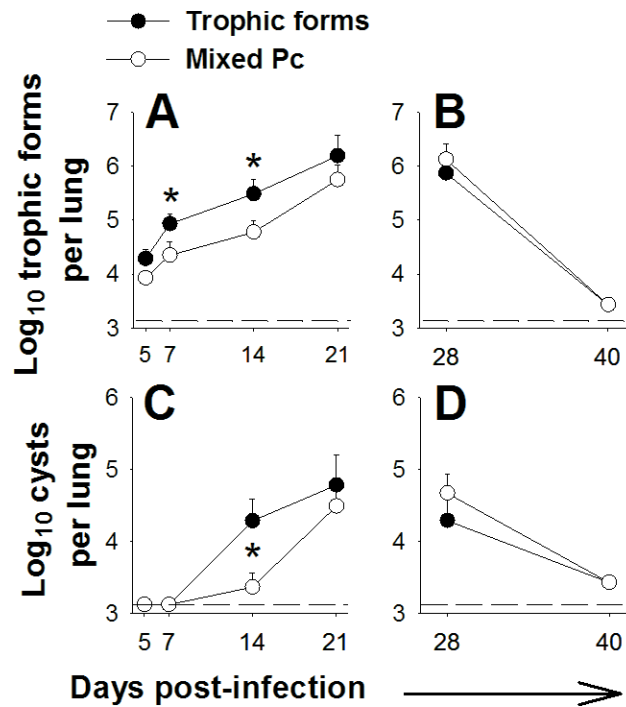
Figure 3-1 Cysts are undetectable during the first week post-infection in BALB/cJ neonates infected with *P. murina* trophic forms.

Neonatal (24-72 h old) mice were infected i.n. with 10^6 trophic forms or mixed *P. murina* organisms. Trophic (**A, B**) and cystic (**C, D**) lung burden in the right lung lobes was determined by enumeration of organisms on DiffQuik stained slides under a microscope. Data represent the mean ±SD of 3-4 mice per group and are representative of 2 separate experiments. The limit of detection was Log_{10} 3.12 nuclei per neonatal right lung lobe. Two way ANOVA with Holm-Sidak post-hoc test was used to compare mean trophic form or cyst number between the groups, *$p \leq 0.05$.
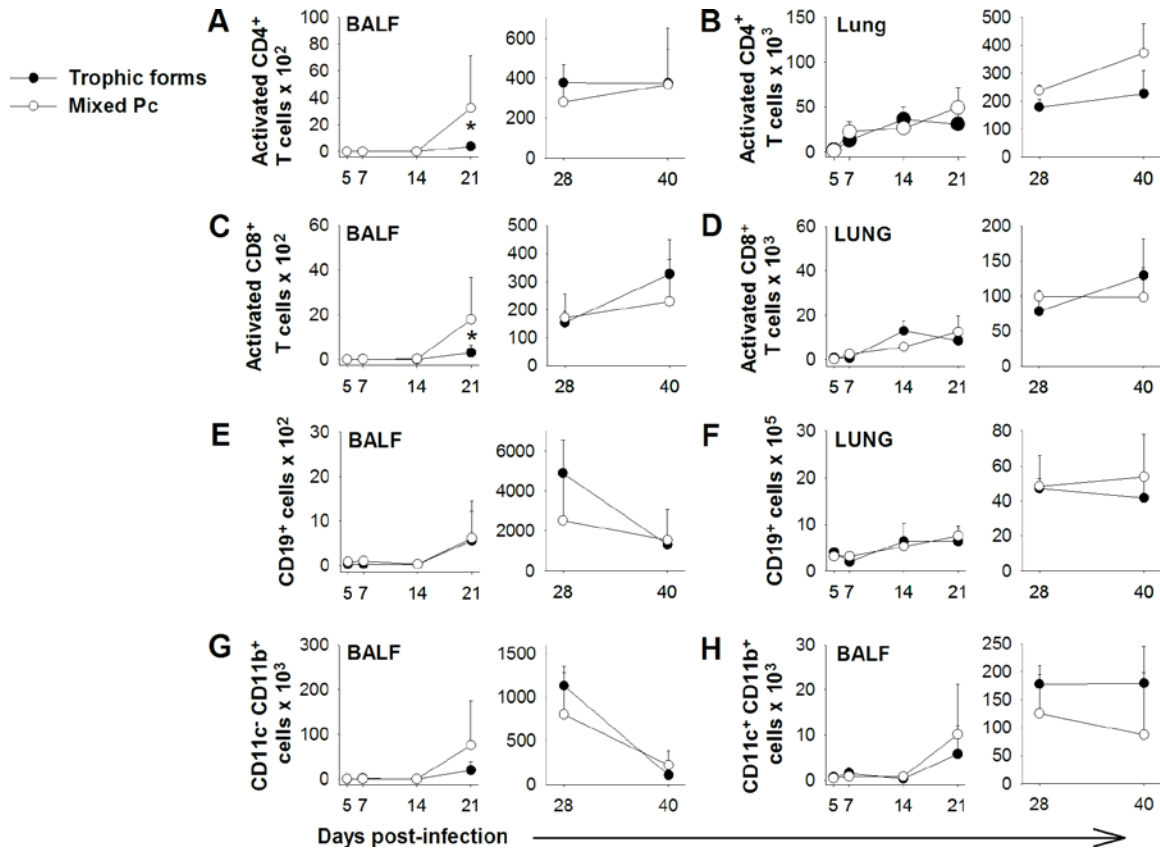
Figure 3-2 Cysts promote the recruitment of activated T cells in the BALF by day 21 post-infection in neonates.

Neonatal (24-72 h old) BALB/cJ mice were infected i.n. with 10^6 trophic forms or mixed *P. murina* organisms. Flow cytometry was used to phenotype activated CD44^{high} CD62L^{low} CD4^{+} T cells (**A, B**), activated CD44^{high} CD62L^{low} CD8^{+} T cells (**C, D**), and CD19^{+} B cells (**E, F**) in the BALF and lung digest. Flow cytometry was used to phenotype CD11c^{-} CD11b^{+} (**G**) and CD11c^{+} CD11b^{+} (**H**) non-lymphocytes with high granularity and size from the BALF. Data represent the mean ±SD of 3-4 mice per group and are representative of 2 separate experiments. T tests were used to compare mean total cell number between the groups at individual timepoints, *p ≤ 0.05.
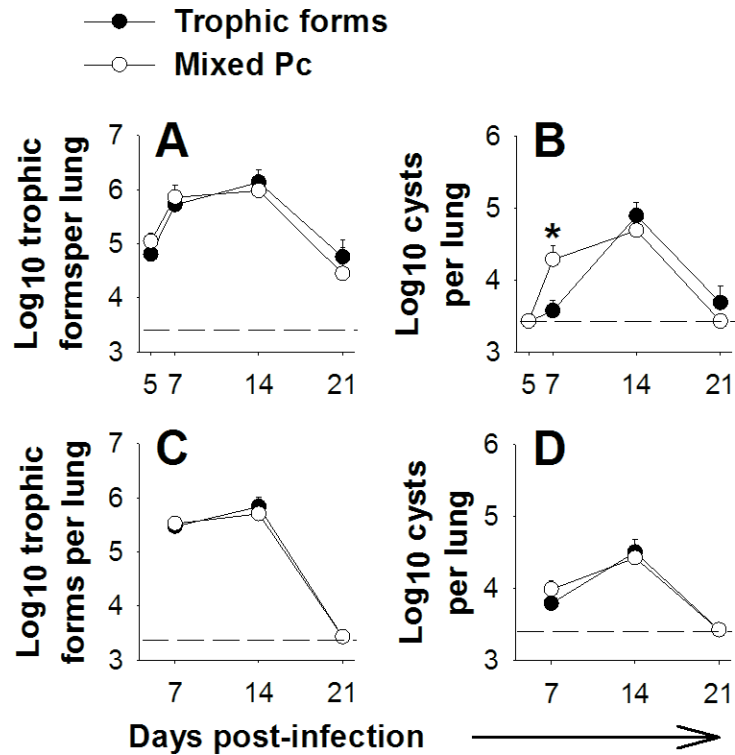
Figure 3-3 Cysts are undetectable before day 7 post-infection in BALB/cJ adults infected with *P. murina* trophic forms.

Adult mice were infected i.t. with 5 X 10^6 trophic forms or mixed *P. murina* organisms. Trophic (**A, C**) and cystic (**B, D**) lung burdens from two separate experiments were determined by enumeration of organisms on DiffQuik stained slides under a microscope. Data represent the mean ±SD of 5 mice per group. The limit of detection was Log_{10} 3.42 nuclei per adult right lung lobe. T tests were used to compare the mean fungal burden between the two groups at individual timepoints, *p ≤ 0.05.
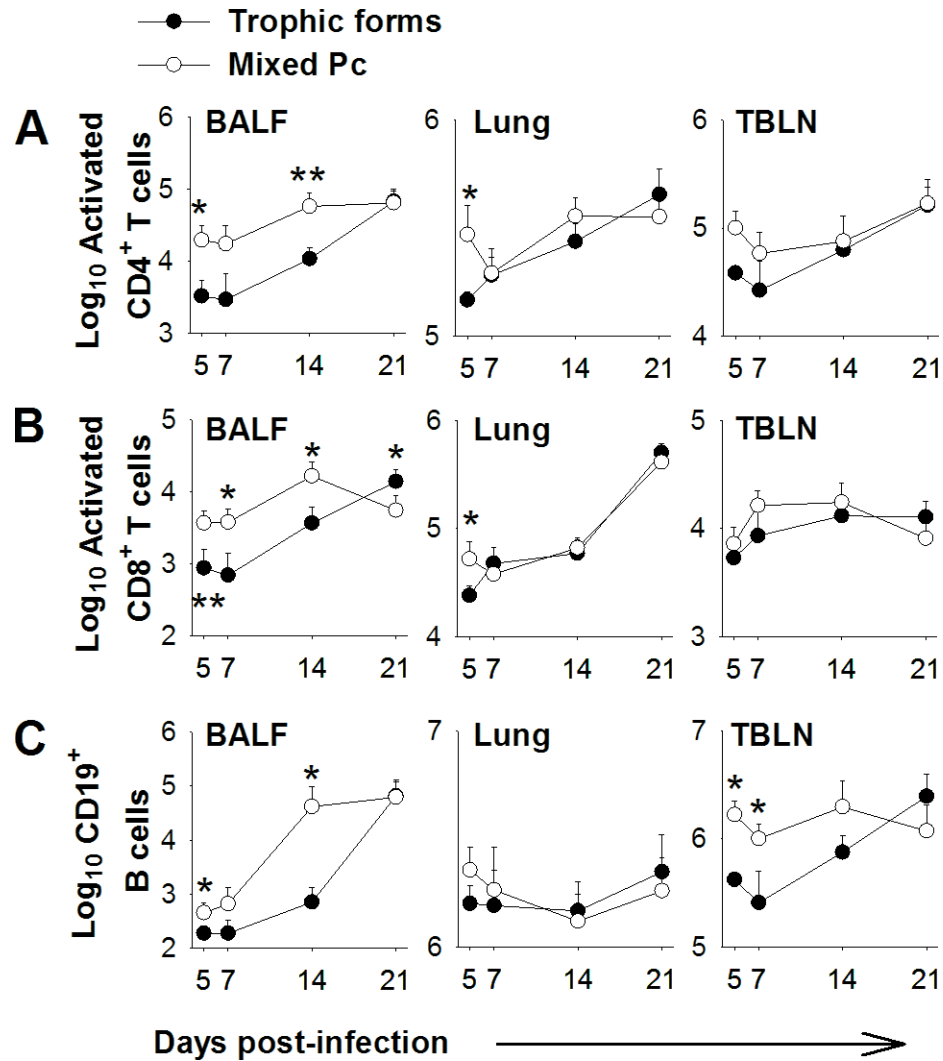
Figure 3-4 Infection with the cyst life cycle stage drives recruitment of T and B cells into the lungs of adult mice.

BALB/cJ adult mice were infected i.t. with 5 X 10^6 trophic forms or mixed *P. murina* organisms. Flow cytometry was used to phenotype activated CD4$^+$ T cells (**A**), activated CD8$^+$ T cells (**B**), and CD19$^+$ B cells (**C**) in the BALF, lung digest, and TBLN. Activation of T cells was evaluated by CD44 and CD62L expression. Data represent the mean ±SD of 5 mice per group and are representative of 2 separate experiments. T test was used to compare mean total cell number between the groups at individual timepoints, *p ≤ 0.05, **p ≤ 0.01, ***p ≤ 0.001.
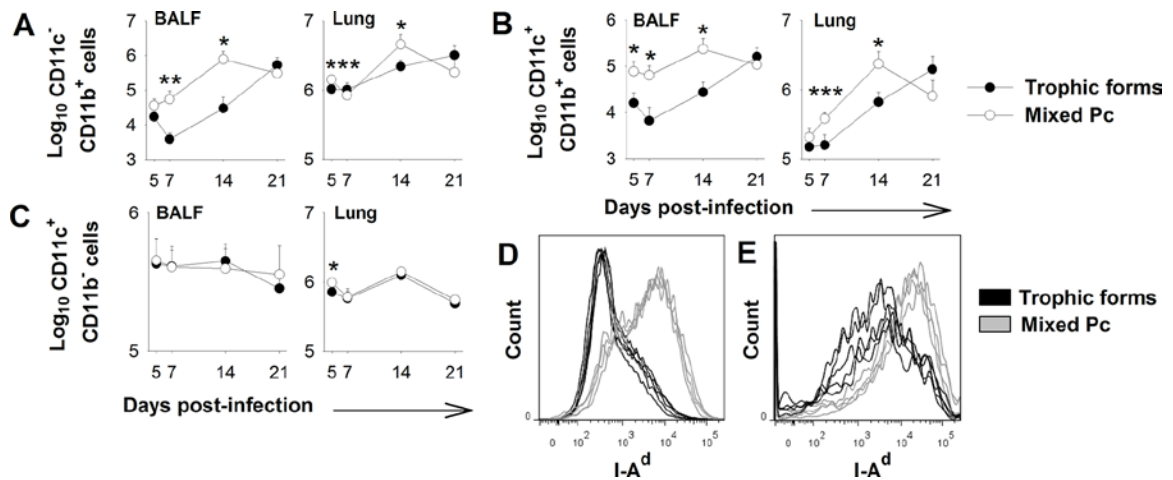
Figure 3-5 Cysts promote the early increase in CD11c$^+$ CD11b$^+$ innate immune cells and infiltration of CD11c$^-$ CD11b$^+$ innate immune cells into the alveolar spaces and lung parenchyma of adult mice.

BALB/cJ adult mice were infected i.t. with 5 X 10^6 trophic forms or mixed *P. murina* organisms. Flow cytometry was used to phenotype CD11c$^-$ CD11b$^+$ (**A**), CD11c$^+$ CD11b$^+$ (**B**) and CD11c$^+$ CD11b$^-$ (**C**) non-lymphocytes with high granularity and size from the BALF and lung digest. Flow cytometry was used to compare expression of the MHC class II molecule I-A^d on CD11c$^+$ CD11b$^-$ (**D**) and CD11c$^+$ CD11b$^+$ (**E**) cells in the BALF. Data represent the mean ±SD of 5 mice per group and are representative of 2 separate experiments. T tests were used to compare mean total cell number between the groups at individual timepoints, *$p \le 0.05$, **$p \le 0.01$, ***$p \le 0.001$.
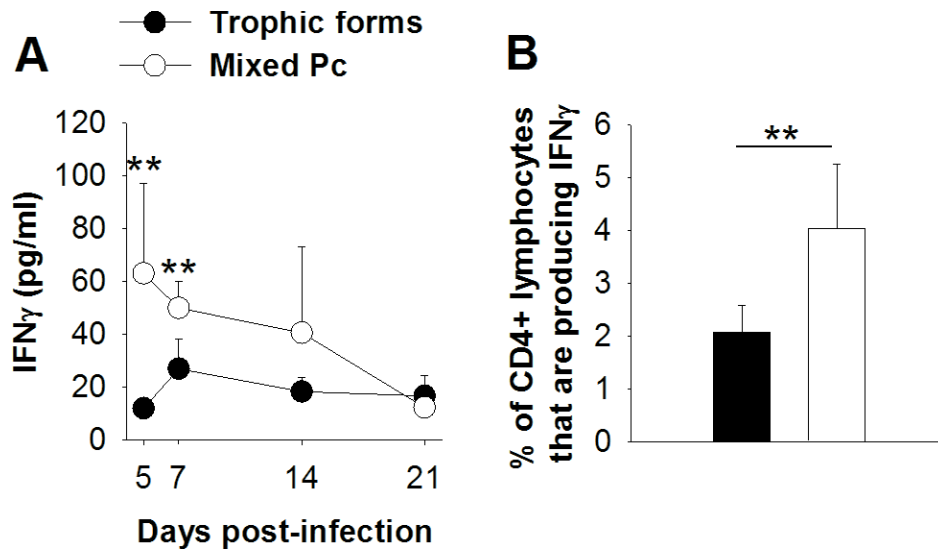
Figure 3-6 Cysts stimulate production of the proinflammatory T_h1-type cytokine IFN-γ in the lungs BALB/cJ adult mice.

Adult mice were infected i.t. with 5 X 10^6 trophic forms or mixed *P. murina* organisms. IFN-γ cytokine production in the supernatant of the first BALF wash was quantified by ELISA (**A**). Flow cytometry was used to evaluate intracellular IFN-γ expression in $CD4^+$ cells in the lung digest at day 7 post-infection (**B**). Data represent the mean ±SD of 5 mice per group and are representative of 2 separate experiments. T tests were used to compare BALF IFN-γ levels between the groups at individual timepoints (A) and to compare the percentage of $CD4^+$ T cells expressing IFN-γ between the groups (B), **p ≤ 0.01.
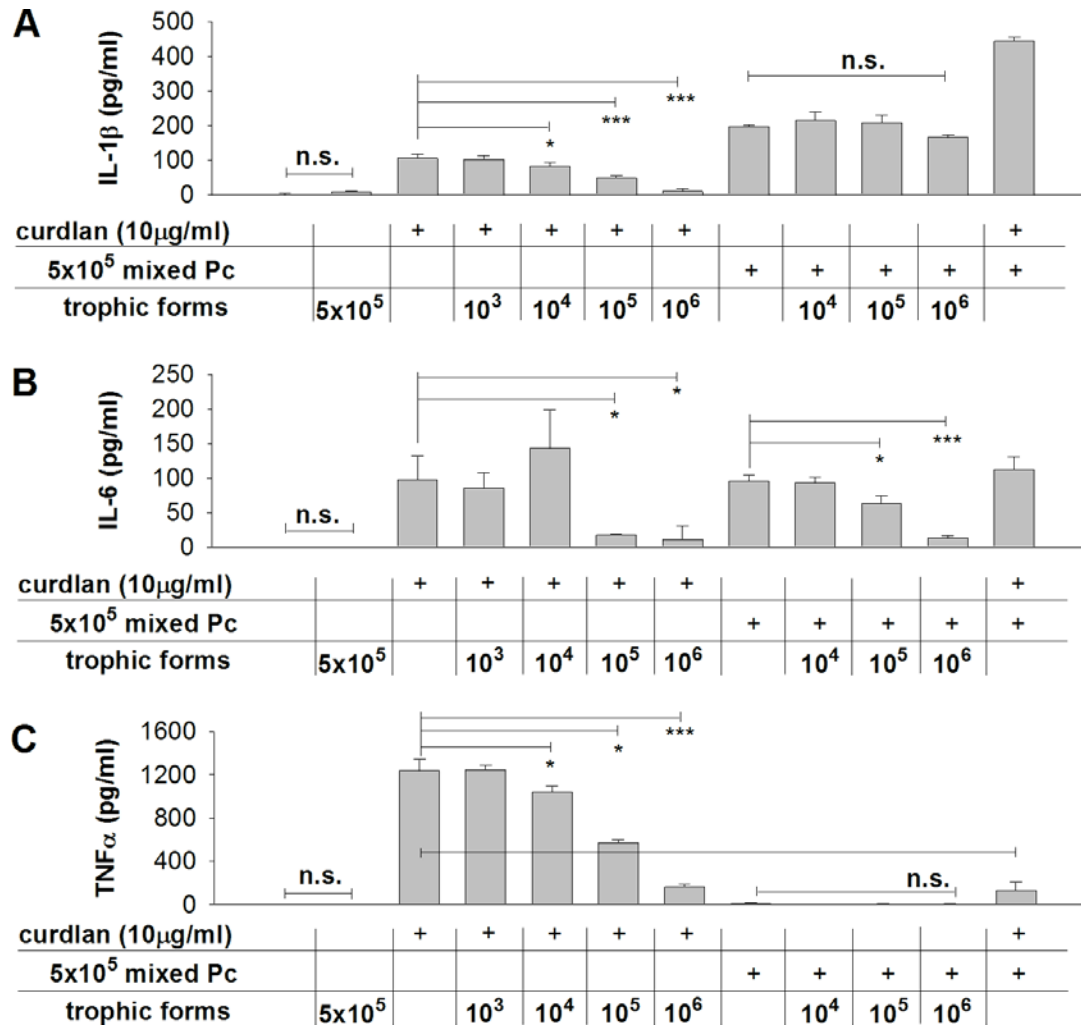
Figure 3-7 Cysts, but not trophic forms, stimulate production of the proinflammatory cytokines IL-1β and IL-6 by BMDCs *in vitro*.

BMDCs from adult BALB/cJ mice were incubated with 5 X 10^5 trophic forms or 5 X 10^5 mixed *P. murina* organisms for 72 h. Curdlan was included as a positive control for cytokine production. IL-1β (**A**), IL-6 (**B**), and TNFα (**C**) cytokine production was quantified by ELISA. Data represent the mean ±SD of 3 biological replicates per group and are representative of at least 2 separate experiments. One way ANOVA with Student-Newman-Keuls post-hoc test was used to compare supernatant cytokine concentration between the groups, *p ≤ 0.05, **p ≤ 0.01, ***p ≤ 0.001, n.s., not statistically significant.
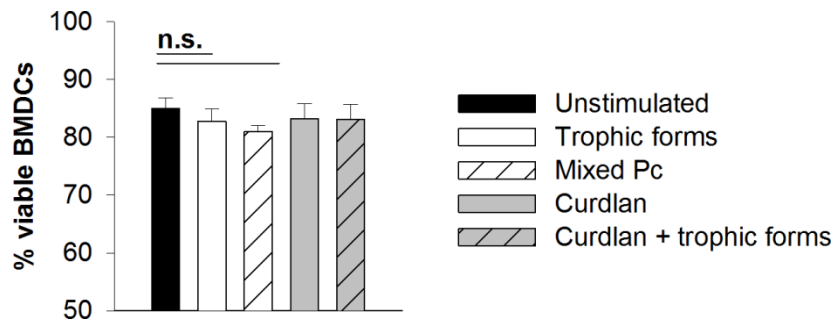
Figure 3-8 Incubation of BMDCs with trophic and cystic forms of *P. murina* does not impact cell viability.

BMDCs from adult BALB/cJ mice were incubated with 5×10^5 trophic forms, 5×10^5 mixed P. murina organisms, 10µg/ml curdlan or curdlan and trophic forms for 72 h. Trypan blue staining was used to determine the percentage of viable BMDCs. Data represent the mean ±SD of 3 biological replicates per group and are representative of 2 separate experiments. One way ANOVA with Student-Newman-Keuls post-hoc test was used to compare the percent of viable BMDCs between the groups, n.s., not statistically significant.
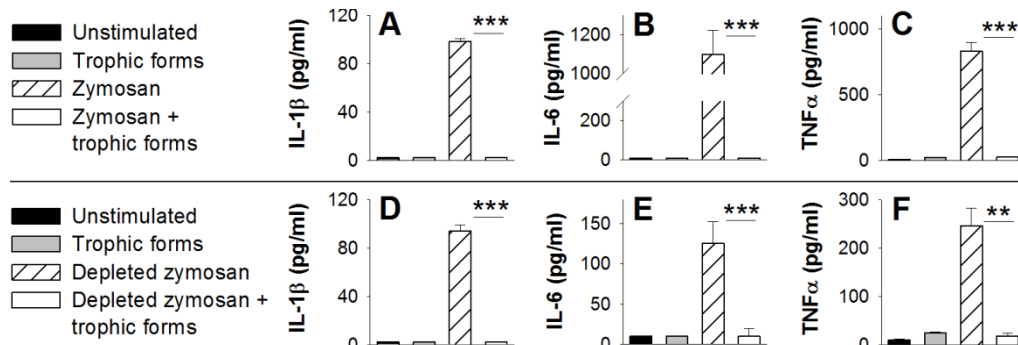
Figure 3-9 Trophic forms suppress the zymosan- and depleted zymosan-stimulated production of proinflammatory cytokines by BMDCs.

BMDCs from adult BALB/cJ mice were incubated with 5 X 10^5 trophic forms, 20µg/ml zymosan (**A-C**) and/or 20µg/ml depleted zymosan (D-F). IL-1β (**A, D**), IL-6 (**B, E**), and TNFα (**C, F**) cytokine production was quantified by ELISA. Data represent the mean ±SD of 3 biological replicates per group and are representative of 3 separate experiments. One way ANOVA with Student-Newman-Keuls post-hoc test was used to compare supernatant cytokine concentration between the groups, **p $\leq$ 0.01, ***p $\leq$ 0.001.
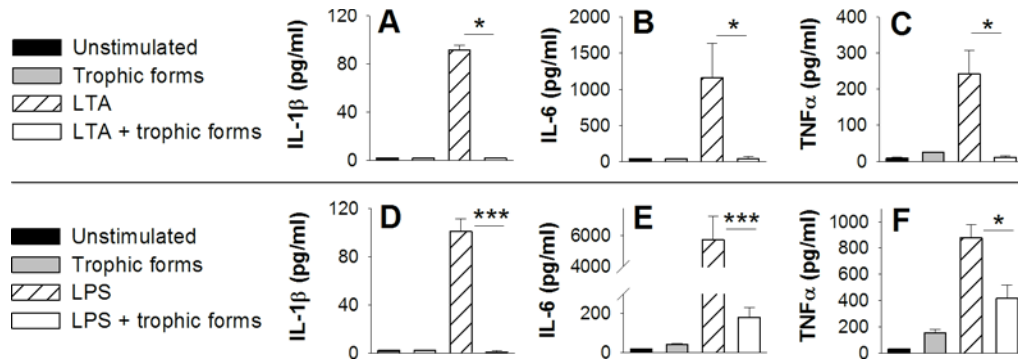
Figure 3-8 Trophic forms suppress LTA- and LPS-mediated cytokine production.

BMDCs from adult BALB/cJ mice were incubated with 5 X 10^5 trophic forms, 10µg/ml LTA (**A-C**), and/or 100ng/ml LPS (**D-F**) for 72 h. IL-1β (**A, D**), IL-6 (**B, E**), and TNFα (**C, F**) cytokine production was quantified by ELISA. Data represent the mean ±SD of 3 biological replicates per group and are representative of three separate experiments. One way ANOVA with Student-Newman-Keuls post-hoc test was used to compare supernatant cytokine concentration among the groups when the data were parametric (**D, E**), ***p $\leq$ 0.001. Kruskal-Wallis one-way ANOVA on ranks was used to compare differences among the groups when the data were nonparametric (**A, B, C, F**), *p $\leq$ 0.05.
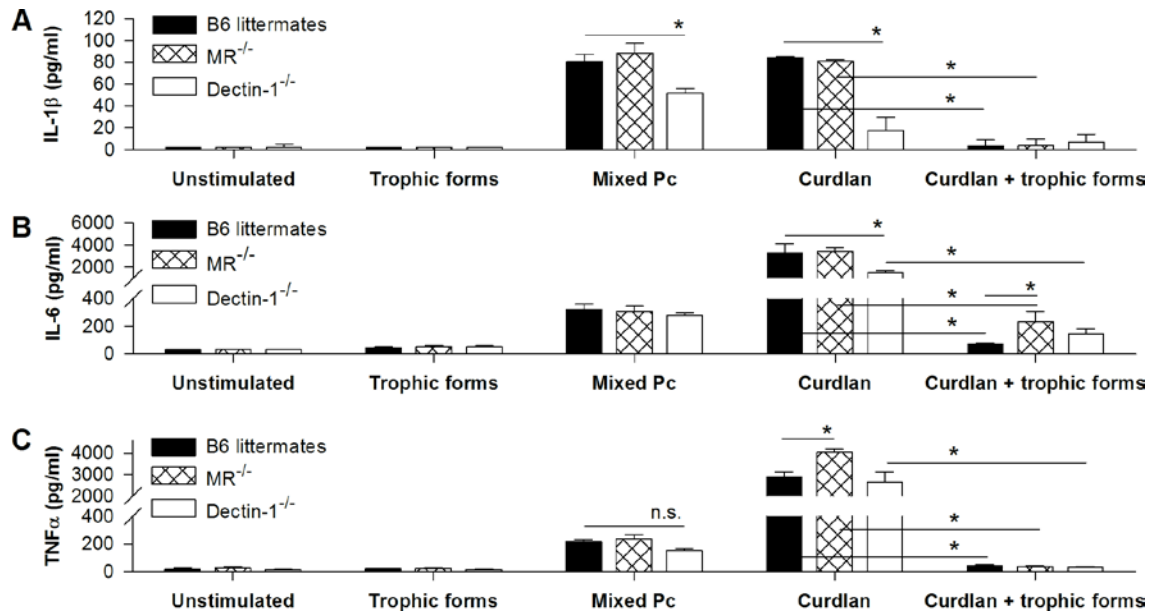
Figure 3-9 The response to trophic forms and cysts is not exclusively dependent on the C-type lectin receptors dectin-1 and mannose receptor.

BMDCs from wildtype C57BL/6 littermate controls, MR$^{-/-}$, and dectin-1$^{-/-}$ adult mice were incubated with 5 X 10^5 trophic forms or 5 X 10^5 mixed *P. murina* organisms for 72 h. Curdlan was included as a positive control for cytokine production. IL-1β (**A**), IL-6 (**B**), and TNFα (**C**) cytokine production was quantified by ELISA. Data represent the mean ±SD of 3 biological replicates per group and are representative of 3 separate experiments. Kruskal-Wallis one-way ANOVA on ranks was used to compare differences among the groups when the data were nonparametric, *p ≤ 0.05.
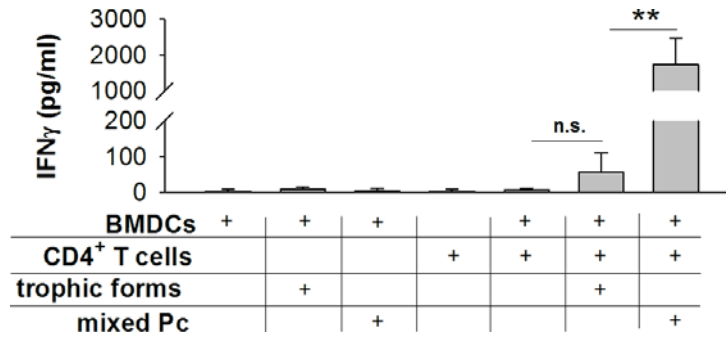
Figure 3-10 Cysts, but not trophic forms, stimulate production of the proinflammatory T$_h$1-type cytokine IFN-γ by CD4$^+$ T cells *in vitro*.

CD4$^+$ T cells and BMDCs from adult BALB/cJ mice were incubated with trophic forms or mixed *P. murina* organisms for 72 h. IFN-γ cytokine production was quantified by ELISA. Data represent the mean ±SD of 3 biological replicates per group and are representative of 3 separate experiments. One way ANOVA with Student-Newman-Keuls post-hoc test was used to compare supernatant IFN-γ concentration between the groups, **p ≤ 0.01, n.s., not statistically significant.

Chapter 4. The trophic life cycle stage of *Pneumocystis* species induces protective adaptive responses without inflammation-mediated progression to pneumonia.

I. Introduction

There are few reports that address how *Pneumocystis* trophic forms and cysts shape the development of the *in vivo* immune response. Previous studies demonstrate that dendritic cells treated with β-1,3-glucan from the cyst wall drive T_h1/T_h17-type CD4$^+$ T cell responses (23, 88). However, the clearance of *Pneumocystis* organisms from the host lung is dependent on a broad range of effector responses, including CD4$^+$ T cell, B cell, and macrophage activity (1-4). Furthermore, T_h2 and T_h17-type CD4$^+$ T cell responses may be generated in response to *Pneumocystis* infection, and clearance of the infection may be mediated by any of the T helper phenotypes within the $T_h1/T_h2/T_h17$ paradigm (24, 111-115).

In Chapter 3, we report that *Pneumocystis* trophic forms suppressed the production of proinflammatory cytokines IL-1β, IL-6, and TNFα by dendritic cells stimulated with a range of PAMPs, including β-glucan, LPS, LTA, zymosan, and depleted zymosan (168). Immunocompetent mice inoculated with purified trophic forms failed to initiate early innate and adaptive immune responses compared to mice inoculated with a mixture of trophic forms and cysts. Despite these delays, the mice inoculated with trophic forms were able to clear the infection within a similar period of time as the mice inoculated with mixed organisms. However, the rapid turnover of trophic forms into cysts in these previous experiments precludes the formation of conclusions regarding which life cycle stage(s) initiate the immune responses that led to clearance.

Basic research into the interactions between this fungal pathogen and the host immune response has the potential to inform novel approaches to reduce morbidity and mortality due to *Pneumocystis* pneumonia. In this Chapter, we sought to determine if trophic forms were capable of stimulating protective CD4$^+$ T cell and B cell responses to *P. murina* infection. Conversely, immune-mediated damage is a major consequence of *Pneumocystis* pneumonia. Therefore, we explored the role of trophic forms in the development of *Pneumocystis* pneumonia. These models employed the inoculation of immunocompetent mice with an enriched population of trophic forms coupled with treatment with a β-1,3-glucan synthesis inhibitor, anidulafungin, to prevent encystment.

Here, we demonstrate that the trophic stage of *P. murina* is sufficient to provoke CD4$^+$ T cell- and antibody-mediated responses leading to clearance of infection, but not progression to PcP. The adoptive transfer of CD4$^+$ T cells generated in the presence of trophic forms was sufficient to mediate the clearance of both trophic forms and cysts from the lungs of RAG2$^{-/-}$ mice. In addition, primary infection with trophic forms was sufficient for the development of antibody-mediated secondary responses leading to clearance of both trophic forms and cysts following reinfection. Recent studies demonstrate that protective immunization against *Pneumocystis* infection is a feasible goal, even in the context of SIV-induced immunosuppression or CD4$^+$ T cell depletion (175, 176). Here, our data suggest that trophic form-mediated immune suppression of innate responses does not impede the development of protective secondary adaptive responses. Conversely, our data suggest that the depletion of the cyst life cycle stage may be sufficient for protection against the inflammation-mediated pathology associated with PcP.

II. Results

Trophic forms are sufficient to provoke CD4$^+$ T cell-mediated clearance of infection.

Here, we employ an adoptive transfer model to evaluate the role of trophic forms in the generation of protective CD4$^+$ T cell responses. Briefly, we treated immunocompetent, wild-type mice ("donors") with the β-1,3-glucan synthesis inhibitor anidulafungin followed by infection with 10^6 purified trophic forms. The mice were treated with anidulafungin i.p. three times per week to prevent formation of the cystic stage, as initially described by Linke et al (24). A control group of mice were treated with saline and infected with a mixture of 10^6 *P. murina* trophic forms and cysts. The mixed *P. murina* inoculum consisted of 10 trophic forms to 1 cyst. CD4$^+$ T cells were isolated from the TBLN 14 days post-infection by positive selection. CD4$^+$ T cells were adoptively transferred by the retro-orbital route to RAG2$^{-/-}$ mice ("recipients"). Recipient mice were treated with either anidulafungin or saline i.p. followed by infection with 5 X 10^5 trophic forms or mixed organisms, respectively. Animals were euthanized at 15 and 30 days post-infection.

As expected, cysts were below the limit of detection in recipient mice treated with anidulafungin (**Fig 4.1A**). Mice that received trophic form-stimulated CD4$^+$ T cells followed by infection with trophic forms had more trophic forms in the lungs at day 15 post-infection compared to all other groups (**Fig 4.1A**). However, all of the recipient mice infected with trophic forms cleared their trophic burden by day 30 post-infection, while only one of four mice infected with mixed organisms cleared the infection by day 30 post-infection. A higher number of activated CD4$^+$ T cells were also observed at day 15

post-infection in the lung parenchyma of the group that received trophic form-stimulated CD4$^+$ T cells followed by infection with trophic forms compared to all other groups (**Fig 4.1B**). These differences were resolved by day 30 post-infection, and no differences in the numbers of activated CD4$^+$ T cells in the alveolar spaces (BALF) or TBLN were observed among the groups. These data indicate that trophic forms are sufficient to drive protective CD4$^+$ T cell responses capable of mediating the clearance of trophic organisms.

Trophic forms promote early CD4$^+$ T cell-mediated IFNγ production in response to infection with trophic forms in the absence of cysts.

Previous experiments by our lab suggest that co-culture of BMDCs with trophic forms is not sufficient for stimulation of IFNγ production by CD4$^+$ T cells (**Chapter 3**). However, adoptive transfer of CD4$^+$ T cells from trophic form-infected donors led to increased expression of IFNγ at day 15 post-infection in the alveolar spaces of recipient mice infected with trophic forms compared to adoptive transfer of CD4$^+$ T cells from mixed *P. murina*-infected donors into recipient mice infected with mixed *P. murina*. (**Fig 4.2**). Statistically significant differences were not observed amongst the groups in regards to TNFα, IL-13, and IL-17A production in the alveolar spaces (**Fig 4.2**). These data indicate that CD4$^+$ T cells generated in the presence of trophic forms are capable of mediating proinflammatory responses following adoptive transfer.

Trophic forms are sufficient to induce B cell-mediated clearance of *P. murina* infection.

Immunocompetent mice inoculated with purified trophic forms display delayed accumulation of B cells into the lungs compared to mice inoculated with a mixture of trophic forms and cysts (168). B cells are required for clearance of primary *P. murina* infection (3, 4). Here, we used a reinfection model with concurrent depletion of CD4$^+$ T cells to evaluate the role of trophic forms in the generation of protective B cell responses. We treated immunocompetent, wild-type mice with the β-1,3-glucan synthesis inhibitor anidulafungin, followed by infection with 3 X 10^6 purified trophic forms. Animals were treated with anidulafungin three times per week throughout the primary infection. Following clearance of the primary infection, anidulafungin treatment was stopped, and anti-CD4 antibody was administered to deplete CD4$^+$ T cells (**Fig 4.3A**). Mice were then treated with either anidulafungin or saline, and re-infected with 5 X 10^6 purified trophic forms or mixed *P. murina* organisms, respectively. Animals were euthanized at day 15 post-infection.

The memory B cell response to trophic forms was sufficient to drive the *P. murina* trophic forms and cysts burdens below the limit of detection (Log$_{10}$ 3.42) by day 15 post-infection (**Fig 4.3B**). No differences in the numbers of CD19$^+$ B cells in the alveolar spaces, lung parenchyma, and TBLN were observed between the mice rechallenged with trophic forms or mixed organisms (**Fig 4.3C**). Likewise, no differences were observed in the expression of the costimulatory molecules CD80 and CD86 on the surface of B cells (data not shown). Differences in the numbers of activated CD8$^+$ T cells in the BALF, lung parenchyma, and TBLN were not observed between the groups (data not shown).

These data indicate that trophic forms are sufficient to induce B cell-mediated clearance of trophic forms and cysts.

Serum antibody from trophic form- or mixed *P. murina*-infected mice binds mixed *P. murina* at higher titer than purified trophic forms.

Pneumocystis-specific antibody is protective against secondary infection, even in the absence of CD4$^+$ T cells (112, 121, 177). To test the specificity of the antibody produced in our B cell rechallenge model, serum was collected at day 15 post-rechallenge. The titer of serum IgG against sonicated mixed *P. murina* organisms was 1:5000, compared to a titer of 1:1000 against an equal protein concentration of sonicated trophic forms (**Fig 4.4**). A similar trend was observed when serum IgG was probed against an equal organism concentration of sonicated trophic forms vs mixed *P. murina* organisms (data not shown). The source of the serum (mice rechallenged with trophic forms vs mixed organisms), did not have an impact on the titer against trophic forms nor mixed organisms (**Fig 4.4**). These data are comparable to the anti-trophic form and anti-mixed organism titers of serum collected from immunocompetent mice following primary infection with mixed organisms (data not shown). These data suggest that serum antibody from *P. murina*-infected mice binds purified trophic forms with a lower affinity or avidity than cysts.

Trophic forms promote early antibody-mediated innate responses to infection with trophic forms in the absence of cysts.

B cells may enhance innate immunity to *Pneumocystis* organisms via antibody-mediated opsonization of the fungal organisms and by the production of cytokines and other signals to maximize antifungal responses (3, 178-180). Here, innate immune cells were phenotyped and quantified at day 15 post-infection in the lungs of CD4-depleted mice rechallenged with trophic forms or mixed *P. murina* (**Fig 4.5**). A 2-fold increase in activated macrophages and lung dendritic cells (CD11c$^+$ CD11b$^+$ innate immune cells) was observed at day 15 post-infection in the alveolar spaces of mice rechallenged with trophic forms (**Fig 4.5**). Differences in the numbers of immature alveolar macrophages and lung dendritic cells (CD11c$^+$ CD11b$^-$), and non-resident innate immune cells (CD11c$^-$ CD11b$^+$) were not observed between the groups (**Fig 4.5**). These data suggest differences in the kinetics of the macrophage or dendritic cell response following clearance of the secondary infection with trophic forms compared to mixed *P. murina* organisms.

Infection with trophic forms in the absence of cysts is not sufficient for progression to PcP in immunocompromised mice.

Pneumocystis pneumonia (PcP) is characterized by inflammation-mediated alveolar damage. Previously, we have shown that trophic forms suppress the production of pro-inflammatory cytokines by BMDCs (Chapter 3) and alveolar macrophages (multiple members of the Garvy lab, data not shown). Here, we evaluate the role of the trophic forms in the development of PcP using mice deficient in T and B cells. We hypothesized that infection with trophic forms in the absence of cysts would delay the onset of

inflammation-mediated PcP. Treatment of immune-reconstituted mice with the β-1,3-glucan synthase inhibitor anidulafungin results in depletion of *Pneumocystis murina* cysts (17). RAG2$^{-/-}$ mice were treated with anidulafungin or saline, followed by infection with 2 X 10^6 purified trophic forms (**Fig 4.6**). Anidulafungin or saline treatment was maintained through the experiment. Saline-treated control mice were euthanized at day 72 post-infection due to symptoms of advanced PcP, including severe weight loss (**Fig 4.6A**). In contrast, mice treated with anidulafungin had no overt symptoms of PcP, and continued to gain weight through the end of the study at day 120 post-infection (**Fig 4.6A**). The lungs of saline-treated control mice contained 8 X 10^7 trophic forms and 5 X 10^6 cysts at day 72 post-infection (**Fig. 4.6B**). No cysts were detected in the lungs of the anidulafungin-treated mice at day 120 post-infection (**Fig 4.6B**). A small population of 4 X 10^5 trophic organisms remained in the lungs of the anidulafungin-treated mice (**Fig 4.6B**).

T cells and B cells are required for clearance of *P. murina* organisms (1, 3, 4). In the absence of adaptive immunity, infection with mixed *P. murina* organisms induces non-protective inflammatory responses, including recruitment of innate immune cells (133, 134). We compared the innate immune responses in the alveolar spaces (BALF) and lung parenchyma of the saline- and anidulafungin-treated mice following euthanasia at day 72 and day 120 post-infection, respectively (**Fig 4.6C-E**). A direct comparison between the groups is not advisable due to the difference in study endpoints. Rather, the following data are presented as a snapshot of the lungs at the time of euthanasia. An average of 119 pg/ml TNFα was detected in the BALF of the saline-treated mice at day 72 post-infection, while the lavage of anidulafungin-treated mice contained an average of

17 pg/ml TNFα at day 120 post-infection (**Fig 4.6C**). The majority of the cells in the alveolar spaces and lung parenchyma of saline-treated mice were $CD11c^-$ $CD11b^+$ non-resident innate immune cells (**Fig 4.6D**). The bulk of cells within this population were $F4/80^{low}$ neutrophils (**Fig 4.6E**). In contrast, most of the cells in the alveolar spaces of the anidulafungin-treated groups were $CD11c^+$ $CD11b^-$ immature macrophages or dendritic cells (**Fig 4.6D**), and the majority of the $CD11c^-$ $CD11b^+$ non-resident cells were $F4/80^{high}$, indicating recruitment of monocytes or macrophages rather than myeloid-derived suppressor cells (MDSCs) or neutrophils (**Fig 4.6E**). These data indicate that cysts are required for the development of inflammatory responses associated with *Pneumocystis* pneumonia. Additionally, trophic forms are able to survive in immunocompromised lungs for extended periods of time in the absence of cysts and without being able to complete their life cycle.

III. Discussion

The data reported here confirm that the trophic stage of *P. murina* is sufficient to induce CD4^{+} T cell- and antibody-mediated responses leading to clearance of infection, but not progression to *Pneumocystis* pneumonia. We have previously reported that cysts are required for robust early innate and adaptive immune responses, including recruitment of CD4^{+} T cells and B cells into the alveolar spaces (168). While the magnitude of the early response was reduced in the animals inoculated with trophic forms alone, both the mice inoculated with trophic forms and the mice inoculated with mixed *P. murina* cleared the infection by 30 days post-inoculation (168). Previously we found that mice infected with trophic forms developed detectable cysts by day 7 in adult mice and day 14 post-infection in neonates (168). Because of this, we were unable to discern whether trophic forms failed to induce protective immune responses, or if the response to trophic forms was merely delayed. Here, we used the β-1,3-glucan synthase inhibitor anidulafungin to evaluate the adaptive and innate immune responses stimulated by trophic forms in the absence of cysts.

Both CD4^{+} T cells and B cells are required for clearance of *P. murina* during primary infection, but either CD4^{+} T cells or antibody are sufficient for clearance during secondary infection (1, 3, 4, 121, 124, 181). We report here that adoptive transfer of CD4^{+} T cells from trophic form- or mixed *P. murina*-infected animals was sufficient to mediate clearance of trophic forms in recipient mice. However, adoptive transfer of CD4^{+} T cells from trophic form- or mixed *P. murina*-infected animals was sufficient to mediate clearance of mixed *P. murina* in only one mouse among the group of four animals by day 30 post-infection. We have previously reported that transfer of CD4^{+} T cells from mixed

P. murina-infected animals is sufficient to mediate clearance of mixed *P. murina* organisms in RAG1$^{-/-}$ mice (124). Therefore, we predicted that mixed *P. murina*-stimulated CD4^{+} T cells would eventually mediate clearance of the infection, given sufficient time.

While macrophages are required for clearance of *Pneumocystis* organisms, these cells are not competent to resolve the infection in the absence of adaptive immunity (1-4). Here, a control population of RAG2$^{-/-}$ mice was infected with mixed *Pneumocystis* organisms and treated with saline, but were not given CD4^{+} T cells. As expected, this group contained a relatively high average fungal burden of 9.89 X 10^{6} trophic forms and 8.69 X 10^{5} cysts at day 30 post-infection, with an average of 11.4 trophic forms to cysts (data not shown). This population reconfirms that the adoptive transfer of CD4^{+} T cells is required for the control of fungal growth. In addition, this control population demonstrates that while the majority of the CD4^{+} T cell recipient mice failed to clear the mixed *P. murina* organisms by day 30 post-infection, the adoptive transfer of CD4^{+} T cells was sufficient to limit fungal growth. This observation is consistent with our prediction that the transfer of *P. murina*-stimulated CD4^{+} T cells would eventually mediate clearance of the mixed *P. murina* infection, given sufficient time. Furthermore, we and others have reported clearance of mixed P. murina infection following adoptive transfer of CD4^{+} T cells in similar models.

Intriguingly, our data suggest that the CD4^{+} T cell-mediated clearance of trophic forms during secondary infection occurs more rapidly in the absence of cysts. This phenomenon occurs independently of the composition of the priming infection. Our previous evidence indicates that cysts enhance, rather than inhibit the inflammatory

response (168). Therefore, we suggest that the more efficient clearance of trophic forms observed in the absence of cysts may be due to slower growth kinetics of trophic forms in the absence of cysts. Linke *et al*. demonstrate that anidulafungin does not limit the expansion of trophic forms during the first two weeks of treatment (24). However, our long-term anidulafungin model (**Fig 4.6**) demonstrates poor expansion of the trophic population due to the prolonged absence of the cyst stage. In the absence of anidulafungin, a single mature cyst produces eight progeny which develop into trophic forms. Clearance of the trophic population by immune cells may be accelerated in the absence of this source of nascent trophic forms.

Previously reported data demonstrate that cysts are required for robust numbers of activated CD4$^+$ T cells within the alveolar spaces and lung parenchyma of infected animals (168). However, we report here that the adoptive transfer of trophic form-stimulated CD4$^+$ T cells leads to increased numbers of activated CD4$^+$ T cells in the lung parenchyma of recipient mice at day 15 post-infection compared to transfer of CD4$^+$ T cells from mixed infection. It is noteworthy that fewer CD4$^+$ T cells were harvested from the draining lymph nodes of the wild-type donor mice infected with trophic forms compared to mixed *P. murina* infection (data not shown). However, the adoptive transfer of equal numbers of CD4$^+$ T cells reveals that these CD4$^+$ T cells are fully capable of mediating clearance.

Our previous data indicated that inoculation with trophic forms leads to fewer IFN-γ-producing CD4$^+$ T cells and suboptimal IFN-γ concentrations in the alveolar spaces compared to inoculation with mixed *P. murina* (168). Furthermore, trophic form-stimulated BDMCs failed to produce TNFα, IL-1β, and IL-6 in response to various other

stimuli, and failed to induce IFNγ production during co-culture with CD4$^+$ T cells (168). Conversely, the data reported here shows that trophic forms are sufficient to drive CD4$^+$ T cell-mediated TNFα, IFN-γ, and IL-13 production *in vivo*. These data suggest that stimulation with trophic forms does not skew the immune response away from T$_h$1 or T$_h$2-type responses. While T$_h$17 responses are critical for control of many fungal infections, including candidiasis, a mixed T helper response is observed in response to *Pneumocystis* infection. This mixed response appears to be largely redundant, as T$_h$1-, T$_h$2-, and T$_h$17-type responses have all been associated with clearance of *P. murina* organisms (24, 111-115). Cumulatively, our data suggest that trophic forms suppress the development of innate immunity, and thus delay the initiation of adaptive responses (168), but trophic forms do not have a direct suppressive effect on CD4$^+$ T cells *in vivo*.

We have reported that cysts are required for an early increase in B cells in the lungs of infected mice (168). However, here we report that primary infection with trophic forms is sufficient to induce antibody-mediated clearance of *P. murina* trophic forms and cysts during secondary infection. No differences in B cell count were observed in the animals rechallenged with trophic forms or mixed *P. murina*. Rechallenge of CD4$^+$ T cell-depleted mice with trophic forms promoted increased numbers of activated macrophages and dendritic cells (CD11c$^+$ CD11b$^+$) in the alveolar spaces compared to mice rechallenged with mixed *P. murina*. However, these data were generated by a single timepoint following clearance (day 15), and differences between the groups may be due to the kinetics of clearance, rather than differences in the magnitude of the response.

Intriguingly, serum antibody bound sonicated mixed *P. murina* antigen at higher titer than trophic antigen. This phenomenon was observed even in serum from

anidulafungin-treated animals that had never developed cysts. Previous studies suggest that there is significant overlap in the glycoproteins, including glycoprotein A (gpA, alternatively, major surface glycoprotein, MSG), on the surface of trophic forms and cysts (20, 165). Our data suggest that serum antibody raised against trophic forms binds conserved material on the cyst life cycle stage. We also observe that serum antibody collected during primary infection in immunocompetent mice bound cysts at higher titer than trophic form, as confirmed by fluorescent microscopy (data not shown). These data indicate that treatment of trophic forms or cysts with anidulafungin was not responsible for the decreased titer of serum antibody against trophic antigen. Rather, these observations again suggest that there may be differences in the identity or quantity of the antigenic material present on the trophic forms and cysts. Alternatively, trophic forms may modulate the T helper response, resulting in the reduction or elimination of a subset of IgG isotypes, leading to a net reduction of total IgG, but not necessarily a reduction in protection. Regardless, our data indicate that while serum antibody binds mixed *P. murina* antigen at higher titer than trophic forms, antibody-mediated responses are sufficient for clearance of both trophic forms and cysts.

While the initiation of innate and adaptive responses is required for clearance of *Pneumocystis* organisms in immunocompetent hosts, the non-specific provocation of inflammation leads to immune-mediated damage in immunocompromised hosts that progress to *Pneumocystis* pneumonia (133, 134). It has been previously reported that treatment of immune-reconstituted mice with the β-1,3-glucan synthase inhibitor anidulafungin results in depletion of cysts and a reduced inflammatory response (24). Here, we report that long-term anidulafungin treatment of trophic form-infected RAG2$^{-/-}$

mice results in the carriage of a relatively small population of trophic forms without progression to pneumonia. Control RAG2$^{-/-}$ mice developed cysts and progressed to pneumonia characterized by weight loss, and recruitment of neutrophils into the lungs. In contrast, the majority of innate immune cells within the alveolar spaces of anidulafungin-treated mice were immature alveolar macrophages and lung dendritic cells.

Linke et al., propose that depletion of cysts would reduce inflammation-induced lung damage in patients, and our data further corroborates this suggestion (24). However, our data highlight the need for a greater understanding of the impact of trophic forms on inflammatory responses and host health. While no overt symptoms of pneumonia were detected in our anidulafungin-treated mice, it has been reported that trophic forms induce direct damage to alveolar epithelial cells due to attachment to the host cell membrane (132). Further studies should evaluate the effect of a chronic infection with trophic forms on the health of alveolar epithelium.

In our model, the fungal lung burden of RAG2$^{-/-}$ mice with severe pneumonia may consist of as many as 1×10^8 trophic forms. It is unclear why the expansion of trophic forms was limited in RAG2$^{-/-}$ mice during long-term treatment with anidulafungin. Cushion *et al*, demonstrate that a short-term course of β-1,3-glucan synthase inhibitor therapy does not hamper expansion of trophic forms (17, 24). However, the extended time course of our study suggests that cysts enhance the growth of the trophic forms.

It is thought that the formation of the cyst requires sexual reproduction, and it is possible that the growth of the fungus is severely limited when the trophic forms are restricted to asexual reproduction (13). Meiosis followed by multiple rounds of mitosis within the maturing cyst results produces eight progeny, which develop into trophic

forms. In the absence of this rapid expansion of organisms via sexual reproduction, it is possible that innate immune cells may kill enough of the trophic forms to limit the growth of the population, but not enough to clear the organisms from the lungs.

Alternatively, a signal or product from the cyst or cyst-stimulated host cells may be required for expansion of trophic forms. Trophic forms are found clustered within a biofilm-like substance that includes material from previously ruptured cysts (14). Depletion of cysts may deprive the trophic forms of this protective shelter, and may permit killing of trophic forms by innate immune cells.

Whatever the mechanism, it is interesting that in an immunosuppressed environment the trophic population persists in the absence of cysts. This indicates that long-term exposure to trophic forms is insufficient to promote widespread activation of lung immune cells, including macrophages, in the absence of signals from T cells and B cells. Furthermore, this may suggest that trophic forms also suppress the production of proinflammatory signals, including cytokines, by alveolar epithelial cells. In Chapter 5, we will demonstrate that dendritic cells are capable of phagocytosing trophic forms. It is possible that, in the absence of the cyst, the trophic population may be limited by random encounters with phagocytes. These encounters may result in the destruction of individual trophic forms, but may serve to suppress the activation of the immune cell and thereby protect the trophic population as a whole. It should also be noted that the long-term carriage of trophic forms results in the infiltration of a population of $CD11c^{-}$ $CD11b^{+}$ cells that are overwhelmingly $F4/80^{high}$. This suggests that trophic forms do not mediate immune suppression by recruiting $F4/80^{low}$ myeloid-derived suppressor cells.

These observations emphasize the need for an improved understanding of the life cycle of *Pneumocystis* species, and the role of the trophic and cystic lifeforms in the development of protective vs detrimental immune responses. The data presented herein suggest that disruption of cyst development (and, thus the elimination of the progeny from sexual reproduction), limits the growth of *Pneumocystis* trophic form and prevents the development of *Pneumocystis* pneumonia. Future studies should evaluate the consequences of long-term carriage of trophic populations within the host lung. Relatively few human populations suffer from an immunodeficient state as pronounced as that modeled in the $RAG2^{-/-}$ mice, thus, additional animal models of immunodeficiency may be employed to identify patient populations capable of clearing this small population of trophic forms. In these populations, treatment with anidulafungin or other echinocandins may remove the threat of immune-mediated lung damage, while providing an opportunity for the host to develop a more modest, yet effective immune response to the trophic population, as Linke *et al.* demonstrated in their model of immune reconstitution syndrome (24).

We have previously reported that infection with trophic forms in the absence of cysts leads to the delayed initiation of innate and adaptive responses against *Pneumocystis* infection (168). Despite these delays, we found here that the trophic stage of *P. murina* is sufficient to induce $CD4^+$ T cell- and antibody-mediated responses leading to clearance of infection, but not progression to *Pneumocystis* pneumonia, as defined by severe weight loss and infiltration of innate immune cells into the lungs. These data suggest that immune evasion by the trophic forms may hinge on the suppression of the initiation of the innate immune response. The development of adaptive

immunity may represent a "point of no return" at which the trophic forms are no longer able to escape clearance.

Manipulation of the immune response to trophic forms and cysts may provide new options for the treatment and prevention of *Pneumocystis* infection, while a failure to consider these differential responses may hamper future efforts. Here, our data indicate that trophic forms elicit adaptive responses, but do not provoke the non-protective inflammation characteristic of *Pneumocystis* pneumonia. Further evaluation of the antigenic determinants on trophic forms and cysts may elicit a vaccine that provides protection while limiting immune-mediated damage, including immune reconstitution syndrome.
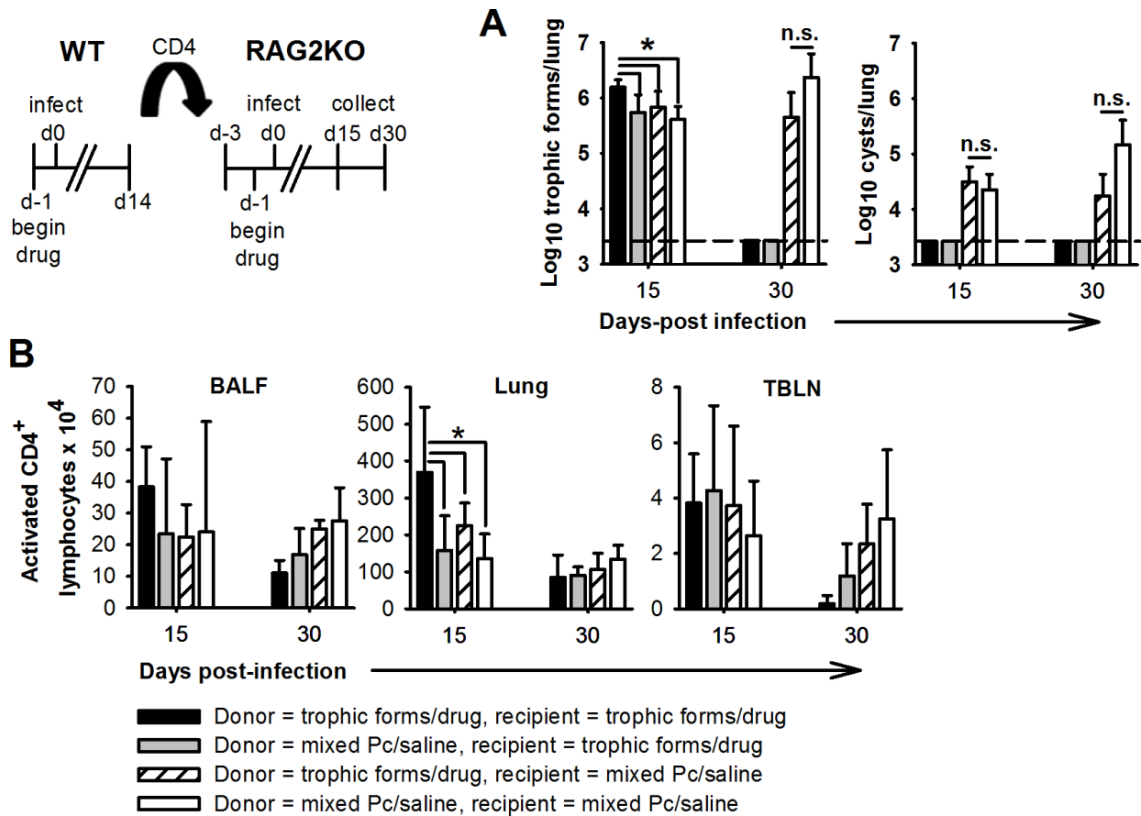
Figure 4-1 Infection with trophic forms is sufficient to provoke CD4$^+$ T cell-mediated clearance of *P. murina* trophic forms.

CD4$^+$ T cells were adoptively transferred from trophic form or mixed *Pneumocystis*-infected BALB/c mice (donors) to RAG2KO mice (recipients). Recipient mice were challenged with trophic forms or mixed *Pneumocystis* organisms. Both donor and recipient mice were treated with anidulafungin or saline throughout the study to maintain trophic or mixed *Pneumocystis* burdens, respectively. Fungal lung burdens (**A**) in the right lung lobes were determined by enumeration of organisms on DiffQuik stained slides under a microscope. Flow cytometry was used to phenotype activated CD44^{high} CD62L^{low} CD4$^+$ T cells (**B**) in the BALF, lung digest, and TBLN. Data represent the mean ±SD of 4 mice per group and are representative of 2 separate experiments. Kruskal-Wallis one-way ANOVA on ranks with Student-Newman-Keuls post-hoc test was used to compare differences among the groups at individual timepoints when the data were nonparametric (**A**). Two-way ANOVA with Student-Newman-Keuls post-hoc test was used to compare cell numbers where the data were parametric (**B**), *$p \leq 0.05$.
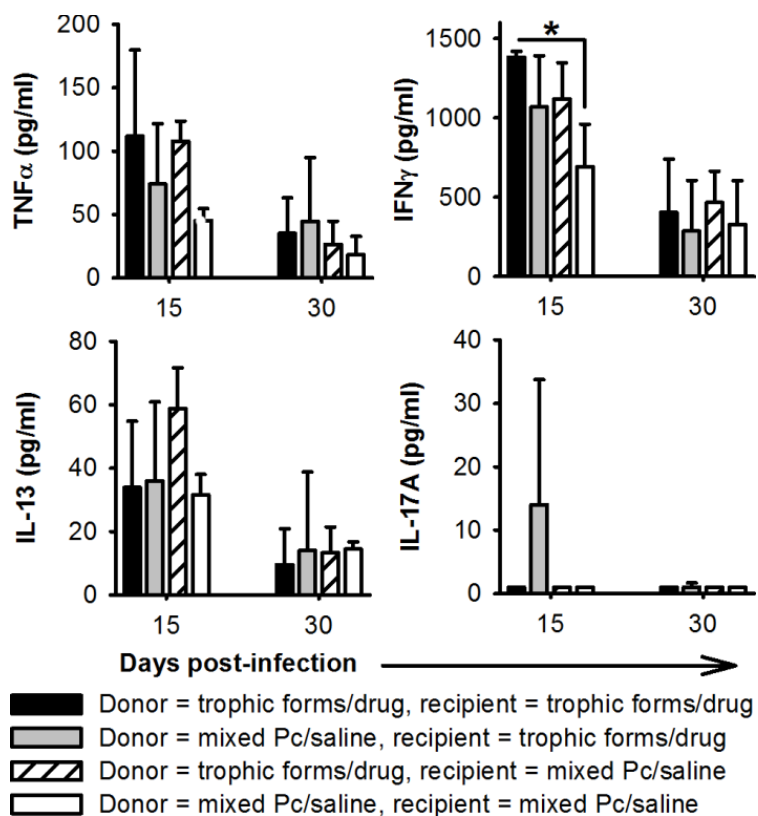
Figure 4-2 Transfer of CD4^{+} T cells from trophic form-infected mice promotes increased production of IFNγ in recipient mice challenged with trophic forms, compared to challenge with mixed *Pneumocystis* organisms.

CD4^{+} T cells were adoptively transferred from trophic form or mixed *Pneumocystis*-infected BALB/c mice (donors) to RAG2KO mice (recipients). Recipient mice were challenged with trophic forms or mixed *Pneumocystis* organisms. Both donor and recipient mice were treated with anidulafungin or saline throughout the study to maintain trophic or mixed *Pneumocystis* burdens, respectively. TNFα, IFNγ, IL-13, and IL-17A concentrations in the supernatant of the first BALF wash were quantified by ELISA. Data represent the mean ±SD of 4 mice per group and are representative of 2 separate experiments. Two-way ANOVA with Student-Newman-Keuls post-hoc test was used to compare cytokine expression, *$p \leq 0.05$.
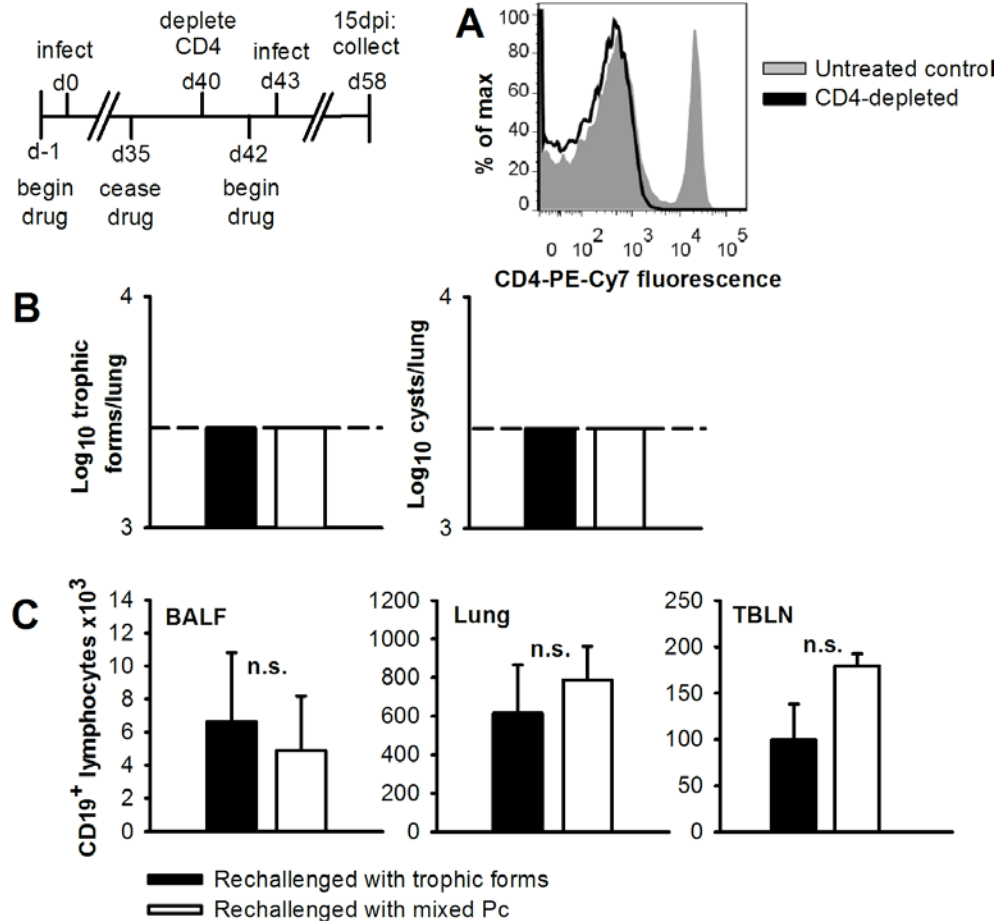
Figure 4-3 Infection with trophic forms is sufficient to provoke antibody-mediated clearance of *P. murina* trophic forms and cysts.

BALB/c adult mice were infected i.t. with trophic forms. Mice were treated with anidulafungin one day prior to infection, and three times per week thereafter until d35 post-infection. Anti-CD4 antibody was administered at d40 post-infection to deplete $CD4^+$ T cells. The depletion of $CD4^+$ T cells was confirmed by flow cytometry three days after treatment with the first dose of anti-CD4 monoclonal antibody (**A**). Treatment with anidulafungin or saline resumed one day prior to rechallenge with trophic forms or mixed *P. murina* organisms, respectively. The depletion of $CD4^+$ T cells was confirmed by flow cytometry on lung homogenate at d43 (**A**). Animals were euthanized 15 days after rechallenge. Fungal lung burdens (**B**) in the right lung lobes were determined by enumeration of organisms on DiffQuik stained slides under a microscope. The limit of detection was Log_{10} 3.42 organisms per adult right lung lobe. Flow cytometry was used to phenotype $CD19^+$ B cells (**C**) in the BALF, lung digest, and TBLN. Data represent the mean ±SD of 3 mice per group and are representative of 2 separate experiments. T tests were used to compare mean fungal burden or total cell number between the groups, *$p \leq$ 0.05.
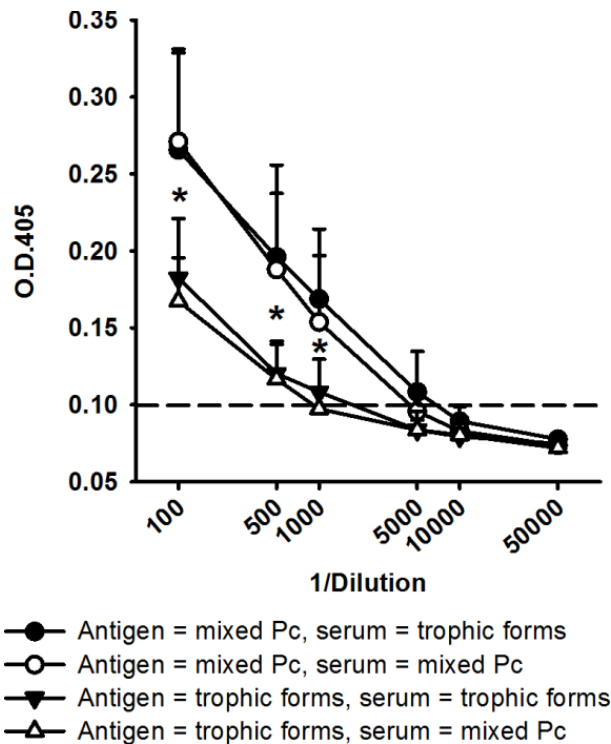
Figure 4-4 Serum antibody collected from trophic form or mixed *P. murina*-infected mice binds trophic forms at lower titer than mixed *P. murina*.

BALB/c adult mice were infected i.t. with trophic forms. Mice were treated with anidulafungin one day prior to infection, and three times per week thereafter until d35 post-infection. Anti-CD4 depleting antibody was administered at d40 post-infection. Treatment with anidulafungin or saline resumed one day prior to rechallenge with trophic forms or mixed *P. murina* organisms, respectively. Animals were euthanized 15 days after rechallenge, and serum antibody was collected. ELISAs were performed on serum to determine the level of trophic form- or mixed *Pneumocystis*-specific IgG. Serum was probed against equal protein concentrations of sonicated trophic or mixed P. murina antigen. Data are expressed as the optical density at 405 nm. Data represent the mean ±SD of 3 mice per group and are representative of 2 separate experiments. Kruskal-Wallis one-way ANOVA on ranks with Student-Newman-Keuls post-hoc test was used to compare mean optical density at 405nm between trophic antigen and mixed antigen groups at individual dilutions, $*p \leq 0.05$.
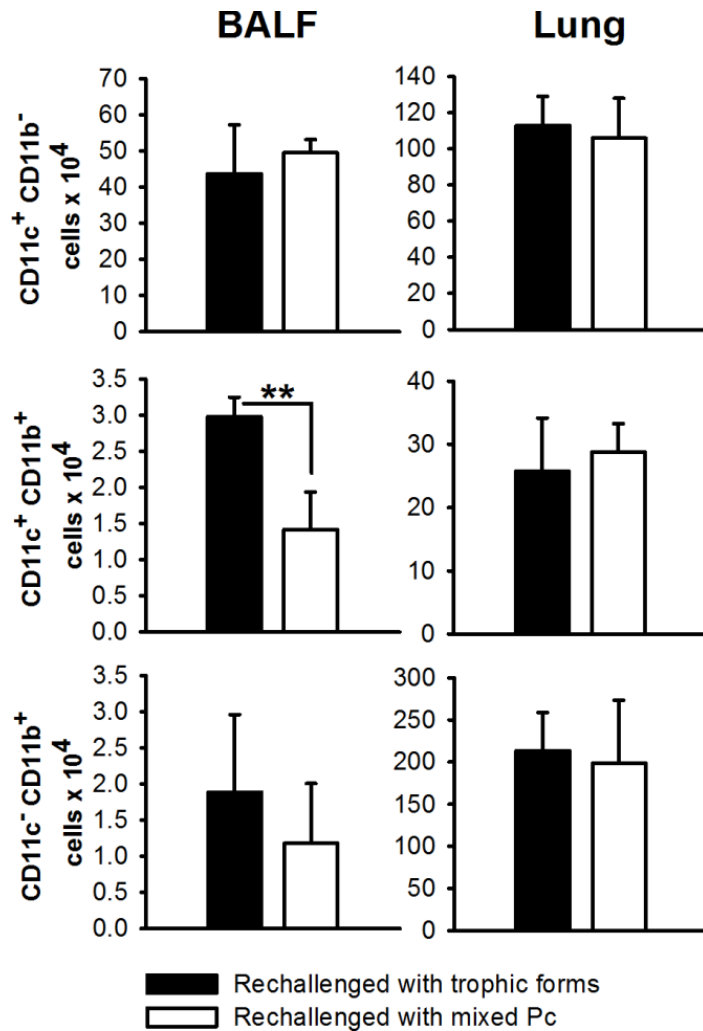
Figure 4-5 The antibody-mediated secondary response to trophic forms promotes an increase in CD11c⁺ CD11b⁺ innate immune cells in the alveolar spaces.

BALB/c adult mice were infected i.t. with trophic forms. Mice were treated with anidulafungin one day prior to infection, and three times per week thereafter until d35 post-infection. Anti-CD4 depleting antibody was administered at d40 post-infection. Treatment with anidulafungin or saline resumed one day prior to rechallenge with trophic forms or mixed *P. murina* organisms, respectively. Animals were euthanized 15 days after rechallenge. Flow cytometry was used to phenotype $CD11c^+$ $CD11b^-$, $CD11c^+$ $CD11b^+$ and $CD11c^-$ $CD11b^+$ non-lymphocytes with high granularity and size from the BALF and lung digest. Data represent the mean ±SD of 3 mice per group and are representative of 2 separate experiments. T tests were used to compare mean total cell number between the groups, $**p \leq 0.01$.
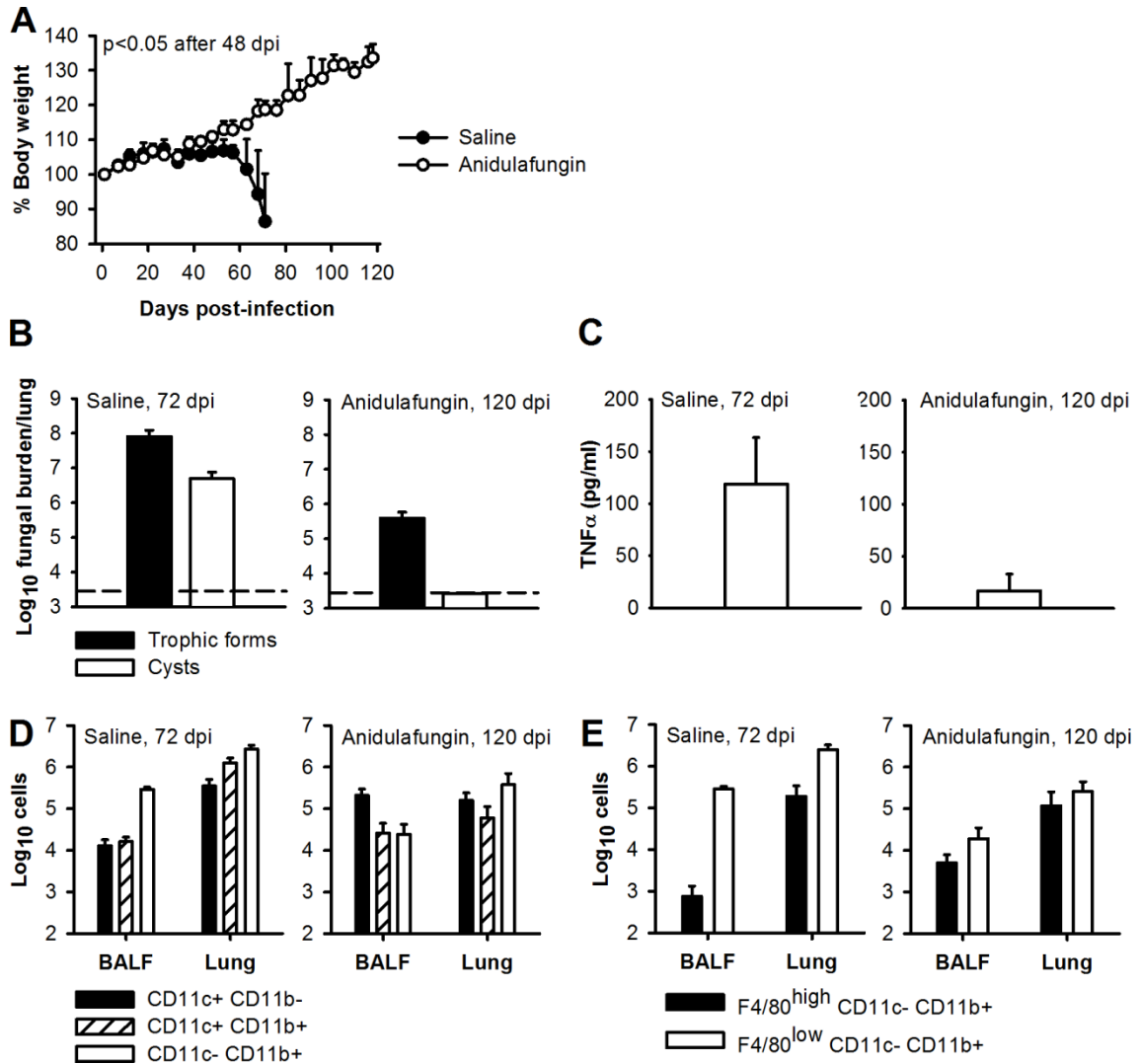
Figure 4-6 Cysts are required for progression to pneumonia in immunocompromised mice infected with *P. murina*.

RAG2KO mice were treated with anidulafungin or saline, followed by infection with 2 X 10^6 purified trophic forms. Anidulafungin or saline treatment was maintained through the experiment. Saline-treated control mice were euthanized at day 72 post-infection due to symptoms of advanced PcP. Mice treated with anidulafungin were euthanized at day 120 post-infection. The change in average body weight was recorded (**A**). Fungal lung burdens (**B**) in the right lung lobes were determined by enumeration of organisms on DiffQuik stained slides under a microscope. TNFα concentrations in the supernatant of the first BALF wash were quantified by ELISA (**C**). Flow cytometry was used to phenotype CD11c$^+$ CD11b$^-$, CD11c$^+$ CD11b$^+$ and CD11c$^-$ CD11b$^+$ non-lymphocytes with high granularity and size from the BALF and lung digest (**D**). CD11c$^-$ CD11b$^+$ cells were further phenotyped by flow cytometry on the basis of F4/80 expression (**E**). Data represent the mean ±SD of 3 mice per group and are representative of 2 separate

experiments. T tests were used to compare body weight between the groups at individual timepoints, *p ≤ 0.05.

Chapter 5: The trophic life cycle stage of the opportunistic fungal pathogen *Pneumocystis murina* hinders the ability of dendritic cells to stimulate CD4+ T cell responses

The following chapter is modified from: Evans HM, Simpson A, Shen S, Stromberg AJ, Pickett CL and Garvy BA. 2017. The trophic life cycle stage of the opportunistic fungal pathogen *Pneumocystis murina* hinders the ability of dendritic cells to stimulate CD4+ T cell responses. Infect Immun. In press. doi:10.1128/IAI.00396-17.

I. Introduction

In Chapter 3, we have reported that the life cycle stages of *Pneumocystis murina* have opposing effects on the immune response (168). The immune response to infection with *P. murina* trophic forms alone was less robust than the response to infection with a physiologically normal mixture of cysts and trophic forms. Infection with trophic forms alone resulted in reduced numbers of CD11c+ innate immune cells in the lungs, as well as reduced recruitment of activated CD4+ and CD8+ T cells, compared to infection with a normal mixture of trophic forms and cysts. *In vitro*, trophic forms suppressed production of the proinflammatory cytokines by dendritic cells stimulated with broad range of fungal and bacterial PAMPs. In addition, trophic form-stimulated BMDCs failed to stimulate production of the T_h1-type cytokine IFN-γ by CD4+ T cells.

In this Chapter, we sought to further characterize the dendritic cell response to trophic forms. Dendritic cells are the principal antigen presenting cells in the lung. However, their role in initiating the adaptive response to *Pneumocystis* has been understudied. Previous reports indicate that β-glucan from the cyst wall is sufficient to

induce dendritic cell-mediated proliferation and polarization of T_h1/T_h17-type CD4^{+} T cells(23, 88). The mechanism for dendritic cell recognition of *Pneumocystis* trophic forms, which do not express β-glucan, is unknown. Both stages express surface glycoproteins and mannoproteins that may serve as pathogen-associated molecular patterns (PAMPs) that could be recognized by receptors on host cells (7-9). However, the breath of the suppression observed in Chapter 3 suggests that, despite the availability of PAMPs, trophic forms induce poor activation of dendritic cells. In contrast, the data presented in Chapter 4 indicate that trophic forms are sufficient to promote CD4^{+} T cell responses.

We sought to further evaluate the effects of trophic forms on dendritic cell activation and antigen presentation. The failure of trophic forms to stimulate key proinflammatory cytokines (Chapter 3) encouraged us to use the NanoString gene expression assay to evaluate the dendritic cell response to trophic forms compared to a mixed population of trophic forms and cysts. NanoString is an array capable of analyzing the relative expression of a predefined panel of target genes. Herein, we employed the NanoString nCounter Mouse Immunology CodeSet to evaluate the expression of 561 immunity-related mouse transcripts in dendritic cells treated with trophic forms or a mixed population of trophic forms and cysts. This technique painted a focused portrait of the dendritic cell response to trophic forms. The NanoString assay more directly addressed our research focus than other, more extensive, methods of gene expression analysis such as RNASeq.

The NanoString assay was a powerful tool to demonstrate the broad failure of dendritic cells to become activated in response to trophic forms. We demonstrate that *P.*

murina trophic forms hinder the ability of dendritic cells to serve in their essential role as stimulators of CD4$^+$ T cell responses by reducing the capacity of dendritic cells to produce proinflammatory cytokines, present antigen, and express costimulatory molecules. Treatment of dendritic cells with trophic forms induced a less robust pattern of expression of immunity-related genes than treatment with a mixture of *P. murina* trophic forms and cysts. In addition, treatment with trophic forms reduced the ability of dendritic cells to increase surface expression of MHC class II and CD40 in response to stimulation with mixed *P. murina* organisms or zymosan. These defects in the expression of MHC class II and costimulatory molecules corresponded with a reduced capacity for trophic form-loaded dendritic cells to stimulate CD4$^+$ T cell proliferation and polarization.

II. Results

P. murina trophic forms induce a suppressive pattern of gene expression in dendritic cells.

Pneumocystis trophic forms suppress the production of proinflammatory cytokines by dendritic cells stimulated with multiple PAMPs (168). These PAMPs are recognized by a range of pattern recognition receptors that mediate diverse signaling pathways within the cell, including, in the case of IL-1β, inflammasome activation. These data suggest that _P. murina_ trophic forms have a broadly suppressive effect on dendritic cells. To evaluate the activity of dendritic cells in response to trophic forms, we employed a target gene expression array to analyze the dendritic cell response to _P. murina_ trophic forms based on the expression of 561 immunity-related mouse transcripts (NanoString nCounter Mouse Immunology CodeSet). BMDCs from adult BALB/cJ mice were incubated with trophic forms or mixed _P. murina_ organisms at a dendritic cell to fungal cell ratio of 1:50. Controls included untreated BMDCs and BMDCs treated with 10 µg/ml of the β-glucan curdlan. Curdlan is a high-molecular-weight β-1,3-glucan isolated from _Alcaligenes faecalis_, and is similar to the β-1,3-glucan that composes the _P. murina_ cyst wall (182, 183). Curdlan is employed in these experiments as a reductive positive control for β-glucan-induced signaling in BMDCs. RNA was extracted after 2, 4, and 8 hr, and analyzed with the preassembled NanoString panel. Raw NanoString data are hosted at doi:10.1128/IAI.00396-17 (Data Set S1). Raw counts were normalized to internal reference transcripts and housekeeping genes.

The normalized data illustrate that trophic forms induced a broader pattern of reduced gene expression in dendritic cells, compared to stimulation with a normal mixture of cystic and trophic forms ("mixed Pc"), or the β-glucan curdlan (**Fig 5.1A-D**). The heat map shown in **Fig 5.1A** depicts the relative values of the 561 transcripts for each sample (n = 5) within each treatment group, at 8 h post-treatment. Data are shown as the relative gene expression value compared to the unstimulated control. A large portion of the immunity-related genes were induced by treatment with curdlan, but downregulated by treatment with trophic forms (**Fig 5.1A**). Stimulation with a mixture of *P. murina* organisms did not induce total gene expression as robustly as the positive control, curdlan (**Fig 5.1A**). However, stimulation with mixed *P. murina* organisms did lead to upregulation of a greater number of genes than stimulation with trophic forms alone (**Fig 5.1A**). Intriguingly, stimulation with trophic forms and mixed *P. murina* organisms led to the upregulation of several genes whose expression was not induced by curdlan (**Fig 5.1A, C**).

Experimental data shown in **Fig 5.1B** represent the principle component analysis-based clustering of the samples within each group after 8 h of treatment. Principle component analysis plots the data in terms of the directions where the data has the most variance (the mathematically-defined "principal components"). Here, each of the groups formed distinct clusters, indicating a unique pattern of gene expression following each treatment. Experimental data shown in **Fig 5.1C-D** represent genes upregulated or downregulated in the treated groups relative to the untreated control. Differences were identified by two-way ANOVA followed by pairwise comparisons using the Least Significant Difference Method. A change was deemed significant if the p value was

<0.01. Notably, BMDCs treated with trophic forms also increased the expression of a subset of genes relative to unstimulated cells. Of the 561 immunity-related transcripts, stimulation with trophic forms induced the statistically significant upregulation of 154 genes (**Fig 5.1C**) and the downregulation of 130 genes (**Fig 5.1D**) relative to the unstimulated control. 121/154 (78.6%) of the genes upregulated (**Fig 5.1C**) by stimulation with trophic forms and 93/130 (71.5%) of the genes downregulated (**Fig 5.1D**) by treatment with trophic forms were also upregulated or downregulated (respectively) in the mixed *P. murina*- and curdlan-treated groups. The pattern of gene expression in response to mixed *P. murina* organisms (a mixture of 10 trophic forms to 1 β-glucan expressing cyst) was similar to the phenotypes induced by either trophic forms or curdlan with few unique genes either up- or down-regulated (**Fig 5.1C-D**). The data shown in **Fig 5.1** demonstrate that trophic forms induced a unique pattern of gene expression in regards to both the identity of gene transcript, and the magnitude of the change in expression. In contrast, treatment with *mixed P. murina* organisms induced a pattern of gene expression that represents an intermediate phenotype between the comparatively less robust pattern of gene expression that is induced by trophic forms and the highly inflammatory pattern that is induced by the β-glucan curdlan.

Trophic forms induce the expression of genes encoding chemokines and complement proteins.

As noted in **Fig 5.1C**, stimulation with trophic forms induced the statistically significant upregulation of 154 genes compared to the unstimulated control. The data shown in **Fig 5.2A** include all of the genes in the NanoString panel with a statistically

significant (p < 0.01) four-fold or greater increase in expression between BMDCs treated with trophic forms compared to unstimulated BMDCs. Several genes on this list are related to the complement system or encode chemokines. Notably, many of these genes, including the genes encoding complement system transcripts, are more highly expressed in cells treated with trophic forms compared to stimulation with curdlan or a mixture of *P. murina* organisms.

The data in **Fig 5.2B-C** represent all genes encoding regulators of inflammation (B) or immunity-related transcription factors (C) with a statistically significant (p < 0.01) two-fold or greater increase in expression between BMDCs treated with trophic forms compared to unstimulated BMDCs. While we have previously reported that trophic forms fail to induce translocation of NFκB in alveolar macrophages and trophic forms suppress the production of IL-1β, IL-6, and TNFα protein by dendritic cells, these data indicate that dendritic cells are responsive to the trophic forms (9, 168). Furthermore, treatment of dendritic cells with trophic forms induces a distinct pattern of gene expression compared to stimulation with curdlan and mixed *P. murina*.

Muc1 is not required for trophic form-mediated suppression of cytokine responses.

A striking finding in our gene expression data is that the expression of *Muc1* is 50-fold greater in BMDCs treated with trophic forms compared to the unstimulated control (**Fig 5.2A**). In contrast, stimulation of BMDCs with mixed *P. murina* organisms or curdlan induced a 10-fold increase in *Muc1* expression compared to the unstimulated control (**Fig 5.2A**). *Muc1* encodes a transmembrane mucin-like glycoprotein that is associated with suppression of TLR-mediated signaling in alveolar epithelial cells (184).

117

In addition to CLRs such as dectin-1, *Pneumocystis* species have been shown to stimulate cytokine production via TLR2 and TLR4 (156, 170). We previously published that *Pneumocystis* trophic forms suppressed the production of proinflammatory cytokines by dendritic cells stimulated with the TLR2 agonist LTA and the TLR4 agonist LPS. To evaluate the role of *Muc1* in trophic form-mediated suppression of TLR signaling, we measured cytokine production by *Muc1*-deficient BMDCs following stimulation with trophic forms, mixed *P. murina* organisms, curdlan, LPS, and/or LTA (**Fig 5.3**). Trophic form-mediated suppression of IL-6 was similar in wild-type and Muc1$^{-/-}$ BMDCs.

Stimulation with trophic forms leads to attenuated expression of multiple cytokine genes compared to treatment with a mixture of trophic forms and cysts.

Dendritic cells are the principal antigen presenting cells in the lung, and are critical for optimal B cell and T cell activation in response to pathogens (reviewed in (84)). Immature lung dendritic cells reside in the alveolar interstitium, where they project their dendritic extensions through the epithelial-tight junctions into the alveolar spaces. Encounters with antigen promote a complex maturation process that prepares the dendritic cell to serve as an antigen-presenting cell. We previously published that *Pneumocystis* trophic forms suppressed the production of proinflammatory cytokines IL-1β, IL-6, and TNFα by dendritic cells stimulated with multiple PAMPs (168). A principle aim of the gene expression array was to identify the extent of the suppressive impact of trophic forms on dendritic cells.

Data shown in **Fig 5.4A** represent the relative gene expression at 8 h post-stimulation of every cytokine included in the preassembled panel. Gene expression is

displayed as the log2 value of the quotient of the treated value divided by the untreated value. Stimulation with trophic forms led to the expression of the vast majority of the cytokine genes included in the panel. However, the magnitude of this upregulation was attenuated compared to treatment with mixed *P. murina* organisms or curdlan. For example, treatment with trophic forms increased the expression of transcripts encoding IL-1β and IL6. However, this upregulation was not as great as that observed in cells stimulated with mixed *P. murina* or curdlan (**Fig 5.4A**). In addition, IL-1β and IL-6 protein were not detectable in the supernatant of dendritic cells stimulated with purified trophic forms (**Fig 5.5**). Treatment with trophic forms failed to induce gene and protein expression of TNFα (**Fig 5.4A** and **Fig 5.5**). Mixed *P. murina* and curdlan both induced expression of the transcript encoding TNFα. However, as previously reported, stimulation with curdlan but not mixed *P. murina* induced protein expression of TNFα (168).

Trophic forms induce less robust expression of multiple transcription factors and positive regulators of inflammation compared to treatment with a mixture of trophic forms and cysts.

Data shown in **Fig 5.4B** represent genes that encode positive regulators of inflammation whose expression was significantly different (greater than 2-fold difference, p<0.01) between the cells treated with trophic forms and mixed *P. murina* organisms at 8 h. Notably, treatment with trophic forms in the absence of cysts lead to less robust expression of a wide range of mediators of inflammation, including the genes encoding the dendritic cell maturation marker SLAMF1, compared to stimulation with a mixed population of trophic forms and cysts. Data shown in **Fig 5.4C** represent genes

that encode immunity-associated transcription factors whose expression was significantly different (greater than 2-fold difference, $p<0.01$) between the cells treated with trophic forms and mixed *P. murina* organisms at 8 h. Conventional dendritic cells (cDCs) may be divided into two broad subsets: $CD8\alpha^+$ $CD103^+$ cDC1s, which promote T_h1 polarization and $CD11b^+$ cDC2s, which promote T_h2 or T_h17-type responses (185-190). Treatment with trophic forms reduced the expression of the transcripts encoding the cDC1-associated transcription factors Batf3 and Irf8 and the expression of the cDC2-associated transcription factor Irf4 below the basal level of expression. In contrast, stimulation with mixed *P. murina* organisms enhanced the expression of each of these markers.

Suppression of the cytokine response is not dependent on trophic form viability, but is partially dependent on direct contact between trophic forms and dendritic cells.

Pneumocystis trophic forms suppress the production of proinflammatory cytokines IL-1β, IL-6, and TNFα by dendritic cells stimulated with multiple PAMPs (**Fig 5.5** and (168)). We report here that trophic forms are capable of suppressing the expression of multiple immunity related genes (**Fig 5.1 and 5.4**) below the basal level of expression. To determine if suppression requires live participation by the trophic forms, we tested the ability of heat-killed (**Fig 5.6A-C**) or sonicated (**Fig. 5.6D-F**) trophic forms to prevent IL-1β, IL-6, and TNFα cytokine production in BMDCs treated with curdlan. Live, heat-killed, and sonicated trophic forms suppressed cytokine production, indicating that troph-mediated suppression is not dependent on the viability of trophic forms. Surprisingly, while intact mixed *P. murina* organisms induce IL-1β and IL-6 production, these data indicate that sonicated mixed *P. murina* organisms suppressed these responses. These

data suggest that intact cysts are required for stimulation of cytokine production, and, in the absence of this stimulation, the trophic material is able to suppress the response to other PAMPs.

Immunosuppression by the trophic forms could be mediated by a secreted factor or by direct contact between the trophic forms and the BMDCs. We measured curdlan-induced IL-1β, IL-6, and TNFα cytokine production by BMDCs separate from trophic forms by Transwell polyester inserts with 0.4µm pores (**Fig 5.6G-I**). Direct contact between the trophic forms and BMDCs was not required for a reduction in IL-1β or TNFα cytokine production (**Fig 5.6G-H**). Intriguingly, direct contact was required for the suppression of IL-6 protein production (**Fig 5.6I**).

A relatively small amount of *P. murina* DNA was detected in the lower Transwell compartment, and quantitative PCR indicated that up to 2×10^3 trophic forms (or equivalent trophic DNA) may have crossed the Transwell membrane (data not shown). However, the addition of greater than 10^6 trophic forms was required to see the level of suppression that was observed in the Transwell system (**Fig 5.7**). In addition, a portion of the supernatant from the lower compartments was cytospun onto slides and examined under a microscope (limit of detection $= 10^2$ organisms, data not shown). No trophic forms were observed, further confirming that a significant proportion of the trophic forms did not cross the membrane. These controls indicate that the suppression of TNFα and IL-1β observed in **Fig 5.6G-I** was due to material shed from trophic forms, rather than the passage of whole trophic forms through the Transwell membrane.

Trophic forms suppress the expression of multiple factors related to antigen presentation, including MHC class II and the costimulatory molecule CD40.

We have previously reported that infection of wild-type mice with trophic forms induces less expression of MHC class II on the surface of CD11c$^+$ CD11b$^-$ and CD11c$^+$ CD11b$^+$ cells within the lungs compared to infection with mixed *P. murina* organisms (168). This effect was consistent through two weeks post-infection. The reduced capacity of BMDCs to express MHC class II correlated with less robust CD4$^+$ T cell recruitment and proliferation in the lungs of mice infected with trophic forms compared to mixed *P. murina* organisms (168).

The preassembled NanoString panel included several genes related to antigen presentation (Fig. 4A). Gene expression is displayed as the log2 value of the quotient of the treated value divided by the untreated value. These data indicate that trophic forms suppress the expression of multiple antigen-presentation genes below the basal level of expression. *Ciita* encodes the class II transactivator, a master regulator of genes related to MHC class II expression. The expression of *Ciita* is 10-fold lower in BMDCs treated with trophic forms compared to the unstimulated control (**Fig 5.8A**). In contrast, stimulation with mixed *P. murina* led to a 3-fold decrease in *Ciita* expression compared to the unstimulated control, while treatment with curdlan did not significantly alter the expression of *Ciita* (Fig. 4A). Data shown in **Fig 5.8B** represent the relative expression of genes encoding costimulatory molecules. Treatment of BMDCs with trophic forms induces lower levels of expression of the transcripts encoding the costimulatory molecules CD40, CD80, CD86, PD-L1 and PD-L2 than stimulation with mixed *P. murina* organisms.

Flow cytometry was used to evaluate protein expression of MHC class II (**Fig 5.8C-E**) and CD40 (**Fig 5.8D-F**) on the surface of BMDCs treated for 24 hours with trophic forms, mixed *P. murina* organisms, and/or zymosan. Zymosan is a protein-carbohydrate preparation from the cell wall of *Saccharomyces cerevisiae*, and, unlike curdlan, zymosan may be processed and presented as protein antigen. Treatment of BMDCs with mixed *P. murina* organisms and/or zymosan resulted in increased surface expression of MHC class II and CD40 compared to the basal level. Treatment with trophic forms failed to induce surface expression of MHC class II and CD40. Addition of trophic forms to BMDCs treated with *P. murina* organisms or zymosan inhibited the expression of MHC class II and CD40. These data indicate that trophic forms suppress the expression of MHC class II and the costimulatory molecule CD40 on the surface of dendritic cells. Maturation of dendritic cells is characterized by an initial burst in antigen presentation and MHC class II expression followed by a reduction in additional antigen processing and presentation. However, surface expression of peptide-MHC class II complexes is highly stable in mature dendritic cells, with a reported half-life of 31 hours observed in dendritic cells stimulated with LPS (191). Therefore, the observed reduction in MHC class II surface expression after 24 hours of stimulation suggests that treatment with trophic forms impedes the maturation of dendritic cells.

Pretreatment of dendritic cells with trophic forms reduces allogenic CD4+ T cell proliferation in a mixed lymphocyte reaction.

In order to determine the significance of reduced MHC class II on BMDCs treated with trophic forms, a mixed lymphocyte reaction was used in which T cell proliferation is

dependent on detection of allogenic MHC class II, but not specific antigen. To test the effect of trophic forms on allogenic CD4$^+$ T cell proliferation, BMDCs generated from Ia^d-expressing BALB/cJ mice were pretreated with trophic forms or mixed *P. murina* organisms for one hour (**Fig 5.9A**). CFSE-stained splenocytes from uninfected Ia^b-expressing C57BL/6 mice were then added to the wells and co-cultured for 6 days. Flow cytometry was used to evaluate the proliferation of C57BL/6 CD4$^+$ T cells (**Fig 5.9A**). Pretreatment of allogeneic BMDCs with trophic forms, but not mixed *P. murina* organisms reduced CD4$^+$ T cell proliferation and IFNγ production in the mixed lymphocyte reaction (**Fig 5.9A**). These data are consistent with trophic forms suppressing MHC class II expression, resulting in the inability of the pretreated dendritic cells to stimulate antigen-independent allogenic T cell proliferation in a mixed lymphocyte reaction.

Trophic form-loaded dendritic cells stimulate less robust CD4$^+$ T cell responses.

CD4$^+$ T cell responses are required for the clearance of *P. murina* (1). We have previously reported that BMDCs loaded with mixed *P. murina*, but not trophic forms, stimulate IFN-γ production by CD4$^+$ T cells *in vitro* (168). To evaluate whether dendritic cells are able to present antigen and induce CD4$^+$ T cell responses when loaded with trophic forms, we broadened our analysis to include proliferation and other T helper cytokines (**Fig 5.9B-E**). BMDCs loaded with mixed *P. murina*, but not trophic forms, stimulated proliferation in CFSE-labeled CD4$^+$ T cells (**Fig 5.9B**). To confirm that trophic forms are phagocytosed by BMDCs, confocal microscopy was used to demonstrate that DDAO-SE-labeled trophic forms were internalized (**Fig 5.10A**).

Furthermore, confocal microscopy (**Fig 5.10B-C**) and flow cytometry (**Fig 5.10D-E**) confirmed that stimulation of dendritic cells with trophic forms does not reduce the ability of dendritic cells to phagocytose pHrodo Green-label zymosan bioparticles, which fluoresce in low pH.

BMDCs loaded with mixed *P. murina* stimulated higher production of the T_h1-type cytokine IFNγ, the T_h2-type cytokine IL-13, and the T_h17-type cytokine IL-17A by CD4$^+$ T cells compared to stimulation with trophic forms alone (**Fig 5.9C-E**). However, stimulation with trophic forms did induce greater production of IL-13 than the unstimulated control (**Fig 5.9D**). These data indicate that while cysts are required for robust proliferation of CD4$^+$ T cells and production of cytokine *in vitro*, BMDCs loaded with trophic forms are capable of driving modest T_h2-type T cell polarization. *P. murina* organisms did not stimulate CD4$^+$ T cell proliferation and cytokine production in the absence of BMDCs (data not shown), indicating that these responses are dependent on antigen presentation by BMDCs.

III. Discussion

We have previously reported that the cyst life cycle stage drives proinflammatory responses that direct the early recruitment of innate and adaptive immune cells. Infection of adult mice with *Pneumocystis* trophic forms in the absence of cysts leads to the establishment of an immunosuppressive environment in the lungs that persists for up to one week following the formation of the cystic stage (168). If cysts are in the inoculum, the trophic form is unable to suppress inflammatory responses in the lungs as effectively. We have reported that the trophic life cycle forms dampen β-glucan and TLR-induced inflammation compared to stimulation with a mixture of trophic forms and cysts (168). Here, our data confirm that *P. murina* trophic forms hinder the ability of dendritic cells to serve in their essential role as stimulators of CD4$^+$ T cell responses by reducing the capacity of dendritic cells to produce proinflammatory cytokines, present MHC class II, and express costimulatory molecules.

We did not define the factor(s) expressed by the trophic forms that induce suppression. However, experiments were presented that have begun to define the nature of these factors. Intriguingly, suppression of the dendritic cell cytokine response was not dependent on trophic form viability and was only partially dependent on direct contact between trophic forms and dendritic cells. It is plausible that either secreted proteins or shed glycosylated proteins such as glycoprotein A (gpA, or major surface glycoprotein, MSG) are responsible for trophic-form mediated suppression. Direct contact between trophic forms and BMDCs was required for suppression of IL-6, but not IL-1β protein production, while TNFα suppression was partially dependent on direct contact. This data may suggest that multiple factors from the trophic forms are responsible for the broad

suppression of the production of inflammatory cytokines by dendritic cells. Alternatively, it is possible that the amount of suppressive material that crossed into the lower compartment is less than the amount that is present when BMDCs are co-cultured with trophic forms in the lower well. The dose-response curve in **Fig 3.7** suggests that suppression of IL-1β requires the addition of fewer trophic forms compared to the suppression of IL-6. Therefore, it is possible that the Transwell assay employed here represents a scenario in which sufficient suppressive material has reached the BMDC to inhibit IL-1β, but not IL-6, production. Further studies should evaluate the dose-response of BMDCs treated with increasing amounts of material from the trophic forms.

Dendritic cell activation is dependent on the expression of a wide range of transcription factors and signaling mediators related to inflammatory responses. Here, we report that trophic forms induced a differential pattern of gene expression in dendritic cells compared to treatment with a normal mixture of trophic forms and cysts. Treatment of dendritic cells with trophic forms induced a less robust pattern of expression of several immunity-related genes than treatment with a mixture of *P. murina* trophic forms and cysts. We previously published that *Pneumocystis* trophic forms suppressed the production of proinflammatory cytokines IL-1β, IL-6, and TNFα by dendritic cells stimulated with multiple PAMPs, including β-glucan, LPS, LTA, zymosan, and depleted zymosan (168). Here, we demonstrate that transcript levels of these proinflammatory cytokines were lower in dendritic cells treated with trophic forms compared to mixed *P. murina*. These data suggest that the cyst life cycle is required for robust cytokine production by dendritic cells.

Treatment of BMDCs with trophic forms induced the expression of several genes encoding complement components. The complement protein C3 is not required for clearance of *P. murina* infection (123). However, it has been proposed that the accumulation of complement components during PcP contributes to immune-mediated lung damage (192). Anaphylatoxins (complement peptides C3a, C4a, and C5a) are formed during the complement cascade, and may promote neutrophil recruitment (193, 194). It is unclear if complement components contributed to the differential immune response that we observed following inoculation with trophic forms or mixed *P. murina* organisms (**Chapter 3**).

Stimulation of BMDCs with trophic forms also induced the expression of several genes that encode chemokines. This list is comprised of chemokines that are chemoattractant for a range of leukocytes, including monocytes, dendritic cells, neutrophils, NK cells, T cells, and B cells. However, our *in vivo* data suggest that inoculation with trophic forms results in delayed recruitment of leukocytes into the host lungs (**Chapter 3**). Our anidulafungin-treated RAG2$^{-/-}$ model demonstrates that the long-term carriage of a trophic population results in the infiltration of a population of CD11c$^-$ CD11b$^+$ cells that are predominately F4/80^{high} (**Fig 4.6**). This suggests that trophic forms promote the recruitment of monocytes or macrophages rather than F4/80^{low} neutrophils or myeloid-derived suppressor cells. Neutrophils are not required for clearance, but their accumulation in the lungs correlates with disease severity in human *Pneumocystis pneumonia* patients (5, 136). Further work is required to determine which chemokine proteins are present in the host lung during infection with trophic forms or mixed *P.*

murina organisms, and to identify the cell populations recruited in response to trophic infection of immunocompetent hosts.

The data in **Fig 5.2B-C** represent all genes encoding regulators of inflammation (B) or immunity-related transcription factors (C) with a statistically significant ($p < 0.01$) two-fold or greater increase in expression between BMDCs treated with trophic forms compared to unstimulated BMDCs. While we have previously reported that trophic forms fail to induce translocation of NFκB in alveolar macrophages and trophic forms suppress the production of IL-1β, IL-6, and TNFα protein by dendritic cells, these data indicate that dendritic cells are responsive to the trophic forms (9, 168). Furthermore, treatment of dendritic cells with trophic forms induces a distinct pattern of gene expression compared to stimulation with curdlan and mixed *P. murina*.

Trophic forms induce differential regulation of several genes related to inflammation and transcription compared to stimulation with mixed *P. murina*. These genes encompass diverse signaling pathways, including genes encoding members of the interferon regulatory factors (IRF) and STAT families. Here, we show that treatment with trophic forms suppressed the expression of Batf3 and Irf8, which mediate the development of T_h1-promoting $CD8\alpha^+$ $CD103^+$ conventional DCs (cDC1). The expression of Irf4, which mediates the development of T_h2/ T_h17-promoting $CD11b^+$ cDCs (cDC2) was also suppressed by treatment with trophic forms but induced by treatment with mixed *P. murina*. These data suggest that trophic forms may broadly suppress the development of multiple dendritic cell subsets, and are consistent with the failure of trophic form-stimulated dendritic cells to induce robust production of T helper cytokines compared to stimulation with mixed *P. murina*. It should be noted, however,

that the BMDCs employed in these experiments more closely resemble monocyte-derived dendritic cells and are not true conventional dendritic cells, which require Flt3L for differentiation (195, 196). The ability of trophic forms to suppress Batf3, Irf8, and Irf4 expression in Flt3L-dependent conventional dendritic cells has not been evaluated.

Some fungal pathogens, including *Candida* spp and *H. capsulatum*, may prevent phagosomal maturation and acidification (197-199). However, our data indicate that stimulation with trophic forms or a mixed *P. murina* does not reduce the phagocytic capacity of the dendritic cell. Rather, our data confirm that treatment with trophic forms reduces the ability of dendritic cells to present antigen. Treatment with trophic forms reduced the ability of dendritic cells to increase surface expression of MHC class II and CD40 in response to stimulation with mixed *P. murina* organisms or zymosan (a *Saccharomyces* cell wall preparation). Our data indicate that this suppression occurred at the level of transcription, as treatment with trophic forms led to downregulation of several genes associated with MHC class II processing and expression, including the gene encoding the master class II transactivator, Ciita. Treatment with trophic forms also resulted in lower expression of the genes encoding the costimulatory molecules CD40, CD80, and CD86, as well as the immune regulatory molecules PD-L1, and PD-L2 compared to treatment with a mixture of organisms that contained cysts. These defects in the expression of MHC class II and costimulatory molecules corresponded with a reduced capacity for trophic form-loaded dendritic cells to stimulate CD4$^+$ T cell proliferation and polarization. Intriguingly, suppression of the dendritic cell cytokine response was not dependent on trophic form viability, nor on direct contact between trophic forms and

dendritic cells. It is possible that this will also be true for expression of MHC class II, however, these experiments are ongoing.

Modulation of the T helper phenotype of the inflammatory response is a common strategy employed by infectious fungi for immune evasion (200). In addition to presentation of antigen, activated dendritic cells produce cytokines that influence the polarization of the T helper response. Shifts in this balance may elicit an inefficient adaptive response. For example, the generation of a T_h2-type response to the fungal commensal *Candida albicans* inhibits T_h1 responses, and promotes pathogen survival by decreasing phagocyte activation (201). However, while T_h1 or T_h17 responses are critical for control of many fungal infections, including candidemia, a mixed T helper response is observed in response to *Pneumocystis* infection. This mixed response appears to be largely redundant, as T_h1-, T_h2-, and T_h17-type responses have each been associated with clearance of *P. murina* organisms (24, 111-115). Broad suppression of cytokine production by trophic forms may be necessary to overcome this redundancy and delay the activation of adaptive immunity against *P. murina*.

Here, the data indicate that dendritic cells loaded with trophic forms stimulate production of the T_h2-type cytokine IL-13, but not production of the T_h1-type cytokine IFNγ or the T_h17-type cytokine IL-17A. These data indicate that trophic forms may polarize the immune response towards a weak T_h2-type response, while suppressing T_h1 and T_h17-type responses. However, the effectiveness of this response in the absence of CD4$^+$ T cell proliferation is unclear. In addition, it is unclear how trophic forms, which suppress IL-6 protein production and fail to induce expression of the genes encoding IL-2, IL-4, and IL-13 as robustly as stimulation with mixed *P. murina* organisms, promote

T_h2 polarization. The CD4$^+$ T cells used in this experiment were generated from the draining lymph nodes of mixed *P. murina*-infected donor mice. We expect that this population included *P. murina*-specific T_h2 CD4$^+$ T cells (113, 115), which may have continued to produce IL-13, but not proliferate in the presence of trophic form-loaded dendritic cells. The failure of trophic forms to induce T_h1 and T_h17 CD4+ T cell polarization is consistent with the attenuated expression of the genes encoding IL-1β, IL-2, IL-6, IL-12, and IL-12β compared to stimulation with mixed *P. murina* organisms.

In addition, trophic forms are capable of inducing the expression of the genes that encode the transcription factors T-bet (*Tbx21*) and Gata3 (**Fig. 5.2**), which mediate T_h1 and T_h2-type responses, respectively. T-bet expression in dendritic cells is required for effective polarization of T_h1 T cells (202-204). GATA3 expression in BMDCs is required for production of the T_h2-type cytokines IL-13 and IL-5 (205). This indicates that the failure of trophic forms to induce robust T_h1 and T_h2-type responses is not due to direct suppression of the transcription of these master regulators.

Tolerogenic dendritic cells promote anergic or regulatory T cell responses by secreting IL-10, TGFβ, and IL-2 and expressing the inhibitory molecules PD-L1 and PD-L2. However, our data indicate that treatment of dendritic cells with trophic forms results in lower levels of gene expression of each of these tolerogenic markers than treatment with a mixture of trophic forms and cysts. Therefore, trophic forms are not likely to induce a classical tolerogenic phenotype in dendritic cells. Rather, our data indicate that treatment with trophic forms broadly reduces the ability of the dendritic cell to provide activation signals to the CD4$^+$ T cells.

In summary, our data indicate that the trophic life cycle stage of *Pneumocystis* limits the ability of dendritic cells to stimulate CD4$^+$ T cell polarization and proliferation by reducing the expression of MHC class II, costimulatory molecules, and proinflammatory cytokines. These defects may be traced back to reduced levels of gene expression of each of these factors, compared to dendritic cells stimulated with a physiologically normal mixture of trophic forms and cysts. We propose that the suppression of immune responses by the trophic forms promotes the colonization of *Pneumocystis* in immunocompetent hosts. This differential immune response to *Pneumocystis* trophic forms and cysts is most certainly a leading contributor to the success of the organisms as human pathogens.
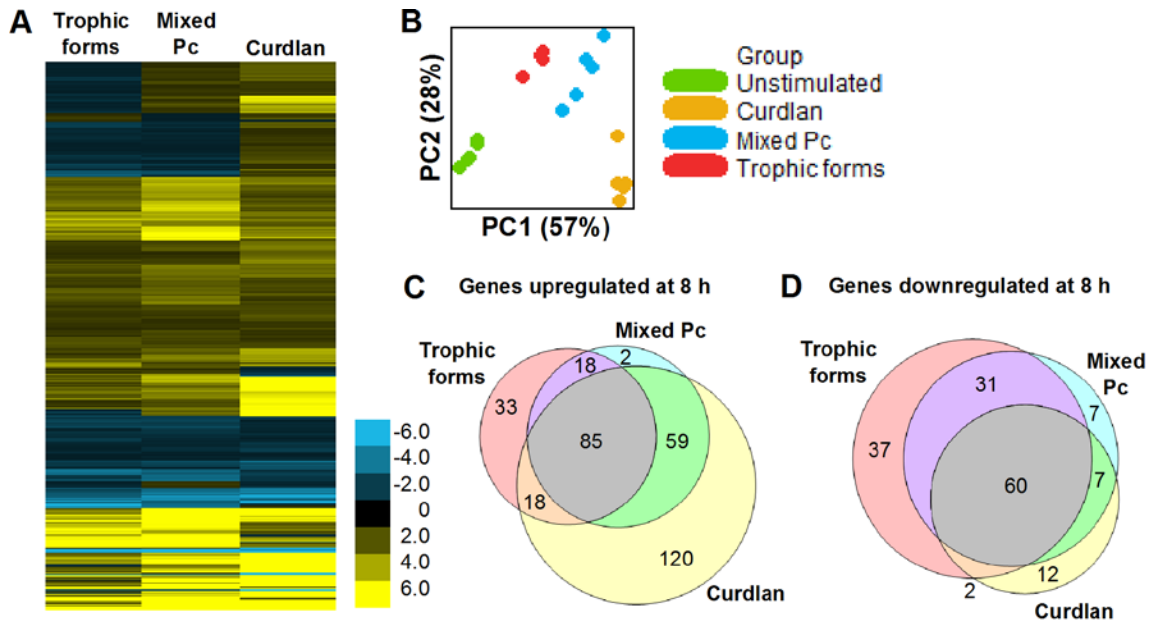
Figure 5-1 Exposure of BMDCs to *P. murina* trophic forms induces a distinct pattern of gene expression.

3×10^5 BMDCs from adult BALB/cJ mice were incubated with 1.5×10^6 trophic forms or 1.5×10^6 mixed *P. murina* organisms. Controls included untreated BMDCs and BMDCs treated with 10μg/ml of the β-glucan curdlan. Cells were lysed after 2, 4, or 8 h of incubation. RNA was extracted. Gene expression analysis was carried out using a preassembled Nanostring Codeset that measures expression of 561 immunity-related mouse transcripts (nCounter Mouse Immunology kit). Analysis and normalization of the raw NanoString data were conducted using nSolver Analysis Software 2.0. Raw counts were normalized to internal positive controls and reference transcripts. A heat map (**A**) was generated to display the treated expression value relative to the untreated value. Principle component analysis (**B**) was used to compare the pattern of gene expression among the untreated and treated groups following 8 h of incubation. Genes upregulated (**C**) or downregulated (**D**) in the treated groups relative to the untreated control were identified by log transformed two way ANOVA followed by pairwise comparisons using the Least Significant Difference Method. Five biological replicates were used per group. A change was deemed significant if the p value was <0.01.
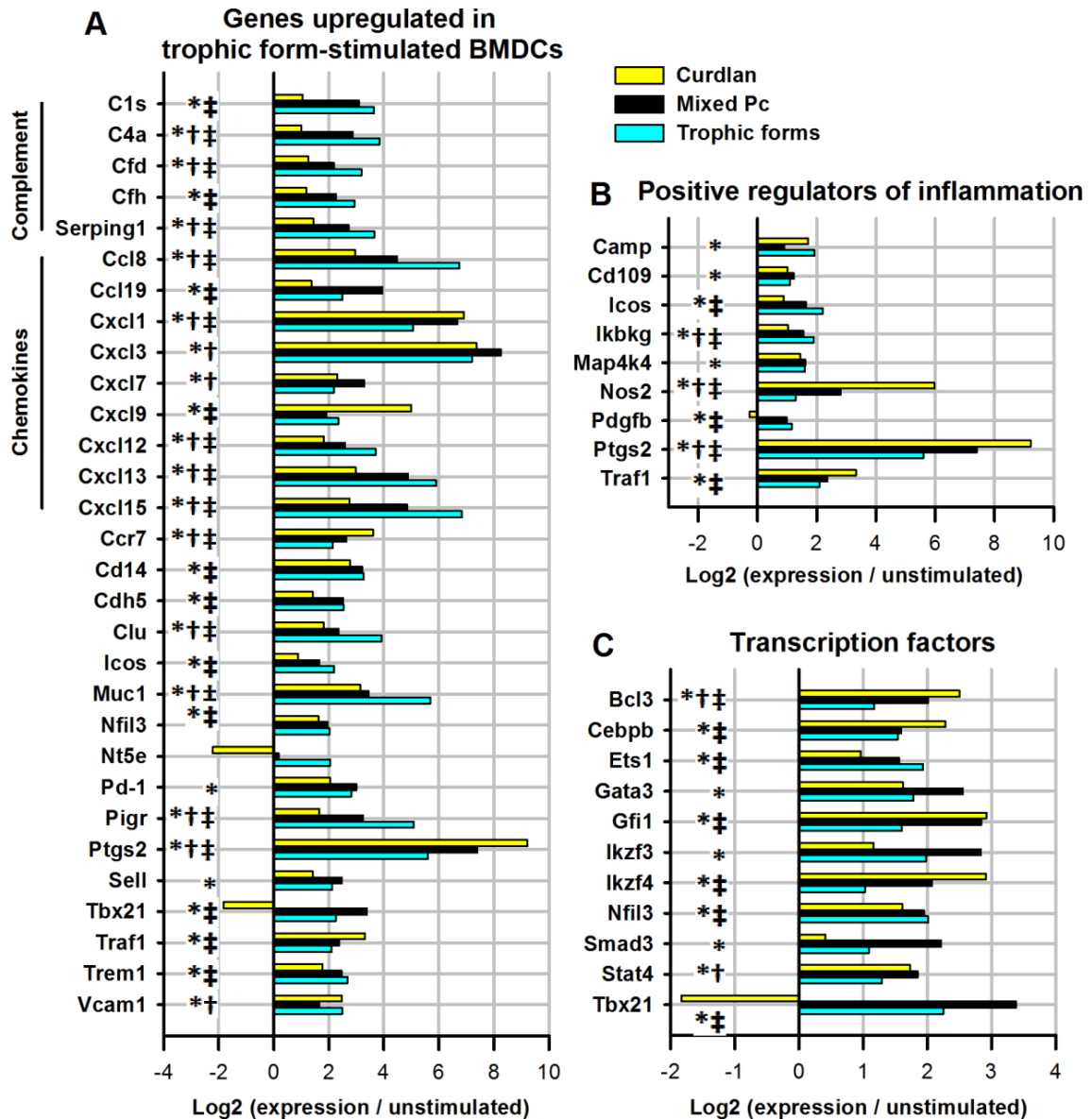
Figure 5-2 Trophic forms induce the expression of genes encoding chemokines and complement proteins.

The relative gene expression after 8 h of treatment was calculated as the log2 value of the quotient of the treated expression value divided by the untreated expression value. The data in **Fig 5.2A** represent genes in the NanoString panel with a statistically significant ($p < 0.01$) four-fold or greater increase in expression between BMDCs treated with trophic forms compared to unstimulated BMDCs. The data represent all genes encoding regulators of inflammation (**B**) or immunity-related transcription factors (**C**) with a statistically significant ($p < 0.01$) two-fold or greater increase in expression between BMDCs treated with trophic forms compared to unstimulated BMDCs. Differences in expression between the groups were identified by log transformed two way ANOVA followed by pairwise comparisons using the Least Significant Difference Method. Five

biological replicates were used per group. Genes with differences in expression with p < 0.01 between BMDCs treated with trophic forms vs unstimulated cells are denoted *, trophic forms vs mixed *P. murina* organisms are denoted †, and trophic forms vs curdlan are denoted ‡.
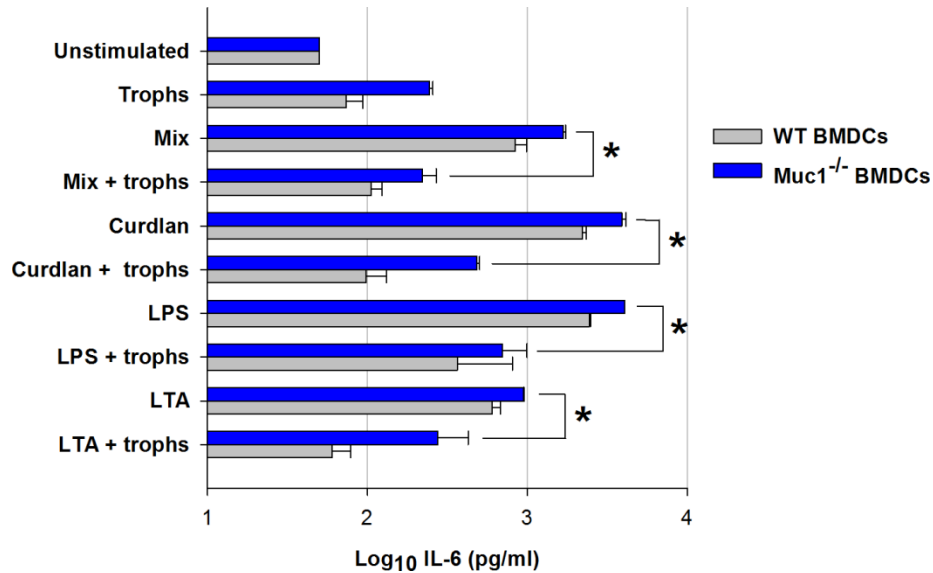
Figure 5-3 Muc1, a negative regulator of TLR-mediated signaling, is not required for trophic-form mediated suppression.

1×10^4 BMDCs from Muc$^{-/-}$ and wild-type BALB/cJ mice were incubated with 5×10^5 trophic forms, 5×10^5 mixed P. murina organisms, 10µg/ml curdlan, 100ng/ml LPS, and 10µg/ml LTA for 72 h. IL-6 production was quantified by ELISA. Data represent the mean ±SD of 3 biological replicates per group and are representative of 2 separate experiments. Kruskal-Wallis one-way ANOVA on ranks was used to compare differences among the Muc1$^{-/-}$ BMDCs treated with a stimulus (mixed Pc, curdlan, LPS, or LTA) compared to a combination of stimulus with trophic forms, $*p < 0.05$.
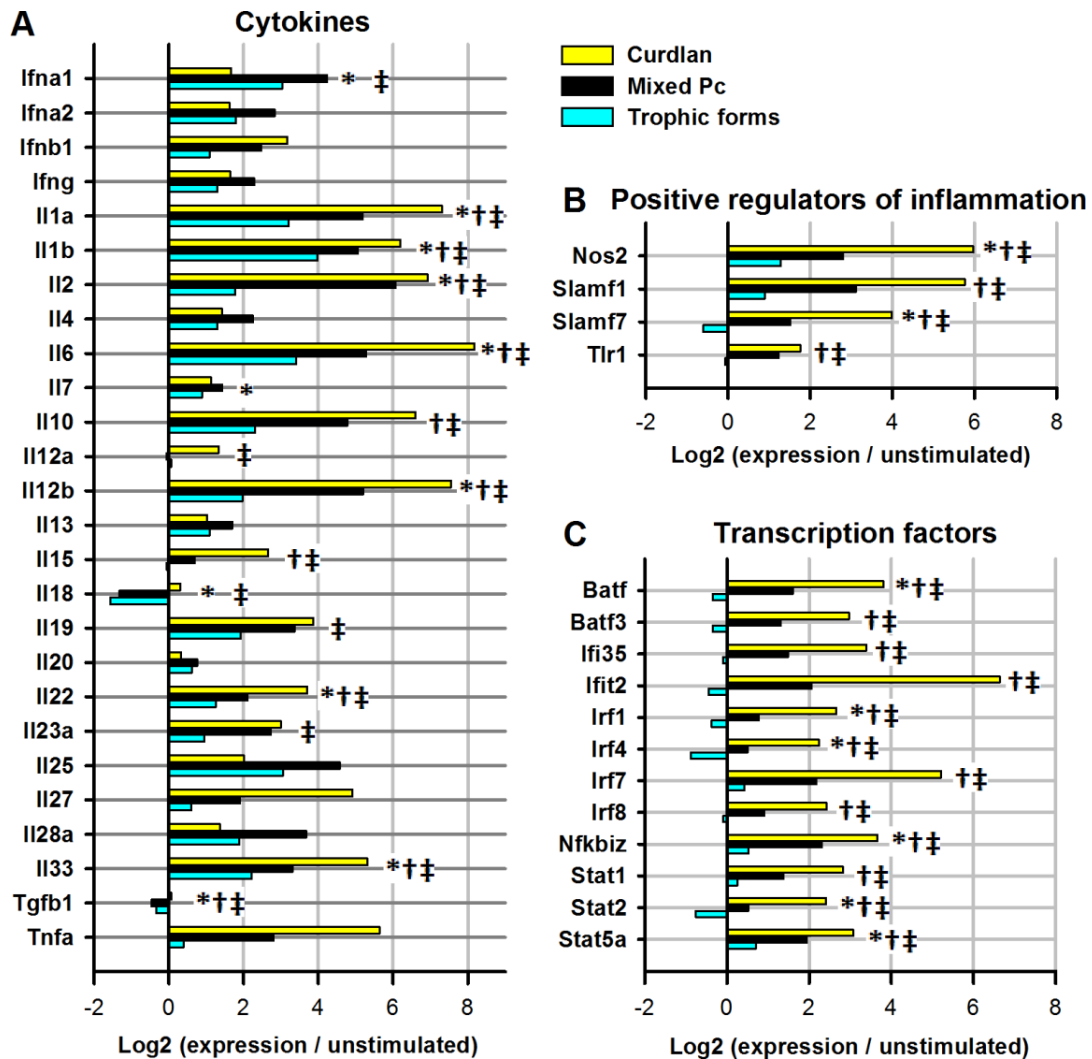
Figure 5-4 Trophic forms induce less robust expression of genes encoding multiple cytokines, positive regulators of inflammation, and transcription factors compared to treatment with a mixture of trophic forms and cysts.

The relative gene expression after 8 h of treatment was calculated as the log2 value of the quotient of the treated expression value divided by the untreated expression value. All cytokine genes in the preassembled NanoString panel are graphed (**A**). The data in **Fig 5.4B-C** represent all genes encoding regulators of inflammation (**B**) or immunity-related transcription factors (**C**) with a statistically significant two-fold or greater difference in expression between BMDCs treated with trophic forms vs mixed *P. murina* organisms. Differences in expression between the groups were identified by log transformed two way ANOVA followed by pairwise comparisons using the Least Significant Difference Method. Five biological replicates were used per group. A change was deemed significant if the p value was <0.01. Genes with differences in expression with p < 0.01 between BMDCs treated with trophic forms vs unstimulated cells are denoted *, trophic forms vs mixed *P. murina* organisms are denoted †, and trophic forms vs curdlan are denoted ‡.

Figure 5-5 Cysts, but not trophic forms, stimulate production of the proinflammatory cytokines IL-1β and IL-6 by BMDCs *in vitro*.

BMDCs from adult BALB/cJ mice were incubated with 3×10^4 trophic forms or 3×10^4 mixed *P. murina* organisms for 72 h. Curdlan was included as a positive control for cytokine production. TNFα (**A**), IL-1β (**B**), and IL-6 (**C**) cytokine production was quantified by ELISA. Data represent the mean ±SD of 3 biological replicates per group and are representative of 2 separate experiments. One way ANOVA with Student-Newman-Keuls post-hoc test was used to compare supernatant cytokine concentration between the groups, **$p \leq 0.01$, ***$p \leq 0.001$, n.s., not statistically significant.
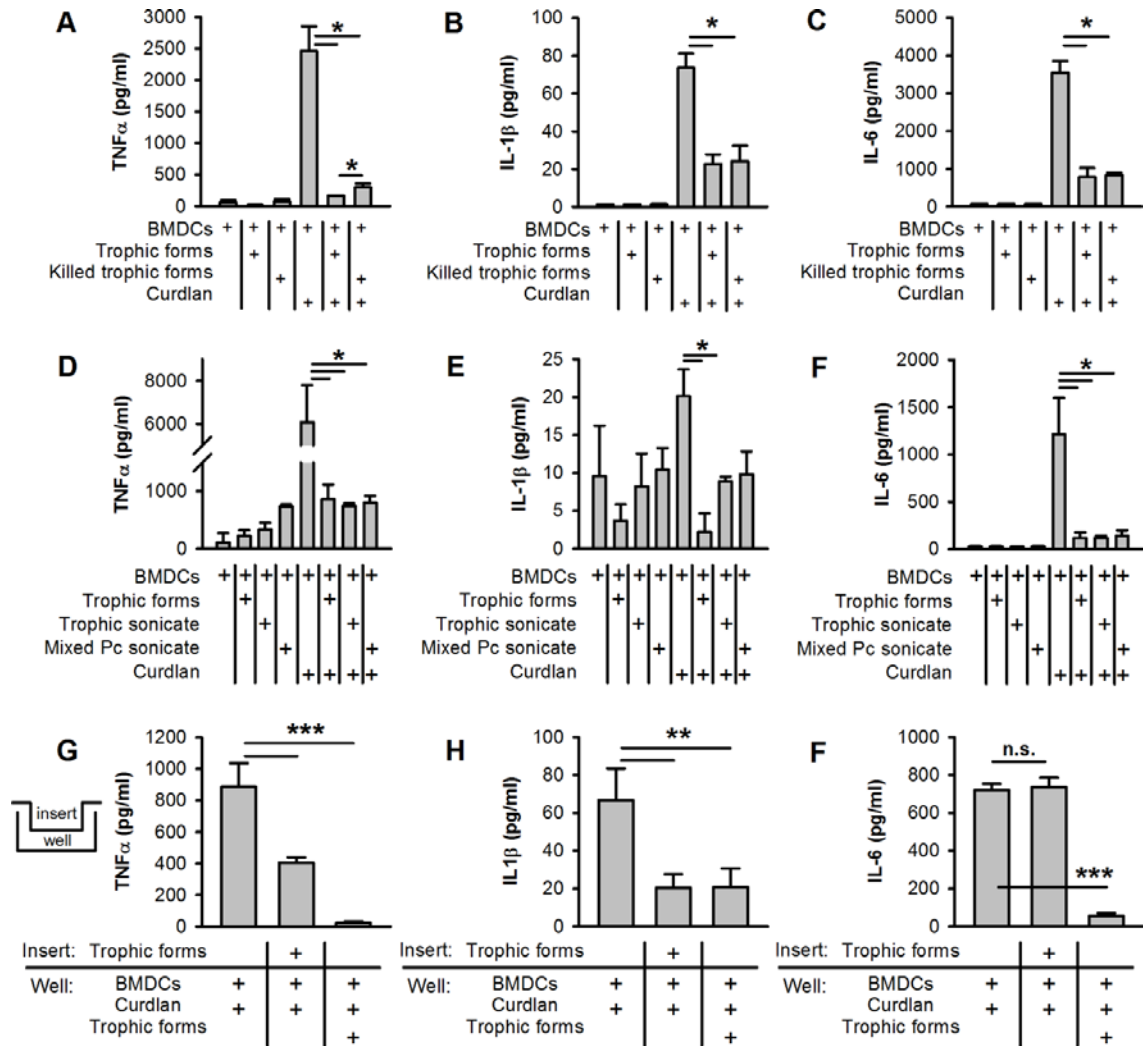
Figure 5-6 Suppression of the cytokine response is not dependent on trophic form viability, but is partially dependent on direct contact between trophic forms and dendritic cells.

1×10^4 BMDCs (**A-F**) from BALB/cJ mice were incubated with 5×10^5 trophic forms, 5×10^5 heat-killed trophic forms, 5×10^5 sonicated trophic forms, 5×10^5 sonicated mixed *P. murina* organisms, and/or 10µg/ml curdlan for 72 h. 1×10^5 BMDCs (**G-I**) from BALB/cJ mice were incubated with 5×10^6 trophic forms and/or 10µg/ml curdlan for 72 h in a Transwell culture plate. TNFα (**A, D, G**), IL-β (**B, E, H**), and IL-6 (**C, F, I**) cytokine production was quantified by ELISA. Data represent the mean ±SD of 3 biological replicates per group and are representative of 2 separate experiments. One-way ANOVA with Student-Newman-Keuls post-hoc test was used to compare differences among the groups where the data were parametric (**A-D, G-I**), *$p \leq 0.05$, ** $p \leq 0.01$, ***$p \leq 0.001$, n.s., not statistically significant. Kruskal-Wallis one-way ANOVA on ranks was used to compare differences among the groups where the data were nonparametric (E-F), *$p \leq 0.05$.
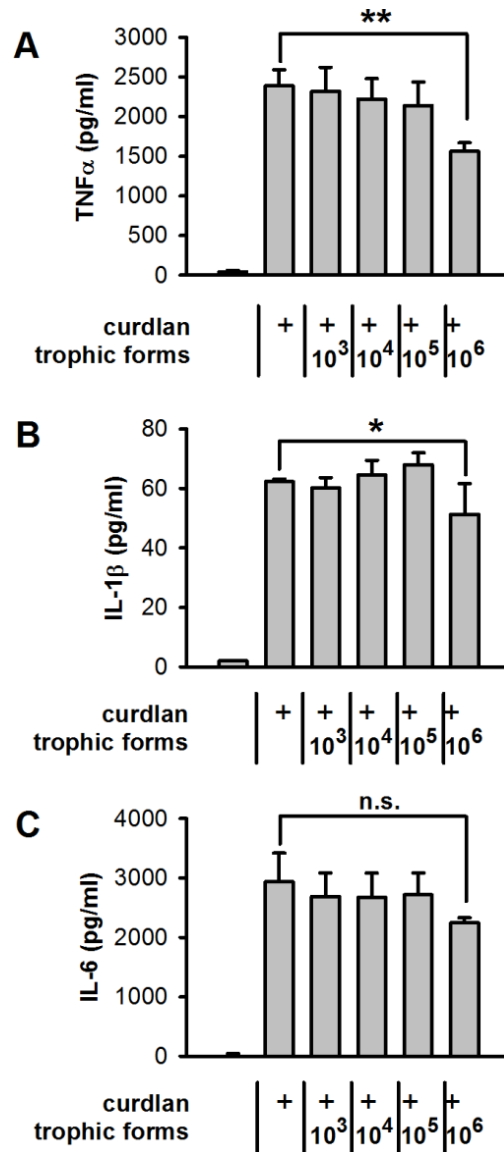
Figure 5-7 A ratio of 10 trophic forms to 1 BMDC is required to for suppression of cytokine expression.

1 X 10^5 BMDCs were incubated with 10 µg/ml curdlan, and increasing numbers of trophic forms for 72 h. TNFα (**A**), IL-1β (**B**), and IL-6 (**C**) cytokine levels in the supernatant were quantified by ELISA. Data represent the mean ±SD of 3 biological replicates per group and are representative of 2 separate experiments. One way ANOVA with Student-Newman-Keuls post-hoc test was used to compare cytokine concentrations among the groups, *p $\leq$ 0.05, n.s., not statistically significant.
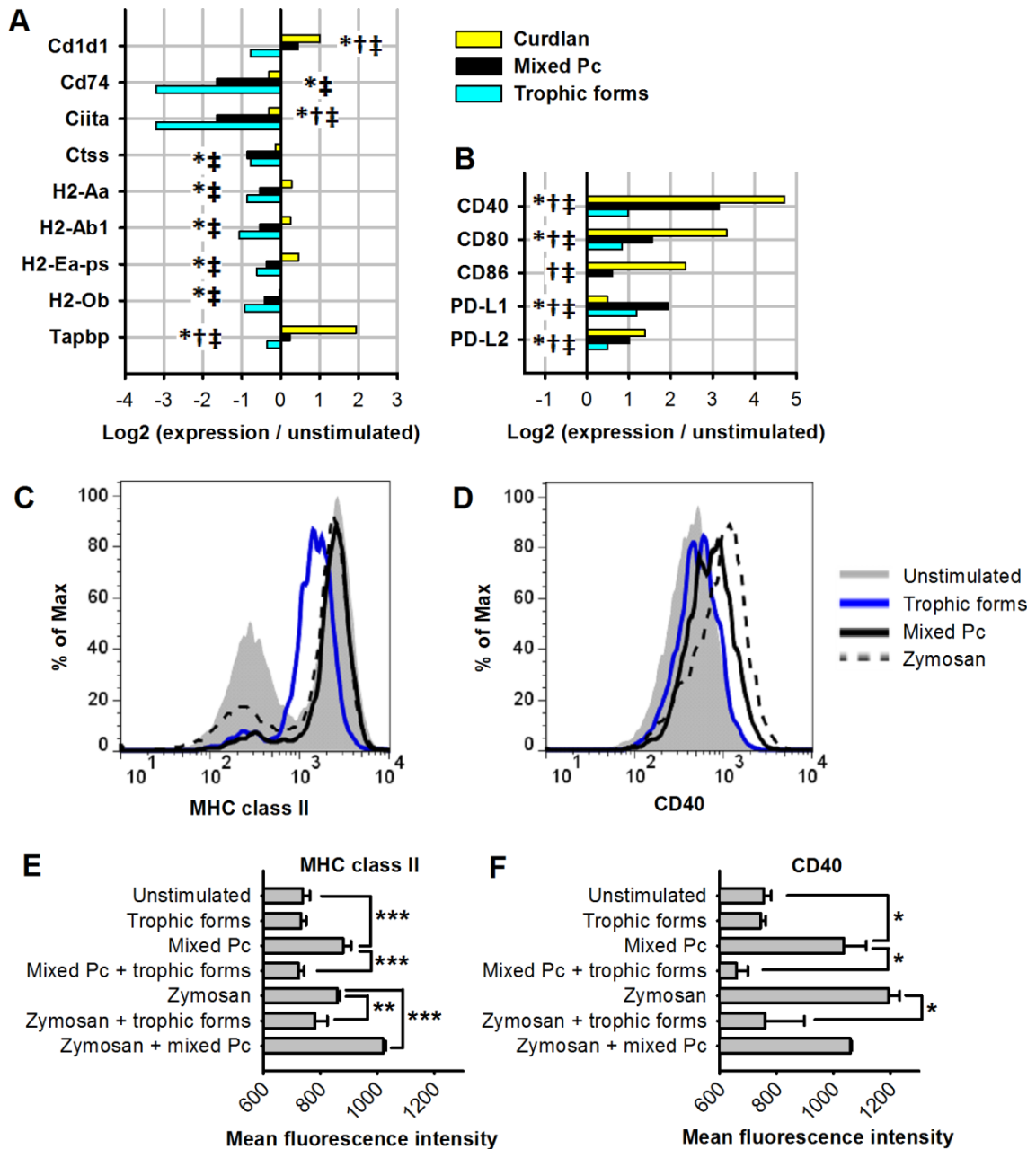
Figure 5-8 Trophic forms suppress the expression of multiple factors related to antigen presentation, including MHC class II and the costimulatory molecule CD40.

The data in **Fig 5.8A-B** represent genes in the NanoString panel encoding transcripts related to antigen-processing and presentation (**A**) or costimulatory molecules (**B**) with a statistically significant ($p < 0.01$) two-fold or greater increase in expression between BMDCs treated with trophic forms compared to unstimulated BMDCs. The relative gene expression after 8 h of treatment was calculated as the log2 value of the quotient of the treated expression value divided by the untreated expression value. Genes with differences in expression with $p < 0.01$ between BMDCs treated with trophic forms vs unstimulated cells are denoted *, trophic forms vs mixed *P. murina* organisms are

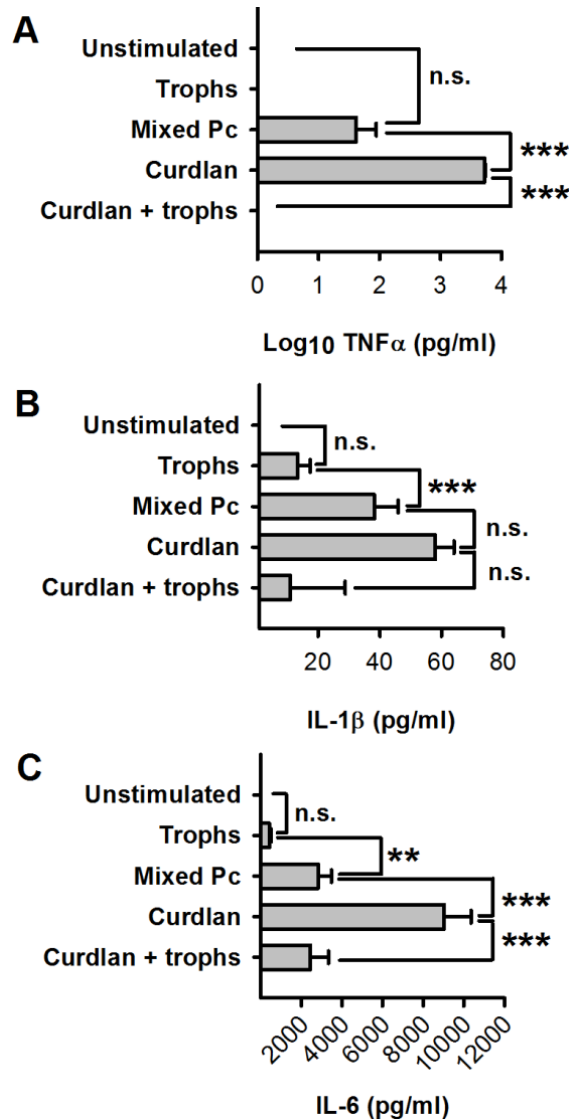denoted *****, trophic forms vs mixed *P. murina* organisms are denoted **†**, and trophic forms vs curdlan are denoted **‡**. Flow cytometry was used to evaluate surface expression of MHC class II (**C, E**) and CD40 (**D, F**) on the surface of BMDCs following 24 hours of treatment with trophic forms, mixed *P. murina*, and/or the fungal cell wall preparation zymosan. Flow cytometry data represent the mean ±SD of 3 biological replicates per group and are representative of 2 separate experiments. One way ANOVA with Student-Newman-Keuls post-hoc test was used to compare the surface expression of MHC class II or CD40 protein among the groups, $*p \leq 0.05$, $** p \leq 0.01$, $***p \leq 0.001$.
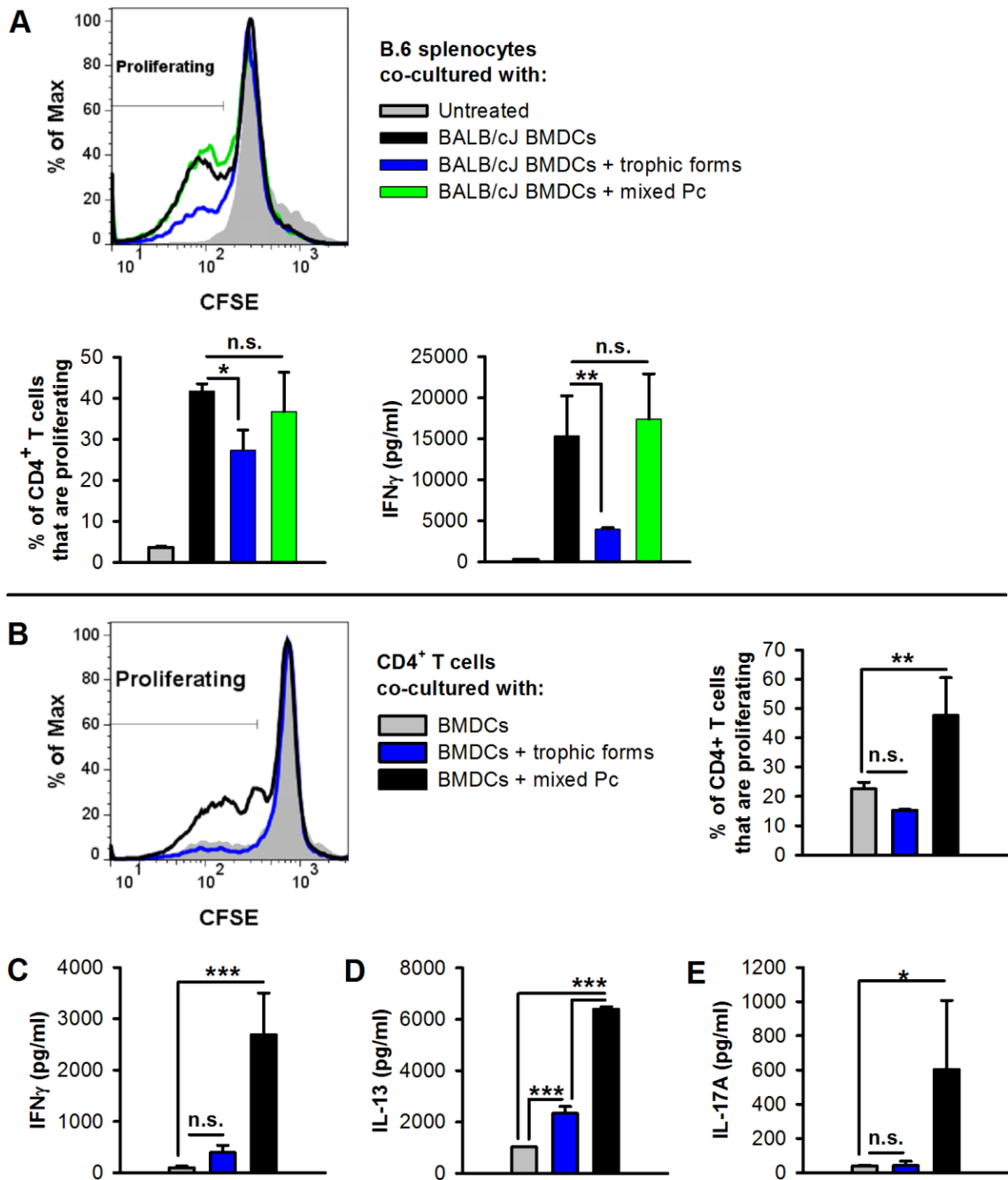
Figure 5-9 Trophic forms reduce dendritic cell-dependent proliferation of CD4+ T cells.

Treatment with trophic forms reduces CD4+ T cell proliferation in response to co-culture with allogeneic BMDCs in a mixed lymphocyte reaction (**A**). BMDCs generated from BALB/cJ mice were pre-treated with trophic forms or mixed *P. murina* organisms for one hour. CFSE-stained splenocytes from uninfected C57BL/6 mice were then added to the wells and co-cultured for 6 days. Flow cytometry was used to identify the CD4+ T cells

and evaluate their proliferation (**A**). BMDCs stimulated with trophic forms induce less proliferation and cytokine protein expression in CD4$^+$ T cells than cells stimulated with mixed *P. murina* (**B-E**). BMDCs and CFSE-stained CD4$^+$ T cells from adult BALB/cJ mice were incubated with trophic forms or mixed *P. murina* for 6 days. Flow cytometry was used to evaluate proliferation of CD4$^+$ T cells (**B**). ELISA was used to evaluate the concentrations of the cytokines IFNγ (**A, C**), IL-13 (**D**) and IL17A (**E**) in the supernatant. Data represent the mean ±SD of 3 biological replicates per group and are representative of at least two separate experiments. Cytokine data in the absence of One-way ANOVA with Student-Newman-Keuls post-hoc test was used to compare the percentage of proliferating CD4$^+$ T cells or supernatant cytokine concentration among the groups, *p ≤ 0.05, ** p ≤ 0.01, ***p ≤ 0.001, n.s., not statistically significant.

A z-stack

10μm

Purple: trophic forms
Green: BMDCs

B

Blue: nuclei
Purple: trophic forms
Green: pHrodo zymosan

C

n.s.

% of BMDCs that are zymosan+

- Unstimulated (grey)
- Trophic forms (blue)
- Mixed Pc (black)

D

n.s.

% of BMDCs that are zymosan+

E

n.s.

MFI of FITC on zymosan+ BMDCS
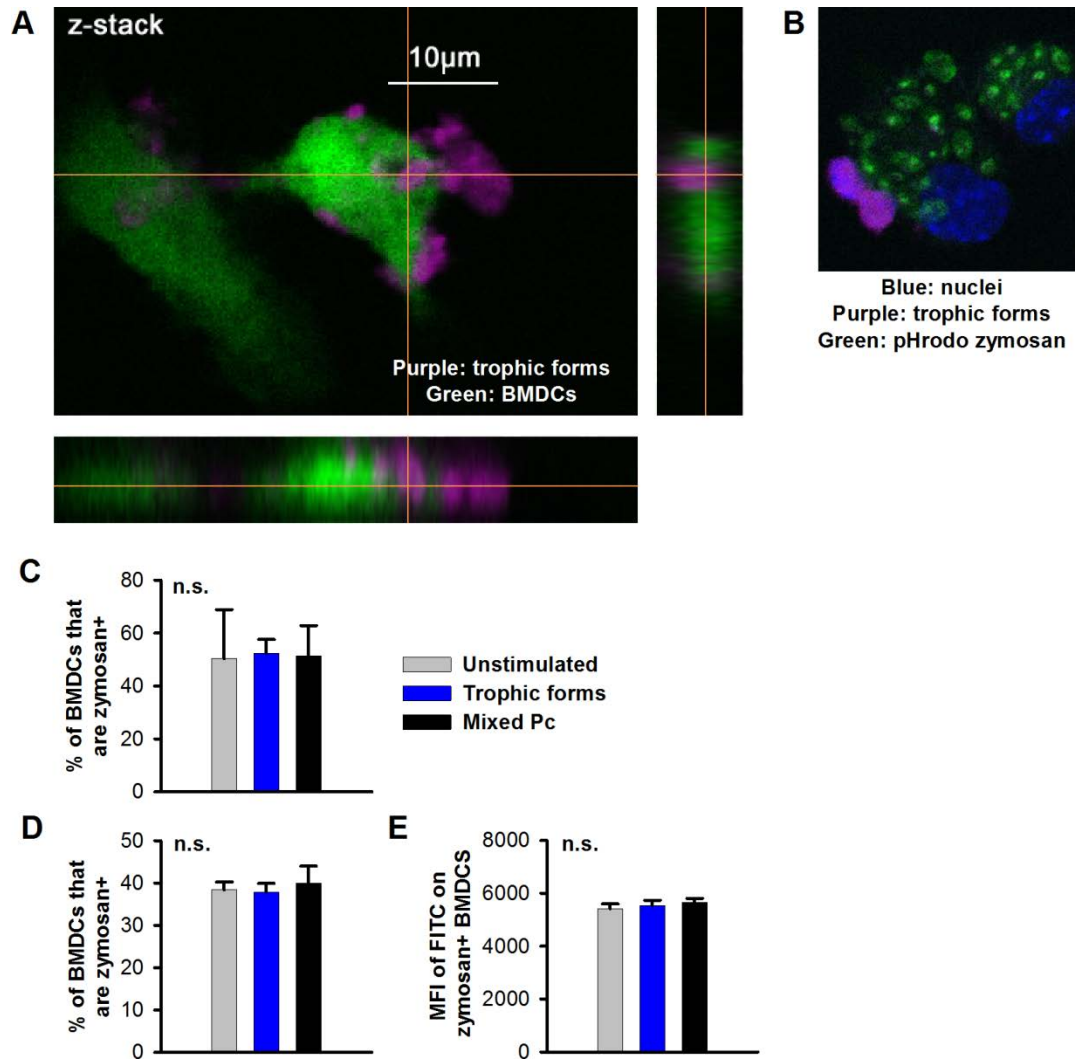
Figure 5-10 Trophic forms do not have a negative impact on the phagocytic capacity of dendritic cells.

CFSE-stained BMDCs from BALB/cJ mice were incubated with DDAO-SE-stained trophic forms or mixed *P. murina* organisms for one hour in a chamber slide (**A**). Cells were fixed in neutral buffered formalin, and confocal microscopy was used to identify internalized trophic forms (**A**). The z-stacks demonstrate that BMDCs internalize DDAO-SE-labeled trophic forms (**A**). BMDCs were incubated with pHrodo Green zymosan bioparticles and/or DDAO-SE-stained trophic forms or mixed *P. murina* organisms for one hour in chamber slides (**B-C**) or FACS tubes (**D-E**). The chamber slides were fixed in neutral buffered formalin, and stained with DAPI (**B-C**). Confocal microscopy was used determine the percentage of BMDCs that had phagocytosed the pH-sensitive pHrodo Green zymosan bioparticles based on at least 100 events per group (**B-C**). Flow cytometry was used to determine the percentage of BMDCs that had phagocytosed the pHrodo Green zymosan bioparticles based on at least 1000 events per group (**D**). The geometric mean fluorescence intensity (MFI) in the FITC channel of the zymosan$^+$ BMDCs was calculated for each group (**E**). Data represent the mean ±SD of 3 biological

replicates per group and are representative of 2 separate experiments. One way ANOVA with Student-Newman-Keuls post-hoc test was used to compare supernatant cytokine concentration between the groups, n.s., not statistically significant ($p > 0.05$).

Chapter 6: Discussion

I. Summary

Pneumocystis species are opportunistic fungal pathogens that cause severe pneumonia in immunocompromised hosts, including HIV/AIDS patients and patients undergoing chemotherapy or immunosuppressive therapy. Failure to clear *Pneumocystis* organisms leads to inflammation-mediated alveolar damage (5). Prior research in the field has overwhelmingly focused on the immune response to infection with a mixture of the trophic and cystic life cycle stages. Certainly, such studies provide valuable information, as the typical immune response to *Pneumocystis* organisms is shaped in the context of infection with both trophic forms and cysts. However, such studies do not provide a nuanced understanding of the distinct roles of the trophic and cystic life cycle stages in the development of the immune response to *Pneumocystis* infection. Here, our goal is to explore the biology of the immune response to these life cycle stages.

Tropic forms are proposed to represent the asexual stage, and are single-nucleated organisms that are typically found in clusters surrounded by a biofilm-like substance consisting of a conglomeration of DNA, β-glucan, and other sugars (13, 14). Cysts are ascus-like structures formed by mitosis, and consist of multiple nuclei surrounded by a fungal cell wall. β-1,3 glucan and β-1,6 glucan serve as the structural components of the cyst wall (13, 15, 16). β-glucan is not detected on the surface of trophic forms (15, 17). Both stages express surface glycoproteins and mannoproteins that may serve as pathogen-associated molecular patterns (PAMPs) that could interact with receptors on

phagocytic cells (18-20). Neither life form produces the classical fungal components ergosterol, chitin or α-glucans (21, 22).

Ultrastructural studies revealed that the trophic forms tightly adhere to the luminal surface of alveolar epithelial cells via microprotusions or invaginations of the trophic plasma membrane (64). This interaction is a risky endeavor for the trophic forms, as alveolar epithelial cells are capable of producing proinflammatory cytokines. In addition, this interaction with the alveolar epithelium places the trophic forms at risk for detection by immature lung dendritic cells, which project their dendritic extensions through the epithelial-tight junctions into the alveolar spaces. This encounter has the potential to induce dendritic cell activation and migration to the draining lymph nodes, where the cell may present antigen to lymphocytes. The involvement of dendritic cells is critical to the recruitment of T and B cells into the airway lumen, particularly as these spaces are largely free of lymphocytes prior to infection. Essentially, this slow-growing obligate parasite has adopted a niche that places it in constant danger of swiftly initiating the adaptive immune responses that will clear the organisms from the lungs.

Herein, we show that the life cycle stages of *Pneumocystis murina* differ in their interactions with the host immune response (**Chapter 3**). Infection with a normal mixture of trophic forms and cysts elicits proinflammatory responses, including early infiltration of T and B cells into the airways. Conversely, the trophic forms of *Pneumocystis murina* suppress the proinflammatory response to multiple pathogen-associated molecular patterns (PAMPs), including β-glucan. Depletion of cysts in immunocompromised RAG2$^{-/-}$ hosts resulted in a trophic burden that grew slowly over a six month period, but

did not induce overt symptoms associated with PcP, such as weight loss and infiltration of innate immune cells into the lungs (**Chapter 4**).

While cysts are required for robust pro-inflammatory responses, including the early recruitment of immune cells into the airways, infection with trophic forms in the absence of cysts is sufficient to drive protective $CD4^+$ T cell and B cell responses (**Chapter 4**). Remarkably, our data indicate that $CD4^+$ T cells generated in the absence of cysts promote faster clearance of infection than $CD4^+$ T cells generated in the presence of mixed *P. murina* organisms (**Chapter 4**). We do not report evidence of a direct suppressive effect of trophic forms on $CD4^+$ T cells or B cells.

Rather, our data indicate that trophic forms broadly inhibit the ability of dendritic cells to fulfill their role as antigen-presenting cells by reducing the expression of cytokines, MHC class II, and costimulatory molecules (**Fig 6.1 and Chapter 5**). These data suggest that immune evasion by the trophic forms may hinge on the suppression of the initiation of the innate immune response, including the inhibition of dendritic cell communication with $CD4^+$ T cells. The rapid establishment of a trophic population may be critical for this fungal pathogen to evade innate immune cells and avoid preemptive clearance of the transmittable, yet inflammatory cyst stage. However, the development of adaptive immunity to *Pneumocystis* may represent a "point of no return" at which the trophic forms are no longer able to escape clearance (**Chapter 3**).

II. Significance

This dissertation represents a major advancement in understanding the interactions between the host immune response and the life cycle stages of *Pneumocystis* species. Past research into the host response to *Pneumocystis* infection has overwhelmingly focused on the sum of the response to a fungal burden that includes a mixture of trophic forms and cysts. However, the capacity of the trophic forms to suppress innate immunity provides a compelling reason for decades of *Pneumocystis* research to be revaluated in the context of differential interactions between the life cycle stages and the host immune response.

1. The role of trophic form-mediated suppression during natural infection

Due to technical restrictions, we have not evaluated the immune response to purified or enriched cysts. However, the data that we have generated regarding the broad, immunosuppressive capabilities of the trophic forms suggest a corollary: the cysts are highly inflammatory. Namely, the net inflammation conditions generated in response to mixed *P. murina* organisms likely necessitates that the cyst must overcome the suppressive capabilities of the trophic forms at physiologically normal ratio of 1 cyst per 10 trophic forms.

The inflammatory potential of the cyst in the face of a 10-fold excess of trophic forms raises questions regarding the relevance of trophic suppression during the tenancy of the host lung. Here, we demonstrate that trophic form-mediated suppression modulates the early kinetics of the immune response, and that this delay persists for one week after the emergence of a population of cysts (**Fig 3.3**). Despite this delay, the immune response is able to clear the infection within the same period of time as observed in the group

inoculated with mixed *P. murina* organisms. It should be noted that this dissertation provides no direct evidence that trophic form-mediated suppression increases the fungal burden or delays clearance.

To address these concerns, we encourage the reader to consider the ecological niche of these ubiquitous fungal species. *Pneumocystis* species have evolved a life cycle characterized by transient infection of immunocompetent hosts. These species appear to occupy a niche somewhere in the gray area between "parasite" and "commensal." We propose that trophic form-mediated suppression is a host defense that has evolved, and has been maintained by selection, within *Pneumocystis* species. If this is true, it would be expected that a mixed *Pneumocystis* population arising from the natural route of infection would benefit from trophic form-mediated suppression. To this effect, we would predict that the inhibition of trophic form-mediated suppression during mixed *P. murina* infection would accelerate the clearance of this population. Conversely, it may be unreasonable to expect that trophic forms, in the absence of cysts, further delay clearance (Chapter 3).

We further propose that there may be other benefits to trophic form-mediated suppression. Inoculation with enriched trophic forms was not sufficient to increase the fungal burden or delay clearance. However, trophic form-mediated suppression may serve in other ways to enhance the fitness of the mixed population. Immune suppression by the trophic forms may improve the early niche within the host lung by dampening the consequences of inflammation, including the limitation of extracellular nutrient availability and the release of antimicrobial products, surfactant, and reactive nitrogen or oxygen species. It is also plausible that inflammatory signals may limit the ability of

Pneumocystis organisms to scavenge nutrients directly from alveolar epithelial cells. Alternatively, we demonstrate that trophic forms inhibit cytokine production in response to a broad range of PAMPs, including bacterial productions such as LPS and LTA. It is possible that trophic forms promote the maintenance of a tolerogenic state within the lung during coinfection of *Pneumocystis* species with bacteria or additional fungal species.

The ultimate aim of trophic form-mediated suppression may not be to delay clearance *per se*, but to enhance the transmission of cysts to a new host. To this effect, we consistently observe a large burst of trophic growth during the first week post-infection (as seen in Fig 3.3) resulting in a trophic form to cyst ratio in excess of 20:1. Based on the work presented in this dissertation, it seems plausible that this energy-intensive expansion of the trophic population may be necessary to preserve favorable conditions within the alveolar spaces, and thus protect the health of the transmittable cysts.

2. Significance for the development of treatments and vaccines

Protective adaptive responses are required for clearance of *Pneumocystis* organisms from the lungs, while, in the absence of protective responses, inflammation-mediated lung damage causes much of the pathology associated with *Pneumocystis* pneumonia. The differential effect of trophic forms and cysts on the host response, therefore, has the potential to shape both positive and negative outcomes associated with *Pneumocystis* infection. Manipulation of this differential response may provide new options for the treatment and prevention of *Pneumocystis* infection, while a failure to consider this differential response may hamper future efforts. Here, our data indicate that trophic forms elicit adaptive responses, but do not provoke the non-protective inflammation

characteristic of *Pneumocystis* pneumonia. Further evaluation of the antigenic determinants on trophic forms and cysts may elicit a vaccine that provides protection while limiting immune-mediated damage.

In Chapter 4, we demonstrate that, the absence of the cyst stage, a small trophic population was maintained in the lungs of RAG2$^{-/-}$ mice without overt evidence of disease. While further studies are required to evaluate the effects of a low trophic burden on the host lung, we report no evidence of the inflammatory conditions associated with *Pneumocystis* pneumonia, including infiltration of immune cells and accumulation of proinflammatory cytokines in the BALF. These observations suggest that the depletion of the cyst stage may provide beneficial treatment options in at-risk patients, particularly those that retain some means of clearing the remaining trophic forms. These patient populations would include those recovering from drug- or virus-induced immunosuppression. The potential benefit of cyst-targeted anti-fungal therapies is highlighted by a report from Linke *et al.* which demonstrates that treatment of rodents with echinocandins reduces inflammation in a model of immune reconstitution syndrome (24). It is our hope that the data presented in this dissertation encourage additional research regarding the influence of trophic forms and cysts on the detrimental proinflammatory response that is characteristic of *Pneumocystis* pneumonia.

3. Pathogen-associated immunosuppression

The identification of the mechanism(s) of trophic form-mediated suppression has the potential to provide highly valuable data for both basic science and translational medicine. The characterization of the suppressive material may suggest a list of

homologous materials expressed by other fungi or, perhaps, other kingdoms of life. These associations may generate hypotheses regarding the mechanism of interaction between the suppressive material and the host cell. Such efforts have the potential to enhance our understanding of immune evasion by a ubiquitous fungal parasite that causes devastating opportunistic infections in immunocompromised hosts.

Furthermore, our data demonstrate that co-culture with trophic forms broadly suppresses the ability of dendritic cells to produce proinflammatory cytokines in response to multiple PAMPs, including LPS, LTA, and zymosan. In addition, we have observed a similar degree of cytokine suppression in J774 macrophages and alveolar macrophages (Garvy lab, unpublished data). The identification of the mechanism(s) involved in suppression may provide pathways or effectors that may be manipulated or mimicked to develop novel anti-inflammatory therapies. Excessive production of proinflammatory cytokines, including IL-1, IL-6, and TNFα, contribute to damage during disease states such as sepsis or influenza-associated cytokine storm (206, 207). Future studies involving trophic form-mediated suppression may identify mechanisms to reduce cytokine production without compromising host immunity.

III. Limitations

This dissertation suffers from the universal limitations surrounding *Pneumocystis* research. Chief among these restrictions is the lack of a long term *ex vivo* culture system for *Pneumocystis* organisms. The inability of *P. jirovecii* to live outside of a human host has limited research on this medically important parasite and opportunistic pathogen. Rat and mouse models have driven critical advances in understanding the immune responses

to *P. carinii* and *P. murina*, respectively. The transmission of *Pneumocystis* organisms and the progression of disease, including the development of interstitial pneumonia, in immunocompromised rodents appear to be homologous to that experienced in humans. Patients with specific immunodeficiencies, including defects in immune cell populations, signaling pathways, and cytokines, have provided evidence regarding the components of the immune response that are essential for clearance of *Pneumocystis* organisms. These observations have been substantiated by a large body of research exploring the immune response to *Pneumocystis* in rodent models.

The complexity of immune cell subsets within the lungs also places limitations on the scope of this dissertation. Dendritic cells are relatively rare within uninfected tissues. cDCs may represent only 1-2% of the total cells within a single-cell suspension from the lungs (208). Furthermore, while some common markers to distinguish dendritic cells, such as CD11c, are applicable in the spleen, the lung is populated by other populations of CD11c$^+$ immune cells subsets that defy basic attempts at identification and isolation. For example, Lancelin and Guerrero-Plata report that positive selection of a single-cell preparation from the lungs yields a mixed population dominated by CD11c^{hi} MHC-II^{lo} macrophages (>70%) (208). Cell sorting for CD11c^{hi} MHC-II^{hi} cells resulted in a population consisting of >96% pure dendritic cells, with a typical yield of 5 X 10^4 cDC per lung (208).

Dendritic cells are relatively rare within tissues, with the exception of the spleen and thymus. Several protocols have been developed to generate primary dendritic cells from bone marrow, permitting researchers to reduce the numbers of animals (and research effort) required to perform dendritic cell studies. Here, we have employed the

methodology developed by Lutz *et al*. (209). Briefly, bone marrow from the tibias and femurs of adult mice was cultured for nine to twelve days in complete culture media containing recombinant murine granulocyte-macrophage colony-stimulating factor (GM-CSF). Every 48 h thereafter, non-adherent cells (including monocytes) were removed and replaced with fresh media with additional GM-CSF. BMDCs were collected by vigorously washing the plates with media to remove loosely adherent cells. In our hands, greater than 80% of recovered cells were CD11c$^+$, and up to 6 X 10^7 BMDCs may be generated from the bone marrow of a single mouse.

However, recent studies have challenged the identity of the BMDCs employed in this model. It has become appreciated that culture of BMDCs with bone marrow yields a mixed population of dendritic cells derived from monocytes and common dendritic cell precursors (210, 211). Neither population may be said to represent bona fide conventional dendritic cells, which require Flt3L for differentiation (195, 196).

It should also be noted that the culture of bone marrow derived cells does not lead to the development of a pure population of dendritic cells. Others have determined that the bone marrow precursors of both dendritic cells and macrophages develop into CD11c$^+$ MHC-II$^+$ cells in the presence of GM-CSF (210, 211). Both subsets undergo activation in response to LPS, while the dendritic cell subset alone is capable of inducing CD4$^+$ T cell responses to OVA antigen (211). The protocol employed here was developed by Lutz *et al*. to enrich for CD11c$^+$ dendritic cells (209). It is unclear if this protocol limits the contamination of CD11c$^+$ MHC-II$^+$ macrophages. While it has been reported that the addition of Flt3L to the culture media reduces the development of macrophages, it should be noted that Flt3L promotes the expansion of a small population of monocytes

in addition to conventional dendritic cells (195, 196). Helft *et al.* suggest that the practice of culturing bone marrow-derived dendritic cells remains a viable model for exploring basic cell function. However, the authors caution researchers to consider the impact of heterogeneous bone marrow-derived populations in their assays. Current protocols for the development of bone marrow-derived dendritic cells reduce, but do not eliminate, the complexity of the heterogeneous cell populations found *in vivo*.

IV. Future directions

This dissertation has provided significant answers regarding the role of the life cycle stages of *Pneumocystis* species in the development of host immunity. It is our hope that this work encourages future research into the biology of *Pneumocystis* organisms and host-pathogen interactions. Perhaps the greatest unanswered questions of this project are: (**1**) identification of the trophic form-associated factor(s) that induce suppression and (**2**) identification of the dendritic cell regulatory mechanisms involved in the suppressive response.

4. Identification of the suppressive factor(s):

This dissertation does not identify the suppressive factor(s) on the trophic forms that induce suppression. However, we have carried out a few preliminary studies regarding this mechanism. Here, we demonstrate that suppression of the cytokine response is not dependent on trophic form viability, nor direct contact between trophic forms and dendritic cells (**Chapter 5**). Live, heat-killed, and sonicated trophic forms suppressed cytokine production by β-glucan-treated BDMCs, indicating that suppression

is not dependent on the viability of trophic forms. Surprisingly, while intact mixed *P. murina* organisms induce IL-1β and IL-6 production, these data indicate that sonicated mixed *P. murina* organisms suppressed these responses. These data suggest that intact cysts are required for stimulation of cytokine production, and, in the absence of this stimulation, the trophic material is able to suppress the response to other PAMPs. Alternatively, it is possible that trophic forms directly reduce the inflammatory potential of the cyst by masking or digesting PAMPs on the cyst surface.

Immunosuppression by the trophic forms could be mediated by a secreted factor or by direct contact between the trophic forms and the BMDCs. Direct contact between the trophic forms and BMDCs was not required for a reduction in IL-1β or TNFα cytokine production (**Chapter 5**). Intriguingly, direct contact was required for the suppression of IL-6 protein production (**Chapter 5**). These experiments suggest that the suppressive effect of trophic forms does not require intact or living organisms, and indicate that suppression of dendritic cell responses is partially induced by some material, less than 0.4 micron in size, that is passively released from trophic forms.

However, it should be noted that these experiments only examined the suppression of IL-1β, IL-6, and TNFα supernatant concentrations. The effects of heat-killing, sonication or separation on trophic-form mediated suppression of other dendritic cell responses (including antigen presentation) have not been evaluated. The inability of trophic forms to suppress IL-6 production in the Transwell system suggests that multiple factors may be required for suppression of certain responses.

The suppressive factor(s) may be a protein or polysaccaharide that is shed from the surface of the trophic forms. Future work in our laboratory will seek to characterize the

suppressive factor using mass spectrometry. Sonication of trophic forms produces a mixture of biomolecules that is too complex for characterization by mass spectrometry. Proper sample preparation for mass spectrometry will require us to reduce the complexity of the sample. Various methods, including treatment with proteinases and glucanases, will be used to digest specific categories of proteins or polysaccharides. Alternatively, proteins may be isolated from the bulk sonicate on the basis of size. The goal will be to characterize by mass spectroscopy the least complex material that retains the suppressive abilities of whole trophic forms.

5.   Identification of the immediate host cell targets of suppression:

Here, we have characterized the suppressive phenotype of dendritic cells stimulated with trophic forms. However, we have not identified the precise mechanism by which trophic forms induce this broad suppressive phenotype. It is possible, for example, that trophic forms induce broad changes in gene expression by manipulating histone modification within the dendritic cell. Alternatively, trophic forms may target one or a handful of genes controlling dendritic cell maturation.

Tolerogenic dendritic cells promote anergic or regulatory T cell responses by secreting IL-10, TGFβ, and IL-2 and expressing the inhibitory molecules PD-L1 and PD-L2. However, our data indicate that treatment of dendritic cells with trophic forms results in lower levels of gene expression of each of these tolerogenic markers than treatment with a mixture of trophic forms and cysts. Therefore, trophic forms are not likely to induce a classical tolerogenic phenotype in dendritic cells. Rather, our data indicate that

treatment with trophic forms broadly reduces the ability of the dendritic cell to provide activation signals to the $CD4^+$ T cells.

The results of the NanoString assay were compared against systems biology databases (InnateDB and others) via tools such as pathway analysis. This analysis assisted in the identification of the antigen presentation genes differentially regulated in trophic form-treated cells (**Chapter 5**). However, such analyses have not yet proved fruitful in the identification of the master regulatory factor(s) targeted by the trophic forms. A large body of research has recently been produced regarding the mechanisms involved in the maturation and polarization of dendritic cells. However, the interactions connecting many of the proteins within the dendritic cell regulome remain unidentified. As these gaps in our understanding are filled, obvious candidates for the trophic target may emerge. In the meantime, more classical approaches may provide fruitful leads. For example, the identification of the suppressive material from the trophic form may permit future studies (such as co-immunoprecipitation assays) to search for interactions with the host cell.

Recent evidence suggests that fungal pathogens may manipulate interactions with C-type lectin receptors to suppress proinflammatory responses. Engagement of the C-type lectin receptor mincle by the fungal skin pathogen *Fonsecaea monophora* was shown to suppress the proinflammatory T_h1- and T_h17-type immune responses induced by dectin-1-mediated signaling (159). Opposing roles for dectin-2 and mincle have been observed in the recognition of *Fonsecaea pedrosoi* (160). We are currently examining whether mincle could mediate the suppressive activity of trophic forms, as was found for *F. monophora* (159).

Mycobacterium tuberculosis provides an additional example of pathogen-mediated manipulation of C-type lectin receptor responses. Pecora *et al*. have reported that *M. tuberculosi*s inhibits MHC class II transactivator (*Ciita*) expression, MHC class II molecule expression, and antigen presentation on macrophages. Lung dendritic cells infected with *M. bovis* BCG express less MHC class II on their surface than uninfected dendritic cells from the same lung (212). *M. tuberculosis* uses terminal mannosylated oligosaccharides to bind mannose receptor and DC-SIGN on host macrophages (213). Internalization via these receptors suppresses, rather than triggers, inflammatory responses in macrophages and dendritic cells. Specifically, the C-type lectin receptor DC-SIGN internalizes *M. tuberculosis* by binding mannosylated lipoarabinomannan, or ManLAM, on the bacterial cell wall. However, binding of ManLAM by the C-type lectin receptor DC-SIGN inhibits *M. tuberculosis* or LPS-induced dendritic cell maturation. The terminal mannosylation of *M. tuberculosis* oligosaccharides may mimic the structures present on host mannoproteins.

Here, we demonstrate that the deletion of mannose receptor on dendritic cells resulted in a modest decrease in the ability of trophic forms to suppress the production of IL-6, but not TNFα and IL-1β, indicating that suppression is mediated through mechanisms other than mannose receptor (**Chapter 3**). Future experiments may evaluate the role of additional mannose-recognizing receptors in the suppression of proinflammatory signaling, MHC class II expression, and induction of CD4^{+} T cell responses.

Other compelling questions, with accompanying speculation, include:

1. How inflammatory are the cysts?

Here, we do not evaluate the immune response to pure cysts. However, our data suggest that stimulation with a 10 to 1 mixture of trophic forms to cysts was sufficient to induce inflammatory responses in the dendritic cell (**Chapter 5**). The inflammatory potential of the cyst to induce a signal over trophic form-mediated suppression should be evaluated. Previous work has demonstrated that dendritic cells activated by *Pneumocystis* cyst cell wall-derived β-glucans increase costimulatory molecule expression and drive T cell polarization towards a T_h1-type response (23). Despite repeated efforts, we have not identified a reliable method to purify cysts from the lungs of mice. However, other groups have enriched *Pneumocystis* cysts from the lungs of infected rats, which are infected with a higher fungal burden than mice. Future studies could evaluate the immune response to purified *P. carinii* cysts from rats, or may continue to evaluate the response to purified *Pneumocystis* cell wall fragments.

2. Does the ratio of trophic forms to cysts influence the host immune response during the course of infection?

Our data suggest that slight shifts in the ratio of trophic forms to cysts may result in differential immune responses. For example, the addition of trophic forms to a mixed population to create a net ratio of 20 trophic forms to one cyst reduces the expression of IL-6 by BMDCs (**Chapter 3**). The *in vivo* effects of such shifts have not been studied, but such research may provide intriguing details regarding the life cycle of the fungus within its host. Over the course of infection, *Pneumocystis* organisms may be found at a

typical ratio of 10 trophic forms to 1 cyst. However, this is not a steady state: cysts are the transmittable life cycle stage, yet a large burst of trophic forms are observed during the first week post-infection (**Chapter 3**). It is possible that this rapid transition may delay recognition of inflammatory PAMPs by dendritic cells in the lung, and may prevent preemptive clearance.

Furthermore, a fungal burden of 20 to 30 trophic forms per cyst is consistently found in the lungs of immunocompromised mice exhibiting severe symptoms of *Pneumocystis* pneumonia. It is possible that inflammatory signals within the lungs promote a shift in the population towards an increase in suppressive trophic forms over inflammatory cysts. This shift could extend the life of the host, albeit at the cost of favoring the production of the non-transmittable trophic forms over the formation of cysts.

3. What impact does the differential response to *Pneumocystis* life forms have on the outcome of the infection in various models of disease?

Our data indicate that infection with trophic forms delays the initiation of innate and adaptive immune responses. Future studies should consider the role of trophic form-mediated suppression in models of various types of immunodeficiency. We found that depletion of cysts from the lungs of RAG2$^{-/-}$ mice results in the formation of a small trophic population that does not cause overt symptoms of *Pneumocystis* pneumonia, including weight loss (**Chapter 4**). Linke et al., demonstrate that depletion of cysts reduced inflammation in a murine model of immune reconstitution inflammatory syndrome (24). However, the range of patients at risk for pneumocystis pneumonia

includes those suffering from a wide range of immunodeficiencies. Does trophic form-mediated suppression increase the risk of developing PcP, or, in the event of PcP, does this suppression reduce inflammation-mediated lung damage in patients undergoing chemotherapy, or corticosteroid treatment? Is suppression of dendritic cell responses more successful in hosts with deficient B cell responses, such as those treated with anti-CD40 antibody therapy? What is the role of trophic form-mediated suppression in HIV/AIDs patients before and after the initiation of HAART? Here, we demonstrate that infection with purified trophic forms leads to a delay in the initiation of immune responses in neonatal mice compared to an infection with a mixture of organisms (**Chapter 3**). What is the impact of trophic form-mediated suppression within the developing lungs of a neonatal host? It is possible that the trophic forms reduce inflammation-mediated lung damage in the lungs of immunocompromised hosts. However, trophic form-mediated suppression may permit the fungal population to expand in the absence of immune pressure. This may prove detrimental if the host develops or regains the ability to respond to the infection, as the increased fungal burden may worsen inflammation-mediated lung damage. Future studies will be required to explore these possibilities.

4. What mechanisms overcome trophic form-mediated immune suppression?

Here, we demonstrate that trophic forms are sufficient to induce protective $CD4^+$ T cell and B cell responses leading to clearance of infection (**Chapter 4**). However, our data indicate that the initiation of these immune responses is delayed if cysts are absent in the inoculum (**Chapter 3**). Furthermore, we demonstrate that trophic form-loaded

dendritic cells are unable to prime CD4$^+$ T cell responses *in vitro*. The populations of immune cells involved in overcoming this delay are unknown. It is possible that trophic forms may not suppress other innate cells as definitively as dendritic cells. For example, alveolar epithelial cells, macrophages, or neutrophils may be more adept than dendritic cells at producing proinflammatory cytokines in the presence of trophic forms. The generation of a local inflammatory environment may promote dendritic cell maturation and activation, leading to presentation of antigen in the draining lymph nodes and the initiation of immune responses.

Research from other members of the Garvy lab indicates that trophic forms also suppress the ability of J774 and alveolar macrophages to express cytokines in response to mixed *P. murina* organisms. However, macrophages produce proinflammatory cytokines at an infectious dose of 10 mixed *P. murina* organisms per phagocyte, compared to the 50 to 1 dose required to yield production of IL-1β and IL-6 by dendritic cells. In our hands, macrophages, but not dendritic cells, produce TNFα in response to mixed P. murina organisms. These data suggest that macrophages may either be more responsive to the cysts or less susceptible to suppression than dendritic cells. However, it should be noted that in Chapter 4, the long-term carriage of trophic forms in RAG2$^{-/-}$ mice (which lack B cells and T cells) failed to promote a substantial accumulation of TNFα in the BALF.

Conversely, B cells may contribute to the initial activation of antigen-presenting cells in the lungs. Opata *et al*. demonstrate that B cells must be present during the first few days post-infection for effective priming of CD4$^+$ T cell responses to mixed *P. murina* infection. This effect occurred independently of antibody production, indicating that B cells provide additional cues for T cell activation (124). B cells are a key source of

TNFα during the response to mixed *Pneumocystis* infection (125). Future studies may characterize the role of B cells in the activation of CD4$^+$ T cells and effector cells in response to trophic forms.

V. Conclusions

Here, we propose that trophic forms broadly inhibit the ability of dendritic cells to fulfill their role as antigen-presenting cells by reducing the expression of cytokines, MHC class II, and costimulatory molecules. These data correspond with suboptimal CD4$^+$ T cell proliferation and polarization *in vitro*, and delayed CD4$^+$ T cell responses *in vivo*. The data presented herein provide compelling evidence for decades of *Pneumocystis* research to be revaluated in the context of interactions between the life cycle stages and the host immune response. The differential immune response to the life cycle stages of *Pneumocystis* shapes both the induction of protective responses and the development of inflammation-associated pathology. Manipulation of this balance may provide new options for the management and prevention of *Pneumocystis* infection, while a failure to consider this differential response may hinder future efforts. Further exploration of the interaction between trophic forms and the host may enhance our basic understanding of the pathways involved in immune activation and suppression. These pursuits may also fuel the discovery of novel anti-inflammatory therapies capable of broadly dampening cytokine production and antigen presentation.
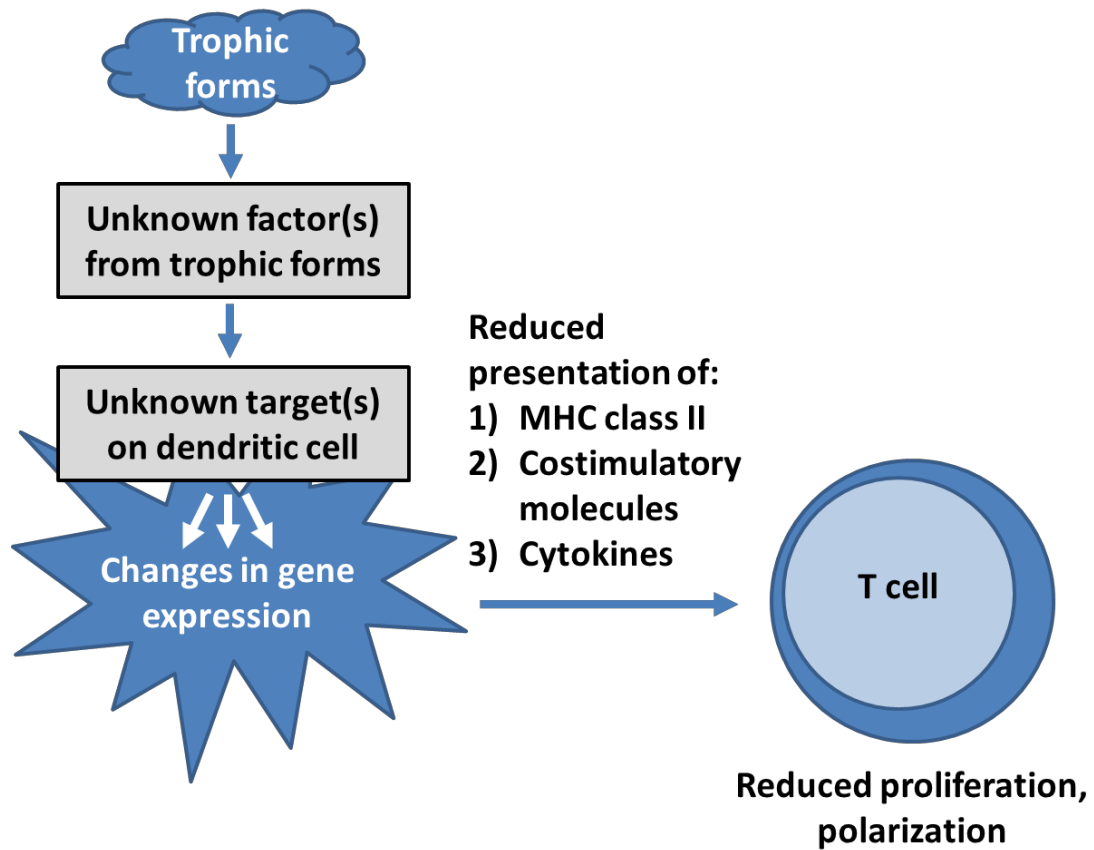
Figure 6-1 Model of trophic form-mediated suppression of dendritic cell function.

Trophic forms inhibit multiple components involved in antigen presentation by dendritic cells, including secretion of inflammatory cytokines and expression of MHC class II and costimulatory molecules on the cell surface. Furthermore, trophic forms suppress the expression of multiple genes related to activation and maturation in dendritic cells. Dendritic cells silenced by trophic forms are unable to induce CD4$^+$ T cell responses *in vitro*. This corresponds with delayed innate and adaptive responses *in vivo*.

Appendix A: List of Abbreviations

AIDS	Acquired immune deficiency syndrome
BMDC	Bone marrow-derived dendritic cells
CLR	C-type lectin receptor
COPD	Chronic obstructive pulmonary disease
ELISA	Enzyme-linked immunosorbent assay
GM-CSF	Granulocyte-macrophage colony-stimulating factor
HAART	High active antiretroviral therapy
HIV	Human immunodeficiency virus
IFNγ	Interferon gamma
IG	Immunoglobulin
IκB	NFκ-B inhibitor
IL	Interleukin
IRIS	Immune reconstitution inflammatory syndrome
IT	Intratracheal
ITAM	Immunoreceptor tyrosine activation motif
J774	Macrophage cell line derived from murine tumor
LPS	Lipopolysaccharides
LTA	Lipoteichoic acid
PAMP	Pathogen-associated molecular pattern
MHC class II	Major histocompatibility class II
MIP	Macrophage inflammatory protein
MR	Mannose receptor
NFAT	Nuclear factor of activated T-cells
NF-κB	Nuclear factor-κ light chain enhancer of activated B cells
NLR	NOD-like receptor
Pc	*Pneumocystis*
PcP	*Pneumocystis* Pneumonia
PRR	Pattern recognition receptor
ROS	Reactive oxygen species
SCID	Severe combined immune deficiency
SIDS	Sudden infant death syndrome
TGFβ	Transforming growth factor β
Th	T helper
TIR	Toll/interleukin-1 receptor
TLR	Toll-like receptor
TMP-SMX	Trimethoprim-sulfamethoxazole
TNFα	Tumor necrosis factor α

References

1. **Harmsen AG, Stankiewicz M.** 1990. Requirement for CD4+ cells in resistance to Pneumocystis carinii pneumonia in mice. J Exp Med 172**:**937-945
2. **Limper AH, Hoyte JS, Standing JE.** 1997. The role of alveolar macrophages in Pneumocystis carinii degradation and clearance from the lung. J Clin Invest 99**:**2110-2117. DOI:10.1172/JCI119384.
3. **Lund FE, Schuer K, Hollifield M, Randall TD, Garvy BA.** 2003. Clearance of Pneumocystis carinii in mice is dependent on B cells but not on P carinii-specific antibody. J Immunol 171**:**1423-1430
4. **Marcotte H, Levesque D, Delanay K, Bourgeault A, de la Durantaye R, Brochu S, Lavoie MC.** 1996. Pneumocystis carinii infection in transgenic B cell-deficient mice. J Infect Dis 173**:**1034-1037
5. **Limper AH, Offord KP, Smith TF, Martin WJ, 2nd.** 1989. Pneumocystis carinii pneumonia. Differences in lung parasite number and inflammation in patients with and without AIDS. Am Rev Respir Dis 140**:**1204-1209. DOI:10.1164/ajrccm/140.5.1204.
6. **Miller RF, Allen E, Copas A, Singer M, Edwards SG.** 2006. Improved survival for HIV infected patients with severe Pneumocystis jirovecii pneumonia is independent of highly active antiretroviral therapy. Thorax 61**:**716-721. DOI:10.1136/thx.2005.055905.
7. **Gajdusek DC.** 1957. Pneumocystis carinii; etiologic agent of interstitial plasma cell pneumonia of premature and young infants. Pediatrics 19**:**543-565
8. **Peglow SL, Smulian AG, Linke MJ, Pogue CL, Nurre S, Crisler J, Phair J, Gold JW, Armstrong D, Walzer PD.** 1990. Serologic responses to Pneumocystis carinii antigens in health and disease. J Infect Dis 161**:**296-306
9. **Kurkjian C, Hollifield M, Lines JL, Rogosky A, Empey KM, Qureshi M, Brown SA, Garvy BA.** 2012. Alveolar macrophages in neonatal mice are inherently unresponsive to Pneumocystis murina infection. Infect Immun 80**:**2835-2846. DOI:10.1128/IAI.05707-11.
10. **Garvy BA, Harmsen AG.** 1996. Susceptibility to Pneumocystis carinii infection: host responses of neonatal mice from immune or naive mothers and of immune or naive adults. Infect Immun 64**:**3987-3992
11. **Garvy BA, Qureshi MH.** 2000. Delayed inflammatory response to Pneumocystis carinii infection in neonatal mice is due to an inadequate lung environment. J Immunol 165**:**6480-6486
12. **Qureshi MH, Garvy BA.** 2001. Neonatal T cells in an adult lung environment are competent to resolve Pneumocystis carinii pneumonia. J Immunol 166**:**5704-5711
13. **Cushion MT, Ruffolo JJ, Walzer PD.** 1988. Analysis of the developmental stages of Pneumocystis carinii, in vitro. Lab Invest 58**:**324-331
14. **Cushion MT, Collins MS, Linke MJ.** 2009. Biofilm formation by Pneumocystis spp. Eukaryot Cell 8**:**197-206. DOI:10.1128/EC.00202-08.
15. **Walker AN, Garner RE, Horst MN.** 1990. Immunocytochemical detection of chitin in Pneumocystis carinii. Infect Immun 58**:**412-415

16. **Kottom TJ, Hebrink DM, Jenson PE, Gudmundsson G, Limper AH.** 2015. Evidence for Proinflammatory beta-1,6 Glucans in the Pneumocystis carinii Cell Wall. Infect Immun 83**:**2816-2826. DOI:10.1128/IAI.00196-15.

17. **Cushion MT, Linke MJ, Ashbaugh A, Sesterhenn T, Collins MS, Lynch K, Brubaker R, Walzer PD.** 2010. Echinocandin treatment of pneumocystis pneumonia in rodent models depletes cysts leaving trophic burdens that cannot transmit the infection. PLoS One 5**:**e8524. DOI:10.1371/journal.pone.0008524.

18. **Gigliotti F, Stokes DC, Cheatham AB, Davis DS, Hughes WT.** 1986. Development of murine monoclonal antibodies to Pneumocystis carinii. J Infect Dis 154**:**315-322

19. **Gigliotti F, Ballou LR, Hughes WT, Mosley BD.** 1988. Purification and initial characterization of a ferret Pneumocystis carinii surface antigen. J Infect Dis 158**:**848-854

20. **De Stefano JA, Myers JD, Du Pont D, Foy JM, Theus SA, Walzer PD.** 1998. Cell wall antigens of Pneumocystis carinii trophozoites and cysts: purification and carbohydrate analysis of these glycoproteins. J Eukaryot Microbiol 45**:**334-343

21. **Ma L, Chen Z, Huang da W, Kutty G, Ishihara M, Wang H, Abouelleil A, Bishop L, Davey E, Deng R, Deng X, Fan L, Fantoni G, Fitzgerald M, Gogineni E, Goldberg JM, Handley G, Hu X, Huber C, Jiao X, Jones K, Levin JZ, Liu Y, Macdonald P, Melnikov A, Raley C, Sassi M, Sherman BT, Song X, Sykes S, Tran B, Walsh L, Xia Y, Yang J, Young S, Zeng Q, Zheng X, Stephens R, Nusbaum C, Birren BW, Azadi P, Lempicki RA, Cuomo CA, Kovacs JA.** 2016. Genome analysis of three Pneumocystis species reveals adaptation mechanisms to life exclusively in mammalian hosts. Nat Commun 7**:**10740. DOI:10.1038/ncomms10740.

22. **Bartlett MS, Queener SF, Shaw MM, Richardson JD, Smith JW.** 1994. Pneumocystis carinii is resistant to imidazole antifungal agents. Antimicrob Agents Chemother 38**:**1859-1861

23. **Carmona EM, Vassallo R, Vuk-Pavlovic Z, Standing JE, Kottom TJ, Limper AH.** 2006. Pneumocystis cell wall beta-glucans induce dendritic cell costimulatory molecule expression and inflammatory activation through a Fas-Fas ligand mechanism. J Immunol 177**:**459-467

24. **Linke MJ, Ashbaugh A, Collins MS, Lynch K, Cushion MT.** 2013. Characterization of a distinct host response profile to Pneumocystis murina asci during clearance of pneumocystis pneumonia. Infect Immun 81**:**984-995. DOI:10.1128/IAI.01181-12.

25. **Chagas C.** 1909. Uber eine neue Trypoanosomiasis des Menschen. Mem Inst Oswaldo Cruz 3**:**1-218

26. **Carini A.** 1910. Formas des eschizogonia do Trypanosoma lewisi. Soc Med Cir São Paulo 38**:**8

27. **Hughes WT.** 2003. Pneumocystis carinii vs. Pneumocystis jiroveci: another misnomer (response to Stringer et al.). Emerg Infect Dis 9**:**276-277; author reply 277-279

28. **Delanoë P. DM.** 1912. Sur les rapports des kystes de Carini du poumon des rats avec le Trypanosoma lewisi. Comptes rendus de "l'Academie des sciences 155**:**658-661

29. **van der meer MG, Brug S.L.** 1942. Infection à Pneumocystis chez l'homme et chez les animaux. Amer Soc Belge Méd Trop 22**:**301-309

30. **Vanek J.** 1951. [Atypical (interstitial) pneumonia in children caused by Pneumocystis carinii]. Cas Lek Cesk 90**:**1121-1124

31. **Jírovec O.** 1952. Pneumocystis carinii puvodce t. zv intertitialnich plasmocelularnich pneumonii kojencw (Pneumocystis carinii, the cause of interstitial plasmacellular pneumonia in neonates). Csl. Hyg epid mikrob 1**:**141

32. **Goetz O, Ohrt B.** 1964. [Long-Term Cortisone Therapy and Interstitial Pneumonia]. Monatsschr Kinderheilkd 112**:**163-164

33. **Smith E, Gaspar IA.** 1968. Pentamidine treatment of Pneumocystis carinii pneumonitis in an adult with lymphatic leukemia. Am J Med 44**:**626-631

34. **Solberg CO, Meuwissen HJ, Needham RN, Good RA, Matsen JM.** 1971. Infectious complications in bone marrow transplant patients. Br Med J 1**:**18-23

35. **Centers for Disease C.** 1981. Pneumocystis pneumonia--Los Angeles. MMWR Morb Mortal Wkly Rep 30**:**250-252

36. **Buchacz K, Lau B, Jing Y, Bosch R, Abraham AG, Gill MJ, Silverberg MJ, Goedert JJ, Sterling TR, Althoff KN, Martin JN, Burkholder G, Gandhi N, Samji H, Patel P, Rachlis A, Thorne JE, Napravnik S, Henry K, Mayor A, Gebo K, Gange SJ, Moore RD, Brooks JT, North American ACCoR, Design of Ie DEA.** 2016. Incidence of AIDS-Defining Opportunistic Infections in a Multicohort Analysis of HIV-infected Persons in the United States and Canada, 2000-2010. J Infect Dis 214**:**862-872. DOI:10.1093/infdis/jiw085.

37. **Deborska-Materkowska D, Kozinska-Przybyl O, Mikaszewska-Sokolewicz M, Durlik M.** 2014. Fatal late-onset Pneumocystis pneumonia after rituximab: administration for posttransplantation recurrence of focal segmental glomerulosclerosis--case report. Transplant Proc 46**:**2908-2911. DOI:10.1016/j.transproceed.2014.09.010.

38. **Elsegeiny W, Eddens T, Chen K, Kolls JK.** 2015. Anti-CD20 antibody therapy and susceptibility to Pneumocystis pneumonia. Infect Immun 83**:**2043-2052. DOI:10.1128/IAI.03099-14.

39. **Mori S, Sugimoto M.** 2015. Pneumocystis jirovecii Pneumonia in Rheumatoid Arthritis Patients: Risks and Prophylaxis Recommendations. Clin Med Insights Circ Respir Pulm Med 9**:**29-40. DOI:10.4137/CCRPM.S23286.

40. **Omer O, P. Cohen, S.F Neong, G.V. Smith.** 2014. Pneumocystis pneumonia complicating immunosuppressive therapy in Crohns disease: A preventable problem? Frontline Gastroenterol 0**:**1-5

41. **Morris A, Sciurba FC, Lebedeva IP, Githaiga A, Elliott WM, Hogg JC, Huang L, Norris KA.** 2004. Association of chronic obstructive pulmonary disease severity and Pneumocystis colonization. Am J Respir Crit Care Med 170**:**408-413. DOI:10.1164/rccm.200401-094OC.

42. **Sivam S, Sciurba FC, Lucht LA, Zhang Y, Duncan SR, Norris KA, Morris A.** 2011. Distribution of Pneumocystis jirovecii in lungs from colonized COPD patients. Diagn Microbiol Infect Dis 71**:**24-28. DOI:10.1016/j.diagmicrobio.2011.05.008.

43. **Fitzpatrick ME, Tedrow JR, Hillenbrand ME, Lucht L, Richards T, Norris KA, Zhang Y, Sciurba FC, Kaminski N, Morris A.** 2014. Pneumocystis

jirovecii colonization is associated with enhanced Th1 inflammatory gene expression in lungs of humans with chronic obstructive pulmonary disease. Microbiol Immunol 58**:**202-211. DOI:10.1111/1348-0421.12135.

44. **Norris KA, Morris A.** 2011. Pneumocystis infection and the pathogenesis of chronic obstructive pulmonary disease. Immunol Res 50**:**175-180. DOI:10.1007/s12026-011-8218-x.

45. **Vargas SL, Ponce CA, Hughes WT, Wakefield AE, Weitz JC, Donoso S, Ulloa AV, Madrid P, Gould S, Latorre JJ, Avila R, Benveniste S, Gallo M, Belletti J, Lopez R.** 1999. Association of primary Pneumocystis carinii infection and sudden infant death syndrome. Clin Infect Dis 29**:**1489-1493. DOI:10.1086/313521.

46. **Morgan DJ, Vargas SL, Reyes-Mugica M, Walterspiel JN, Carver W, Gigliotti F.** 2001. Identification of Pneumocystis carinii in the lungs of infants dying of sudden infant death syndrome. Pediatr Infect Dis J 20**:**306-309

47. **Vargas SL, Ponce CA, Galvez P, Ibarra C, Haas EA, Chadwick AE, Krous HF.** 2007. Pneumocystis is not a direct cause of sudden infant death syndrome. Pediatr Infect Dis J 26**:**81-83. DOI:10.1097/01.inf.0000247071.40739.fd.

48. **Vargas SL, Ponce CA, Gallo M, Perez F, Astorga JF, Bustamante R, Chabe M, Durand-Joly I, Iturra P, Miller RF, Aliouat el M, Dei-Cas E.** 2013. Near-universal prevalence of Pneumocystis and associated increase in mucus in the lungs of infants with sudden unexpected death. Clin Infect Dis 56**:**171-179. DOI:10.1093/cid/cis870.

49. **Walzer PD, Evans HE, Copas AJ, Edwards SG, Grant AD, Miller RF.** 2008. Early predictors of mortality from Pneumocystis jirovecii pneumonia in HIV-infected patients: 1985-2006. Clin Infect Dis 46**:**625-633. DOI:10.1086/526778.

50. **Ko Y, Jeong BH, Park HY, Koh WJ, Suh GY, Chung MP, Kwon OJ, Jeon K.** 2014. Outcomes of Pneumocystis pneumonia with respiratory failure in HIV-negative patients. J Crit Care 29**:**356-361. DOI:10.1016/j.jcrc.2013.12.005.

51. **Roux A, Canet E, Valade S, Gangneux-Robert F, Hamane S, Lafabrie A, Maubon D, Debourgogne A, Le Gal S, Dalle F, Leterrier M, Toubas D, Pomares C, Bellanger AP, Bonhomme J, Berry A, Durand-Joly I, Magne D, Pons D, Hennequin C, Maury E, Roux P, Azoulay E.** 2014. Pneumocystis jirovecii pneumonia in patients with or without AIDS, France. Emerg Infect Dis 20**:**1490-1497. DOI:10.3201/eid2009.131668.

52. **Stringer JR, Cushion MT, Wakefield AE.** 2001. New nomenclature for the genus Pneumocystis. J Eukaryot Microbiol Suppl**:**184S-189S

53. **Stringer JR, Beard CB, Miller RF, Wakefield AE.** 2002. A new name (Pneumocystis jiroveci) for Pneumocystis from humans. Emerg Infect Dis 8**:**891-896. DOI:10.3201/eid0809.020096.

54. **Keely SP, Fischer JM, Cushion MT, Stringer JR.** 2004. Phylogenetic identification of Pneumocystis murina sp. nov., a new species in laboratory mice. Microbiology 150**:**1153-1165. DOI:10.1099/mic.0.26921-0.

55. **Dei-Cas E, Chabe M, Moukhlis R, Durand-Joly I, Aliouat el M, Stringer JR, Cushion M, Noel C, de Hoog GS, Guillot J, Viscogliosi E.** 2006. Pneumocystis oryctolagi sp. nov., an uncultured fungus causing pneumonia in rabbits at weaning: review of current knowledge, and description of a new taxon on

genotypic, phylogenetic and phenotypic bases. FEMS Microbiol Rev 30**:**853-871. DOI:10.1111/j.1574-6976.2006.00037.x.

56. **Copland JW.** 1974. Canine pneumonia caused by Pneumocystis carinii. Aust Vet J 50**:**515-518

57. **Peters SE, Wakefield AE, Whitwell KE, Hopkin JM.** 1994. Pneumocystis carinii pneumonia in thoroughbred foals: identification of a genetically distinct organism by DNA amplification. J Clin Microbiol 32**:**213-216

58. **Guillot J, Demanche C, Hugot JP, Berthelemy M, Wakefield AE, Dei-Cas E, Chermette R.** 2001. Parallel phylogenies of Pneumocystis species and their mammalian hosts. J Eukaryot Microbiol Suppl**:**113S-115S

59. **Riebold D, Mohr E, Sombetzki M, Fritzsche C, Loebermann M, Reisinger EC.** 2012. Pneumocystis species in Brown Leghorn laying hens--a hint for an extra-mammalian reservoir. Poult Sci 91**:**1813-1818. DOI:10.3382/ps.2011-01930.

60. **Gigliotti F, Harmsen AG, Haidaris CG, Haidaris PJ.** 1993. Pneumocystis carinii is not universally transmissible between mammalian species. Infect Immun 61**:**2886-2890

61. **Cushion MT, Keely SP, Stringer JR.** 2004. Molecular and phenotypic description of Pneumocystis wakefieldiae sp. nov., a new species in rats. Mycologia 96**:**429-438

62. **Aliouat-Denis CM, Martinez A, Aliouat el M, Pottier M, Gantois N, Dei-Cas E.** 2009. The Pneumocystis life cycle. Mem Inst Oswaldo Cruz 104**:**419-426

63. **Almeida JM, Cisse OH, Fonseca A, Pagni M, Hauser PM.** 2015. Comparative genomics suggests primary homothallism of Pneumocystis species. MBio 6. DOI:10.1128/mBio.02250-14.

64. **Long EG, Smith JS, Meier JL.** 1986. Attachment of Pneumocystis carinii to rat pneumocytes. Lab Invest 54**:**609-615

65. **Pottratz ST, Martin WJ, 2nd.** 1990. Role of fibronectin in Pneumocystis carinii attachment to cultured lung cells. J Clin Invest 85**:**351-356. DOI:10.1172/JCI114445.

66. **Pottratz ST.** 1998. Pneumocystis carinii interactions with respiratory epithelium. Semin Respir Infect 13**:**323-329

67. **Joffrion TM, Cushion MT.** 2010. Sterol biosynthesis and sterol uptake in the fungal pathogen Pneumocystis carinii. FEMS Microbiol Lett 311**:**1-9. DOI:10.1111/j.1574-6968.2010.02007.x.

68. **Cambi A, Netea MG, Mora-Montes HM, Gow NA, Hato SV, Lowman DW, Kullberg BJ, Torensma R, Williams DL, Figdor CG.** 2008. Dendritic cell interaction with Candida albicans critically depends on N-linked mannan. J Biol Chem 283**:**20590-20599. DOI:10.1074/jbc.M709334200.

69. **Saijo S, Fujikado N, Furuta T, Chung SH, Kotaki H, Seki K, Sudo K, Akira S, Adachi Y, Ohno N, Kinjo T, Nakamura K, Kawakami K, Iwakura Y.** 2007. Dectin-1 is required for host defense against Pneumocystis carinii but not against Candida albicans. Nat Immunol 8**:**39-46. DOI:10.1038/ni1425.

70. **Hughes WT.** 1982. Natural mode of acquisition for de novo infection with Pneumocystis carinii. J Infect Dis 145**:**842-848

71.   **An CL, Gigliotti F, Harmsen AG.** 2003. Exposure of immunocompetent adult mice to Pneumocystis carinii f. sp. muris by cohousing: growth of P. carinii f. sp. muris and host immune response. Infect Immun 71**:**2065-2070

72.   **Dumoulin A, Mazars E, Seguy N, Gargallo-Viola D, Vargas S, Cailliez JC, Aliouat EM, Wakefield AE, Dei-Cas E.** 2000. Transmission of Pneumocystis carinii disease from immunocompetent contacts of infected hosts to susceptible hosts. Eur J Clin Microbiol Infect Dis 19**:**671-678

73.   **Chabe M, Dei-Cas E, Creusy C, Fleurisse L, Respaldiza N, Camus D, Durand-Joly I.** 2004. Immunocompetent hosts as a reservoir of pneumocystis organisms: histological and rt-PCR data demonstrate active replication. Eur J Clin Microbiol Infect Dis 23**:**89-97. DOI:10.1007/s10096-003-1092-2.

74.   **Gigliotti F, Harmsen AG, Wright TW.** 2003. Characterization of transmission of Pneumocystis carinii f. sp. muris through immunocompetent BALB/c mice. Infect Immun 71**:**3852-3856

75.   **de Boer MG, de Fijter JW, Kroon FP.** 2011. Outbreaks and clustering of Pneumocystis pneumonia in kidney transplant recipients: a systematic review. Med Mycol 49**:**673-680. DOI:10.3109/13693786.2011.571294.

76.   **Gianella S, Haeberli L, Joos B, Ledergerber B, Wuthrich RP, Weber R, Kuster H, Hauser PM, Fehr T, Mueller NJ.** 2010. Molecular evidence of interhuman transmission in an outbreak of Pneumocystis jirovecii pneumonia among renal transplant recipients. Transpl Infect Dis 12**:**1-10. DOI:10.1111/j.1399-3062.2009.00447.x.

77.   **Vargas SL, Hughes WT, Santolaya ME, Ulloa AV, Ponce CA, Cabrera CE, Cumsille F, Gigliotti F.** 2001. Search for primary infection by Pneumocystis carinii in a cohort of normal, healthy infants. Clin Infect Dis 32**:**855-861. DOI:10.1086/319340.

78.   **Rivero L, de la Horra C, Montes-Cano MA, Rodriguez-Herrera A, Respaldiza N, Friaza V, Morilla R, Gutierrez S, Varela JM, Medrano FJ, Calderon EJ.** 2008. Pneumocystis jirovecii transmission from immunocompetent carriers to infant. Emerg Infect Dis 14**:**1116-1118. DOI:10.3201/eid1407.071431.

79.   **Thomas CF, Jr., Limper AH.** 2007. Current insights into the biology and pathogenesis of Pneumocystis pneumonia. Nat Rev Microbiol 5**:**298-308. DOI:10.1038/nrmicro1621.

80.   Panel on Opportunistic Infections in HIV-Infected Adults and Adolescents. Guidelines for the prevention and treatment of opportunistic infections in HIV-infected adults and adolescents: recommendations from the Centers for Disease Control and Prevention, the National Institutes of Health, and the HIV Medicine Association of the Infectious Diseases Society of America. Available at http://aidsinfo.nih.gov/contentfiles/lvguidelines/adult_oi.pdf. Accessed July 30, 2017.

81.   **Ioannidis JP, Cappelleri JC, Skolnik PR, Lau J, Sacks HS.** 1996. A meta-analysis of the relative efficacy and toxicity of Pneumocystis carinii prophylactic regimens. Arch Intern Med 156**:**177-188

82.   **Martin SI, Fishman JA, Practice ASTIDCo.** 2013. Pneumocystis pneumonia in solid organ transplantation. Am J Transplant 13 Suppl 4**:**272-279. DOI:10.1111/ajt.12119.

83. **Armstrong-James D, Stebbing J, John L, Murungi A, Bower M, Gazzard B, Nelson M.** 2011. A trial of caspofungin salvage treatment in PCP pneumonia. Thorax 66**:**537-538. DOI:10.1136/thx.2010.135350.

84. **Condon TV, Sawyer RT, Fenton MJ, Riches DW.** 2011. Lung dendritic cells at the innate-adaptive immune interface. J Leukoc Biol 90**:**883-895. DOI:10.1189/jlb.0311134.

85. **Macagno A, Atzori C, Fantoni B, Valerio A, Cargnel A, Groettrup M.** 2001. Pneumocystis carinii does not induce maturation of human dendritic cells. J Eukaryot Microbiol Suppl**:**167S-168S

86. **Kobayashi H, Worgall S, O'Connor TP, Crystal RG.** 2007. Interaction of Pneumocystis carinii with dendritic cells and resulting host responses to P. carinii. J Immunother 30**:**54-63. DOI:10.1097/01.cji.0000211314.13492.64.

87. **Zheng M, Shellito JE, Marrero L, Zhong Q, Julian S, Ye P, Wallace V, Schwarzenberger P, Kolls JK.** 2001. CD4+ T cell-independent vaccination against Pneumocystis carinii in mice. J Clin Invest 108**:**1469-1474. DOI:10.1172/JCI13826.

88. **Carmona EM, Kottom TJ, Hebrink DM, Moua T, Singh RD, Pagano RE, Limper AH.** 2012. Glycosphingolipids mediate pneumocystis cell wall beta-glucan activation of the IL-23/IL-17 axis in human dendritic cells. Am J Respir Cell Mol Biol 47**:**50-59. DOI:10.1165/rcmb.2011-0159OC.

89. **Masur H, Jones TC.** 1978. The interaction in vitro of Pneumocystis carinii with macrophages and L-cells. J Exp Med 147**:**157-170

90. **Von Behren LA, Pesanti EL.** 1978. Uptake and degradation of Pneumocystis carinii by macrophages in vitro. Am Rev Respir Dis 118**:**1051-1059. DOI:10.1164/arrd.1978.118.6.1051.

91. **Pottratz ST, Martin WJ, 2nd.** 1990. Mechanism of Pneumocystis carinii attachment to cultured rat alveolar macrophages. J Clin Invest 86**:**1678-1683. DOI:10.1172/JCI114891.

92. **Ezekowitz RA, Williams DJ, Koziel H, Armstrong MY, Warner A, Richards FF, Rose RM.** 1991. Uptake of Pneumocystis carinii mediated by the macrophage mannose receptor. Nature 351**:**155-158. DOI:10.1038/351155a0.

93. **Steele C, Marrero L, Swain S, Harmsen AG, Zheng M, Brown GD, Gordon S, Shellito JE, Kolls JK.** 2003. Alveolar macrophage-mediated killing of Pneumocystis carinii f. sp. muris involves molecular recognition by the Dectin-1 beta-glucan receptor. J Exp Med 198**:**1677-1688. DOI:10.1084/jem.20030932.

94. **Hidalgo HA, Helmke RJ, German VF, Mangos JA.** 1992. Pneumocystis carinii induces an oxidative burst in alveolar macrophages. Infect Immun 60**:**1-7

95. **Downing JF, Kachel DL, Pasula R, Martin WJ, 2nd.** 1999. Gamma interferon stimulates rat alveolar macrophages to kill Pneumocystis carinii by L-arginine- and tumor necrosis factor-dependent mechanisms. Infect Immun 67**:**1347-1352

96. **Lasbury ME, Liao CP, Hage CA, Durant PJ, Tschang D, Wang SH, Zhang C, Lee CH.** 2011. Defective nitric oxide production by alveolar macrophages during Pneumocystis pneumonia. Am J Respir Cell Mol Biol 44**:**540-547. DOI:10.1165/rcmb.2009-0367OC.

97. **Kandil O, Fishman JA, Koziel H, Pinkston P, Rose RM, Remold HG.** 1994. Human immunodeficiency virus type 1 infection of human macrophages

modulates the cytokine response to Pneumocystis carinii. Infect Immun 62**:**644-650

98. **Zhang J, Zhu J, Imrich A, Cushion M, Kinane TB, Koziel H.** 2004. Pneumocystis activates human alveolar macrophage NF-kappaB signaling through mannose receptors. Infect Immun 72**:**3147-3160. DOI:10.1128/IAI.72.6.3147-3160.2004.

99. **Deckman JM, Kurkjian CJ, McGillis JP, Cory TJ, Birket SE, Schutzman LM, Murphy BS, Garvy BA, Feola DJ.** 2017. Pneumocystis infection alters the activation state of pulmonary macrophages. Immunobiology 222**:**188-197. DOI:10.1016/j.imbio.2016.10.003.

100. **Wang J, Gigliotti F, Bhagwat SP, George TC, Wright TW.** 2010. Immune modulation with sulfasalazine attenuates immunopathogenesis but enhances macrophage-mediated fungal clearance during Pneumocystis pneumonia. PLoS Pathog 6**:**e1001058. DOI:10.1371/journal.ppat.1001058.

101. **Nelson MP, Christmann BS, Werner JL, Metz AE, Trevor JL, Lowell CA, Steele C.** 2011. IL-33 and M2a alveolar macrophages promote lung defense against the atypical fungal pathogen Pneumocystis murina. J Immunol 186**:**2372-2381. DOI:10.4049/jimmunol.1002558.

102. **Hanano R, Reifenberg K, Kaufmann SH.** 1998. Activated pulmonary macrophages are insufficient for resistance against Pneumocystis carinii. Infect Immun 66**:**305-314

103. **Hahn PY, Evans SE, Kottom TJ, Standing JE, Pagano RE, Limper AH.** 2003. Pneumocystis carinii cell wall beta-glucan induces release of macrophage inflammatory protein-2 from alveolar epithelial cells via a lactosylceramide-mediated mechanism. J Biol Chem 278**:**2043-2050. DOI:10.1074/jbc.M209715200.

104. **Evans SE, Hahn PY, McCann F, Kottom TJ, Pavlovic ZV, Limper AH.** 2005. Pneumocystis cell wall beta-glucans stimulate alveolar epithelial cell chemokine generation through nuclear factor-kappaB-dependent mechanisms. Am J Respir Cell Mol Biol 32**:**490-497. DOI:10.1165/rcmb.2004-0300OC.

105. **Evans SE, Kottom TJ, Pagano RE, Limper AH.** 2012. Primary alveolar epithelial cell surface membrane microdomain function is required for Pneumocystis beta-glucan-induced inflammatory responses. Innate Immun 18**:**709-716. DOI:10.1177/1753425912436763.

106. **Carmona EM, Lamont JD, Xue A, Wylam M, Limper AH.** 2010. Pneumocystis cell wall beta-glucan stimulates calcium-dependent signaling of IL-8 secretion by human airway epithelial cells. Respir Res 11**:**95. DOI:10.1186/1465-9921-11-95.

107. **Pottratz ST, Reese S, Sheldon JL.** 1998. Pneumocystis carinii induces interleukin 6 production by an alveolar epithelial cell line. Eur J Clin Invest 28**:**424-429

108. **Roths JB, Sidman CL.** 1992. Both immunity and hyperresponsiveness to Pneumocystis carinii result from transfer of CD4+ but not CD8+ T cells into severe combined immunodeficiency mice. J Clin Invest 90**:**673-678. DOI:10.1172/JCI115910.

109. **Wiley JA, Harmsen AG.** 1995. CD40 ligand is required for resolution of Pneumocystis carinii pneumonia in mice. J Immunol 155**:**3525-3529

110. **Beck JM, Blackmon MB, Rose CM, Kimzey SL, Preston AM, Green JM.** 2003. T cell costimulatory molecule function determines susceptibility to infection with Pneumocystis carinii in mice. J Immunol 171**:**1969-1977

111. **Fraser IP, Takahashi K, Koziel H, Fardin B, Harmsen A, Ezekowitz RA.** 2000. Pneumocystis carinii enhances soluble mannose receptor production by macrophages. Microbes Infect 2**:**1305-1310

112. **Garvy BA, Wiley JA, Gigliotti F, Harmsen AG.** 1997. Protection against Pneumocystis carinii pneumonia by antibodies generated from either T helper 1 or T helper 2 responses. Infect Immun 65**:**5052-5056

113. **Shellito JE, Tate C, Ruan S, Kolls J.** 2000. Murine CD4+ T lymphocyte subsets and host defense against Pneumocystis carinii. J Infect Dis 181**:**2011-2017. DOI:10.1086/315487.

114. **Rudner XL, Happel KI, Young EA, Shellito JE.** 2007. Interleukin-23 (IL-23)-IL-17 cytokine axis in murine Pneumocystis carinii infection. Infect Immun 75**:**3055-3061. DOI:10.1128/IAI.01329-06.

115. **Myers RC, Dunaway CW, Nelson MP, Trevor JL, Morris A, Steele C.** 2013. STAT4-dependent and -independent Th2 responses correlate with protective immunity against lung infection with Pneumocystis murina. J Immunol 190**:**6287-6294. DOI:10.4049/jimmunol.1300431.

116. **Gigliotti F, Crow EL, Bhagwat SP, Wright TW.** 2006. Sensitized CD8+ T cells fail to control organism burden but accelerate the onset of lung injury during Pneumocystis carinii pneumonia. Infect Immun 74**:**6310-6316. DOI:10.1128/IAI.00668-06.

117. **Wright TW, Pryhuber GS, Chess PR, Wang Z, Notter RH, Gigliotti F.** 2004. TNF receptor signaling contributes to chemokine secretion, inflammation, and respiratory deficits during Pneumocystis pneumonia. J Immunol 172**:**2511-2521

118. **Pryhuber GS, Huyck HL, Bhagwat S, O'Reilly MA, Finkelstein JN, Gigliotti F, Wright TW.** 2008. Parenchymal cell TNF receptors contribute to inflammatory cell recruitment and respiratory failure in Pneumocystis carinii-induced pneumonia. J Immunol 181**:**1409-1419

119. **Kolls JK, Habetz S, Shean MK, Vazquez C, Brown JA, Lei D, Schwarzenberger P, Ye P, Nelson S, Summer WR, Shellito JE.** 1999. IFN-gamma and CD8+ T cells restore host defenses against Pneumocystis carinii in mice depleted of CD4+ T cells. J Immunol 162**:**2890-2894

120. **Wells J, Haidaris CG, Wright TW, Gigliotti F.** 2006. Complement and Fc function are required for optimal antibody prophylaxis against Pneumocystis carinii pneumonia. Infect Immun 74**:**390-393. DOI:10.1128/IAI.74.1.390-393.2006.

121. **Harmsen AG, Chen W, Gigliotti F.** 1995. Active immunity to Pneumocystis carinii reinfection in T-cell-depleted mice. Infect Immun 63**:**2391-2395

122. **de la Rua NM, Samuelson DR, Charles TP, Welsh DA, Shellito JE.** 2016. CD4(+) T-Cell-Independent Secondary Immune Responses to Pneumocystis Pneumonia. Front Immunol 7**:**178. DOI:10.3389/fimmu.2016.00178.

123. **Lund FE, Hollifield M, Schuer K, Lines JL, Randall TD, Garvy BA.** 2006. B cells are required for generation of protective effector and memory CD4 cells in response to Pneumocystis lung infection. J Immunol 176**:**6147-6154

124. **Opata MM, Hollifield ML, Lund FE, Randall TD, Dunn R, Garvy BA, Feola DJ.** 2015. B Lymphocytes Are Required during the Early Priming of CD4+ T Cells for Clearance of Pneumocystis Infection in Mice. J Immunol 195**:**611-620. DOI:10.4049/jimmunol.1500112.

125. **Opata MM, Ye Z, Hollifield M, Garvy BA.** 2013. B cell production of tumor necrosis factor in response to Pneumocystis murina infection in mice. Infect Immun 81**:**4252-4260. DOI:10.1128/IAI.00744-13.

126. **Hoyt TR, Dobrinen E, Kochetkova I, Meissner N.** 2015. B cells modulate systemic responses to Pneumocystis murina lung infection and protect on-demand hematopoiesis via T cell-independent innate mechanisms when type I interferon signaling is absent. Infect Immun 83**:**743-758. DOI:10.1128/IAI.02639-14.

127. **Huertas A, Testa U, Riccioni R, Petrucci E, Riti V, Savi D, Serra P, Bonsignore MR, Palange P.** 2010. Bone marrow-derived progenitors are greatly reduced in patients with severe COPD and low-BMI. Respir Physiol Neurobiol 170**:**23-31. DOI:10.1016/j.resp.2009.10.003.

128. **Huertas A, Palange P.** 2011. COPD: a multifactorial systemic disease. Ther Adv Respir Dis 5**:**217-224. DOI:10.1177/1753465811400490.

129. **Brown TT, McComsey GA.** 2006. Osteopenia and osteoporosis in patients with HIV: a review of current concepts. Curr Infect Dis Rep 8**:**162-170

130. **Isgro A, Leti W, De Santis W, Marziali M, Esposito A, Fimiani C, Luzi G, Pinti M, Cossarizza A, Aiuti F, Mezzaroma I.** 2008. Altered clonogenic capability and stromal cell function characterize bone marrow of HIV-infected subjects with low CD4+ T cell counts despite viral suppression during HAART. Clin Infect Dis 46**:**1902-1910. DOI:10.1086/588480.

131. **Qureshi MH, Empey KM, Garvy BA.** 2005. Modulation of proinflammatory responses to Pneumocystis carinii f. sp. muris in neonatal mice by granulocyte-macrophage colony-stimulating factor and IL-4: role of APCs. J Immunol 174**:**441-448

132. **Yoneda K, Walzer PD.** 1981. Mechanism of pulmonary alveolar injury in experimental Pneumocystis carinii pneumonia in the rat. Br J Exp Pathol 62**:**339-346

133. **Gigliotti F, Wright TW.** 2005. Immunopathogenesis of Pneumocystis carinii pneumonia. Expert Rev Mol Med 7**:**1-16. DOI:10.1017/S1462399405010203.

134. **Wright TW, Gigliotti F, Finkelstein JN, McBride JT, An CL, Harmsen AG.** 1999. Immune-mediated inflammation directly impairs pulmonary function, contributing to the pathogenesis of Pneumocystis carinii pneumonia. J Clin Invest 104**:**1307-1317. DOI:10.1172/JCI6688.

135. **Barry SM, Lipman MC, Deery AR, Johnson MA, Janossy G.** 2002. Immune reconstitution pneumonitis following Pneumocystis carinii pneumonia in HIV-infected subjects. HIV Med 3**:**207-211

136. **Azoulay E, Parrot A, Flahault A, Cesari D, Lecomte I, Roux P, Saidi F, Fartoukh M, Bernaudin JF, Cadranel J, Mayaud C.** 1999. AIDS-related Pneumocystis carinii pneumonia in the era of adjunctive steroids: implication of

BAL neutrophilia. Am J Respir Crit Care Med 160**:**493-499. DOI:10.1164/ajrccm.160.2.9901019.

137. **Mason GR, Hashimoto CH, Dickman PS, Foutty LF, Cobb CJ.** 1989. Prognostic implications of bronchoalveolar lavage neutrophilia in patients with Pneumocystis carinii pneumonia and AIDS. Am Rev Respir Dis 139**:**1336-1342. DOI:10.1164/ajrccm/139.6.1336.

138. **Swain SD, Wright TW, Degel PM, Gigliotti F, Harmsen AG.** 2004. Neither neutrophils nor reactive oxygen species contribute to tissue damage during Pneumocystis pneumonia in mice. Infect Immun 72**:**5722-5732. DOI:10.1128/IAI.72.10.5722-5732.2004.

139. **Harmsen AG, Chen W.** 1992. Resolution of Pneumocystis carinii pneumonia in CD4+ lymphocyte-depleted mice given aerosols of heat-treated Escherichia coli. J Exp Med 176**:**881-886

140. **Zhang C, Lei GS, Shao S, Jung HW, Durant PJ, Lee CH.** 2012. Accumulation of myeloid-derived suppressor cells in the lungs during Pneumocystis pneumonia. Infect Immun 80**:**3634-3641. DOI:10.1128/IAI.00668-12.

141. **Lei GS, Zhang C, Lee CH.** 2015. Myeloid-derived suppressor cells impair alveolar macrophages through PD-1 receptor ligation during Pneumocystis pneumonia. Infect Immun 83**:**572-582. DOI:10.1128/IAI.02686-14.

142. **Sepkowitz KA.** 1993. Pneumocystis carinii pneumonia in patients without AIDS. Clin Infect Dis 17 Suppl 2**:**S416-422

143. **Garcia-Vidal C, Viasus D, Carratala J.** 2013. Pathogenesis of invasive fungal infections. Curr Opin Infect Dis 26**:**270-276. DOI:10.1097/QCO.0b013e32835fb920.

144. **Kawai T, Akira S.** 2011. Toll-like receptors and their crosstalk with other innate receptors in infection and immunity. Immunity 34**:**637-650. DOI:10.1016/j.immuni.2011.05.006.

145. **Netea MG, Van der Graaf C, Van der Meer JW, Kullberg BJ.** 2004. Recognition of fungal pathogens by Toll-like receptors. Eur J Clin Microbiol Infect Dis 23**:**672-676. DOI:10.1007/s10096-004-1192-7.

146. **Adams EL, Rice PJ, Graves B, Ensley HE, Yu H, Brown GD, Gordon S, Monteiro MA, Papp-Szabo E, Lowman DW, Power TD, Wempe MF, Williams DL.** 2008. Differential high-affinity interaction of dectin-1 with natural or synthetic glucans is dependent upon primary structure and is influenced by polymer chain length and side-chain branching. J Pharmacol Exp Ther 325**:**115-123. DOI:10.1124/jpet.107.133124.

147. **Gantner BN, Simmons RM, Canavera SJ, Akira S, Underhill DM.** 2003. Collaborative induction of inflammatory responses by dectin-1 and Toll-like receptor 2. J Exp Med 197**:**1107-1117. DOI:10.1084/jem.20021787.

148. **Goodridge HS, Reyes CN, Becker CA, Katsumoto TR, Ma J, Wolf AJ, Bose N, Chan AS, Magee AS, Danielson ME, Weiss A, Vasilakos JP, Underhill DM.** 2011. Activation of the innate immune receptor Dectin-1 upon formation of a 'phagocytic synapse'. Nature 472**:**471-475. DOI:10.1038/nature10071.

149. **LeibundGut-Landmann S, Gross O, Robinson MJ, Osorio F, Slack EC, Tsoni SV, Schweighoffer E, Tybulewicz V, Brown GD, Ruland J, Reis e Sousa C.** 2007. Syk- and CARD9-dependent coupling of innate immunity to the

induction of T helper cells that produce interleukin 17. Nat Immunol 8**:**630-638. DOI:10.1038/ni1460.

150. **Leibundgut-Landmann S, Osorio F, Brown GD, Reis e Sousa C.** 2008. Stimulation of dendritic cells via the dectin-1/Syk pathway allows priming of cytotoxic T-cell responses. Blood 112**:**4971-4980. DOI:10.1182/blood-2008-05-158469.

151. **Sancho D, Reis e Sousa C.** 2012. Signaling by myeloid C-type lectin receptors in immunity and homeostasis. Annu Rev Immunol 30**:**491-529. DOI:10.1146/annurev-immunol-031210-101352.

152. **Dennehy KM, Ferwerda G, Faro-Trindade I, Pyz E, Willment JA, Taylor PR, Kerrigan A, Tsoni SV, Gordon S, Meyer-Wentrup F, Adema GJ, Kullberg BJ, Schweighoffer E, Tybulewicz V, Mora-Montes HM, Gow NA, Williams DL, Netea MG, Brown GD.** 2008. Syk kinase is required for collaborative cytokine production induced through Dectin-1 and Toll-like receptors. Eur J Immunol 38**:**500-506. DOI:10.1002/eji.200737741.

153. **Esteban A, Popp MW, Vyas VK, Strijbis K, Ploegh HL, Fink GR.** 2011. Fungal recognition is mediated by the association of dectin-1 and galectin-3 in macrophages. Proc Natl Acad Sci U S A 108**:**14270-14275. DOI:10.1073/pnas.1111415108.

154. **Valera I, Fernandez N, Trinidad AG, Alonso S, Brown GD, Alonso A, Crespo MS.** 2008. Costimulation of dectin-1 and DC-SIGN triggers the arachidonic acid cascade in human monocyte-derived dendritic cells. J Immunol 180**:**5727-5736

155. **Douglas CM.** 2001. Fungal beta(1,3)-D-glucan synthesis. Med Mycol 39 Suppl 1**:**55-66

156. **Zhang C, Wang SH, Lasbury ME, Tschang D, Liao CP, Durant PJ, Lee CH.** 2006. Toll-like receptor 2 mediates alveolar macrophage response to Pneumocystis murina. Infect Immun 74**:**1857-1864. DOI:10.1128/IAI.74.3.1857-1864.2006.

157. **O'Riordan DM, Standing JE, Limper AH.** 1995. Pneumocystis carinii glycoprotein A binds macrophage mannose receptors. Infect Immun 63**:**779-784

158. **Peters M, Guidato PM, Peters K, Megger DA, Sitek B, Classen B, Heise EM, Bufe A.** 2016. Allergy-Protective Arabinogalactan Modulates Human Dendritic Cells via C-Type Lectins and Inhibition of NF-kappaB. J Immunol 196**:**1626-1635. DOI:10.4049/jimmunol.1502178.

159. **Wevers BA, Kaptein TM, Zijlstra-Willems EM, Theelen B, Boekhout T, Geijtenbeek TB, Gringhuis SI.** 2014. Fungal engagement of the C-type lectin mincle suppresses dectin-1-induced antifungal immunity. Cell Host Microbe 15**:**494-505. DOI:10.1016/j.chom.2014.03.008.

160. **Wuthrich M, Wang H, Li M, Lerksuthirat T, Hardison SE, Brown GD, Klein B.** 2015. Fonsecaea pedrosoi-induced Th17-cell differentiation in mice is fostered by Dectin-2 and suppressed by Mincle recognition. Eur J Immunol 45**:**2542-2552. DOI:10.1002/eji.201545591.

161. **Zhang J, Tachado SD, Patel N, Zhu J, Imrich A, Manfruelli P, Cushion M, Kinane TB, Koziel H.** 2005. Negative regulatory role of mannose receptors on

human alveolar macrophage proinflammatory cytokine release in vitro. J Leukoc Biol 78**:**665-674. DOI:10.1189/jlb.1204699.

162. **Cisse OH, Pagni M, Hauser PM.** 2014. Comparative genomics suggests that the human pathogenic fungus Pneumocystis jirovecii acquired obligate biotrophy through gene loss. Genome Biol Evol 6**:**1938-1948. DOI:10.1093/gbe/evu155.

163. **Hauser PM.** 2014. Genomic insights into the fungal pathogens of the genus pneumocystis: obligate biotrophs of humans and other mammals. PLoS Pathog 10**:**e1004425. DOI:10.1371/journal.ppat.1004425.

164. **Hauser PM, Burdet FX, Cisse OH, Keller L, Taffe P, Sanglard D, Pagni M.** 2010. Comparative genomics suggests that the fungal pathogen pneumocystis is an obligate parasite scavenging amino acids from its host's lungs. PLoS One 5**:**e15152. DOI:10.1371/journal.pone.0015152.

165. **Angus CW, Tu A, Vogel P, Qin M, Kovacs JA.** 1996. Expression of variants of the major surface glycoprotein of Pneumocystis carinii. J Exp Med 183**:**1229-1234

166. **den Dunnen J, Gringhuis SI, Geijtenbeek TB.** 2009. Innate signaling by the C-type lectin DC-SIGN dictates immune responses. Cancer Immunol Immunother 58**:**1149-1157. DOI:10.1007/s00262-008-0615-1.

167. **Tachado SD, Zhang J, Zhu J, Patel N, Cushion M, Koziel H.** 2007. Pneumocystis-mediated IL-8 release by macrophages requires coexpression of mannose receptors and TLR2. J Leukoc Biol 81**:**205-211. DOI:10.1189/jlb.1005580.

168. **Evans HM, Bryant GL, 3rd, Garvy BA.** 2016. The life cycle stages of Pneumocystis murina have opposing effects on the immune response to this opportunistic, fungal pathogen. Infect Immun. DOI:10.1128/IAI.00519-16.

169. **Harding CV, Canaday D, Ramachandra L.** 2010. Choosing and preparing antigen-presenting cells. Curr Protoc Immunol Chapter 16**:**Unit 16 11. DOI:10.1002/0471142735.im1601s88.

170. **Ding K, Shibui A, Wang Y, Takamoto M, Matsuguchi T, Sugane K.** 2005. Impaired recognition by Toll-like receptor 4 is responsible for exacerbated murine Pneumocystis pneumonia. Microbes Infect 7**:**195-203. DOI:10.1016/j.micinf.2004.10.010.

171. **Thornton BP, Vetvicka V, Pitman M, Goldman RC, Ross GD.** 1996. Analysis of the sugar specificity and molecular location of the beta-glucan-binding lectin site of complement receptor type 3 (CD11b/CD18). J Immunol 156**:**1235-1246

172. **Wang J, Gigliotti F, Maggirwar S, Johnston C, Finkelstein JN, Wright TW.** 2005. Pneumocystis carinii activates the NF-kappaB signaling pathway in alveolar epithelial cells. Infect Immun 73**:**2766-2777. DOI:10.1128/IAI.73.5.2766-2777.2005.

173. **Zimmerman JW, Lindermuth J, Fish PA, Palace GP, Stevenson TT, DeMong DE.** 1998. A novel carbohydrate-glycosphingolipid interaction between a beta-(1-3)-glucan immunomodulator, PGG-glucan, and lactosylceramide of human leukocytes. J Biol Chem 273**:**22014-22020

174. **Ferwerda G, Meyer-Wentrup F, Kullberg BJ, Netea MG, Adema GJ.** 2008. Dectin-1 synergizes with TLR2 and TLR4 for cytokine production in human

primary monocytes and macrophages. Cell Microbiol 10**:**2058-2066. DOI:10.1111/j.1462-5822.2008.01188.x.

175. **Kling HM, Norris KA.** 2016. Vaccine-Induced Immunogenicity and Protection Against Pneumocystis Pneumonia in a Nonhuman Primate Model of HIV and Pneumocystis Coinfection. J Infect Dis 213**:**1586-1595. DOI:10.1093/infdis/jiw032.

176. **Tesini BL, Wright TW, Malone JE, Haidaris CG, Harber M, Sant AJ, Nayak JL, Gigliotti F.** 2017. Immunization with Pneumocystis Cross-Reactive Antigen 1 (Pca1) Protects Mice against Pneumocystis Pneumonia and Generates Antibody to Pneumocystis jirovecii. Infect Immun 85. DOI:10.1128/IAI.00850-16.

177. **Pascale JM, Shaw MM, Durant PJ, Amador AA, Bartlett MS, Smith JW, Gregory RL, McLaughlin GL.** 1999. Intranasal immunization confers protection against murine Pneumocystis carinii lung infection. Infect Immun 67**:**805-809

178. **Laursen AL, Obel N, Rungby J, Andersen PL.** 1993. Phagocytosis and stimulation of the respiratory burst in neutrophils by Pneumocystis carinii. J Infect Dis 168**:**1466-1471

179. **Laursen A, Obel NS, Holmskov U, Jensenius JC, Aliouat el M, Andersen PL.** 2003. Activation of the respiratory burst by Pneumocystis carinii. Efficiency of different antibody isotypes, complement, lung surfactant protein D, and mannan-binding lectin. APMIS 111**:**405-415

180. **Empey KM, Hollifield M, Schuer K, Gigliotti F, Garvy BA.** 2004. Passive immunization of neonatal mice against Pneumocystis carinii f. sp. muris enhances control of infection without stimulating inflammation. Infect Immun 72**:**6211-6220. DOI:10.1128/IAI.72.11.6211-6220.2004.

181. **Samuelson DR, de la Rua NM, Charles TP, Ruan S, Taylor CM, Blanchard EE, Luo M, Ramsay AJ, Shellito JE, Welsh DA.** 2016. Oral Immunization of Mice with Live Pneumocystis murina Protects against Pneumocystis Pneumonia. J Immunol 196**:**2655-2665. DOI:10.4049/jimmunol.1502004.

182. **Matsumoto Y, Matsuda S, Tegoshi T.** 1989. Yeast glucan in the cyst wall of Pneumocystis carinii. J Protozool 36**:**21S-22S

183. **Nollstadt KH, Powles MA, Fujioka H, Aikawa M, Schmatz DM.** 1994. Use of beta-1,3-glucan-specific antibody to study the cyst wall of Pneumocystis carinii and effects of pneumocandin B0 analog L-733,560. Antimicrob Agents Chemother 38**:**2258-2265

184. **Ueno K, Koga T, Kato K, Golenbock DT, Gendler SJ, Kai H, Kim KC.** 2008. MUC1 mucin is a negative regulator of toll-like receptor signaling. Am J Respir Cell Mol Biol 38**:**263-268. DOI:10.1165/rcmb.2007-0336RC.

185. **Edelson BT, Kc W, Juang R, Kohyama M, Benoit LA, Klekotka PA, Moon C, Albring JC, Ise W, Michael DG, Bhattacharya D, Stappenbeck TS, Holtzman MJ, Sung SS, Murphy TL, Hildner K, Murphy KM.** 2010. Peripheral CD103+ dendritic cells form a unified subset developmentally related to CD8alpha+ conventional dendritic cells. J Exp Med 207**:**823-836. DOI:10.1084/jem.20091627.

186. **Hildner K, Edelson BT, Purtha WE, Diamond M, Matsushita H, Kohyama M, Calderon B, Schraml BU, Unanue ER, Diamond MS, Schreiber RD, Murphy TL, Murphy KM.** 2008. Batf3 deficiency reveals a critical role for

CD8alpha+ dendritic cells in cytotoxic T cell immunity. Science 322**:**1097-1100. DOI:10.1126/science.1164206.

187. **Schlitzer A, Ginhoux F.** 2014. Organization of the mouse and human DC network. Curr Opin Immunol 26**:**90-99. DOI:10.1016/j.coi.2013.11.002.

188. **Merad M, Sathe P, Helft J, Miller J, Mortha A.** 2013. The dendritic cell lineage: ontogeny and function of dendritic cells and their subsets in the steady state and the inflamed setting. Annu Rev Immunol 31**:**563-604. DOI:10.1146/annurev-immunol-020711-074950.

189. **Schlitzer A, McGovern N, Teo P, Zelante T, Atarashi K, Low D, Ho AW, See P, Shin A, Wasan PS, Hoeffel G, Malleret B, Heiseke A, Chew S, Jardine L, Purvis HA, Hilkens CM, Tam J, Poidinger M, Stanley ER, Krug AB, Renia L, Sivasankar B, Ng LG, Collin M, Ricciardi-Castagnoli P, Honda K, Haniffa M, Ginhoux F.** 2013. IRF4 transcription factor-dependent CD11b+ dendritic cells in human and mouse control mucosal IL-17 cytokine responses. Immunity 38**:**970-983. DOI:10.1016/j.immuni.2013.04.011.

190. **Plantinga M, Guilliams M, Vanheerswynghels M, Deswarte K, Branco-Madeira F, Toussaint W, Vanhoutte L, Neyt K, Killeen N, Malissen B, Hammad H, Lambrecht BN.** 2013. Conventional and monocyte-derived CD11b(+) dendritic cells initiate and maintain T helper 2 cell-mediated immunity to house dust mite allergen. Immunity 38**:**322-335. DOI:10.1016/j.immuni.2012.10.016.

191. **Simmons DP, Wearsch PA, Canaday DH, Meyerson HJ, Liu YC, Wang Y, Boom WH, Harding CV.** 2012. Type I IFN drives a distinctive dendritic cell maturation phenotype that allows continued class II MHC synthesis and antigen processing. J Immunol 188**:**3116-3126. DOI:10.4049/jimmunol.1101313.

192. **Lasbury ME, Durant PJ, Tschang D, Wang SH, Zhang C, Liao CP, Lee CH.** 2006. Expression and activation of complement protein and alveolar damage during Pneumocystis pneumonia. J Eukaryot Microbiol 53 Suppl 1**:**S136-137. DOI:10.1111/j.1550-7408.2006.00204.x.

193. **Perez HD, Ohtani O, Banda D, Ong R, Fukuyama K, Goldstein IM.** 1983. Generation of biologically active, complement-(C5) derived peptides by cathepsin H. J Immunol 131**:**397-402

194. **Perez HD.** 1984. Biologically active complement (C5)-derived peptides and their relevance to disease. Crit Rev Oncol Hematol 1**:**199-225

195. **Xu Y, Zhan Y, Lew AM, Naik SH, Kershaw MH.** 2007. Differential development of murine dendritic cells by GM-CSF versus Flt3 ligand has implications for inflammation and trafficking. J Immunol 179**:**7577-7584

196. **Mayer CT, Ghorbani P, Nandan A, Dudek M, Arnold-Schrauf C, Hesse C, Berod L, Stuve P, Puttur F, Merad M, Sparwasser T.** 2014. Selective and efficient generation of functional Batf3-dependent CD103+ dendritic cells from mouse bone marrow. Blood 124**:**3081-3091. DOI:10.1182/blood-2013-12-545772.

197. **Eissenberg LG, Goldman WE, Schlesinger PH.** 1993. Histoplasma capsulatum modulates the acidification of phagolysosomes. J Exp Med 177**:**1605-1611

198. **Marcil A, Gadoury C, Ash J, Zhang J, Nantel A, Whiteway M.** 2008. Analysis of PRA1 and its relationship to Candida albicans- macrophage interactions. Infect Immun 76**:**4345-4358. DOI:10.1128/IAI.00588-07.

199. **Seider K, Brunke S, Schild L, Jablonowski N, Wilson D, Majer O, Barz D, Haas A, Kuchler K, Schaller M, Hube B.** 2011. The facultative intracellular pathogen Candida glabrata subverts macrophage cytokine production and phagolysosome maturation. J Immunol 187**:**3072-3086. DOI:10.4049/jimmunol.1003730.

200. **Chai LY, Netea MG, Vonk AG, Kullberg BJ.** 2009. Fungal strategies for overcoming host innate immune response. Med Mycol 47**:**227-236. DOI:10.1080/13693780802209082.

201. **Romani L.** 1999. Immunity to Candida albicans: Th1, Th2 cells and beyond. Curr Opin Microbiol 2**:**363-367. DOI:10.1016/S1369-5274(99)80064-2.

202. **Lugo-Villarino G, Maldonado-Lopez R, Possemato R, Penaranda C, Glimcher LH.** 2003. T-bet is required for optimal production of IFN-gamma and antigen-specific T cell activation by dendritic cells. Proc Natl Acad Sci U S A 100**:**7749-7754. DOI:10.1073/pnas.1332767100.

203. **Lugo-Villarino G, Ito S, Klinman DM, Glimcher LH.** 2005. The adjuvant activity of CpG DNA requires T-bet expression in dendritic cells. Proc Natl Acad Sci U S A 102**:**13248-13253. DOI:10.1073/pnas.0506638102.

204. **Heckman KL, Radhakrishnan S, Peikert T, Iijima K, McGregor HC, Bell MP, Kita H, Pease LR.** 2008. T-bet expression by dendritic cells is required for the repolarization of allergic airway inflammation. Eur J Immunol 38**:**2464-2474. DOI:10.1002/eji.200737952.

205. **Yashiro T, Kubo M, Ogawa H, Okumura K, Nishiyama C.** 2015. PU.1 Suppresses Th2 Cytokine Expression via Silencing of GATA3 Transcription in Dendritic Cells. PLoS One 10**:**e0137699. DOI:10.1371/journal.pone.0137699.

206. **Chaudhry H, Zhou J, Zhong Y, Ali MM, McGuire F, Nagarkatti PS, Nagarkatti M.** 2013. Role of cytokines as a double-edged sword in sepsis. In Vivo 27**:**669-684

207. **Liu Q, Zhou YH, Yang ZQ.** 2016. The cytokine storm of severe influenza and development of immunomodulatory therapy. Cell Mol Immunol 13**:**3-10. DOI:10.1038/cmi.2015.74.

208. **Lancelin W, Guerrero-Plata A.** 2011. Isolation of mouse lung dendritic cells. J Vis Exp. DOI:10.3791/3563.

209. **Lutz MB, Kukutsch N, Ogilvie AL, Rossner S, Koch F, Romani N, Schuler G.** 1999. An advanced culture method for generating large quantities of highly pure dendritic cells from mouse bone marrow. J Immunol Methods 223**:**77-92

210. **Helft J, Bottcher JP, Chakravarty P, Zelenay S, Huotari J, Schraml BU, Goubau D, Reis ESC.** 2016. Alive but Confused: Heterogeneity of CD11c(+) MHC Class II(+) Cells in GM-CSF Mouse Bone Marrow Cultures. Immunity 44**:**3-4. DOI:10.1016/j.immuni.2015.12.014.

211. **Helft J, Bottcher J, Chakravarty P, Zelenay S, Huotari J, Schraml BU, Goubau D, Reis e Sousa C.** 2015. GM-CSF Mouse Bone Marrow Cultures Comprise a Heterogeneous Population of CD11c(+)MHCII(+) Macrophages and Dendritic Cells. Immunity 42**:**1197-1211. DOI:10.1016/j.immuni.2015.05.018.

212. **Pecora ND, Fulton SA, Reba SM, Drage MG, Simmons DP, Urankar-Nagy NJ, Boom WH, Harding CV.** 2009. Mycobacterium bovis BCG decreases MHC-II expression in vivo on murine lung macrophages and dendritic cells during aerosol infection. Cell Immunol 254**:**94-104. DOI:10.1016/j.cellimm.2008.07.002.

213. **Torrelles JB, Schlesinger LS.** 2010. Diversity in Mycobacterium tuberculosis mannosylated cell wall determinants impacts adaptation to the host. Tuberculosis (Edinb) 90**:**84-93. DOI:10.1016/j.tube.2010.02.003.

VITA

Heather Marie Evans

Place of Birth: Lebanon, Kentucky

Education

2007-2011   Eastern Kentucky University, Richmond KY
             Bachelor of Science, Biology

Professional Positions

2010-2011   Laboratory technician, Department of Biological Science, Eastern
             Kentucky University
2010   Research assistant, Undergraduate Research Experience in Virology,
             University of Nebraska-Lincoln
2011-2017   Graduate research assistant, Department of Microbiology, Immunology,
             and Molecular Genetics, University of Kentucky

Scholastic and Professional Honors

2015-2016   Kentucky Opportunity Fellowship
2014   American Association of Immunologists Trainee Poster Award
2013-2014   Kentucky Opportunity Fellowship
2011-2012   University of Kentucky Graduate School Academic Year Fellowship

Publications

Evans H.E., G.L. Bryant III, and B.A. Garvy (2016). The life cycle stages of
Pneumocystis murina have opposing effects on the immune response to this
opportunistic, fungal pathogen. Infect Immun, 84(11):3195-205.
DOI:10.1128/IAI.00519-16.

Evans H.E., A. Simpson, S. Shen, A.J. Stromberg, C.L. Pickett, and B.A. Garvy
(accepted, July 2017). The trophic life cycle stage of the opportunistic fungal pathogen
Pneumocystis murina hinders the ability of dendritic cells to stimulate CD4^{+} T cell
responses. Infect Immun. DOI: 10.1128/IAI.00396-17.